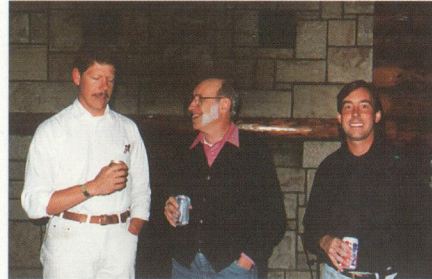


The Journal of Weather Modification



Volume 27 Number 1

April 1995

Weather Modification Association

- THE JOURNAL OF WEATHER MODIFICATION -

COVER: *Cover photos by Editor of attendees at the North Dakota Tracer Experiment and North Dakota Thunderstorm Project Analysis Meeting, Oct 12-14, 1994 at Ranch A - South of Beulah, WY*

EDITED BY:

*James R. Miller, Editor
Joie L. Robinson, Editorial Assistant
Institute of Atmospheric Sciences
South Dakota School of Mines and Technology
501 E. St. Joseph Street
Rapid City, South Dakota 57701-3995 U.S.A.
Phone: (605) 394-2293
FAX: (605) 394-6061*

PUBLISHED BY:

*The Weather Modification Association
P. O. Box 8116
Fresno, California 93747 U.S.A.
Phone: (209) 434-3486*

Additional copies of the Journal of Weather Modification are available for U.S. \$25.00 each (members) and U.S. \$50.00 each (non-members). U.S. \$600.00 for complete set of all 27 volumes/29 issues (members and non-members).

PRINTED BY:

*Fenske Printing
Rapid City, South Dakota U.S.A.*

Membership information is available by contacting the WMA Association at the Fresno, California, address shown above.

Appreciation to the South Dakota Community Foundation for partial support for the production of Volume 27 is gratefully acknowledged.

ISBN: 0739-1781

**- THE JOURNAL OF WEATHER MODIFICATION -
WEATHER MODIFICATION ASSOCIATION**

VOLUME 27

NUMBER 1

APRIL 1995

<u>TABLE OF CONTENTS:</u>	<u>PAGE</u>
THE WEATHER MODIFICATION ASSOCIATION	vi
PRESIDENT'S MESSAGE and EDITOR'S MESSAGE George Bomar and James R. Miller	vii
IN MEMORY OF LAWRENCE "BUD" YOUNGREN	ix

- REVIEWED SECTION -

COMPARATIVE CHARACTERIZATIONS OF THE ICE NUCLEUS ABILITY OF AgI AEROSOLS BY THREE METHODS Paul J. DeMott, Arlin B. Super, Gerhard Langer, David C. Rogers and Jack T. McPartland	1
ON THE CONSUMPTION OF AgI SEEDING AGENT: DEPENDENCE OF THE LIQUID WATER CONTENT IN THE SEEDING ZONE Mladjen Ćuric and Dejan Janc	17
OPERATIONAL EFFICIENCY ASSESSMENT OF HAIL SUPPRESSION FOR AGRICULTURE IN GREECE N. R. Dalezios and S. I. Spanos	21
OBSERVATIONS AND MODEL SIMULATION OF AgI SEEDING WITH A WINTER STORM OVER UTAH'S WASATCH PLATEAU Edmond W. Holroyd III, James A. Heimbach and Arlin B. Super	36
CASE STUDIES OF MICROPHYSICAL RESPONSES TO VALLEY-RELEASED OPERATIONAL AgI SEEDING OF THE WASATCH PLATEAU, UTAH Arlin B. Super	57
A STATUS REPORT ON LIQUID PROPANE DISPENSER TESTING IN UTAH WITH EMPHASIS ON A FULLY- AUTOMATED SEEDING SYSTEM Arlin B. Super, Erick Faatz, Arlen J. Hilton, V. Clark Ogden and Roger D. Hansen	84

- NON-REVIEWED SECTION -

CLOUD SEEDING AND ATMOSPHERIC TRACER PROGRAM CONDUCTED IN THE TSENGWEN RESERVOIR AREA OF TAIWAN DURING THE 1992 MEI-YU SEASON	94
Jack Ming-Sen Lin and Paul Tai-Kuang Chiou, Don A. Griffith, George W. Wilkerson and Mark E. Solak	
THE NOAA ATMOSPHERIC MODIFICATION PROGRAM - A 1995 UPDATE	99
Joseph H. Golden	
A SUMMARY OF WEATHER MODIFICATION ACTIVITIES REPORTED IN THE UNITED STATES DURING 1993	110
Joseph H. Golden	

- WEATHER MODIFICATION ASSOCIATION - GENERAL INFORMATION -

ARTICLES OF INCORPORATION OF THE WEATHER MODIFICATION ASSOCIATION	113
STATEMENT ON STANDARDS AND ETHICS FOR WEATHER MODIFICATION OPERATORS	116
QUALIFICATIONS AND PROCEDURES FOR CERTIFICATION	118
WMA CERTIFIED WEATHER MODIFICATION OPERATORS/MANAGERS AND HONORARY MEMBERS	120
WEATHER MODIFICATION ASSOCIATION OFFICERS AND COMMITTEES	121
WMA AWARDS - THUNDERBIRD AWARD, BLACK CROW AWARD, SCHAEFER AWARD, INTERNATIONAL AWARD	122
WMA MEMBERSHIP DIRECTORY - INDIVIDUAL AND CORPORATE MEMBERS	124
JOURNAL OF WEATHER MODIFICATION - 29 AVAILABLE PUBLICATIONS'	130
HISTORIC INDEX OF PUBLISHED PAPERS IN THE JOURNAL OF WEATHER MODIFICATION, VOL. 22, NO. 1 (Apr 1990) THROUGH VOL. 26, No. 1 (Apr 1994)	132

JOURNAL NOTES, ADVERTISEMENT INFORMATION, SCHEDULED WMA MEETINGS - 1995/96	138
AUTHOR'S GUIDE	139
ADVERTISEMENT	
TO COMMEMORATE THE RETIREMENT OF RAY JAY DAVIS	
(The end of the "tale" - or "trail" -- or is it a new beginning??)	

COMPARATIVE CHARACTERIZATIONS OF THE ICE NUCLEUS ABILITY OF AgI AEROSOLS BY THREE METHODS

Paul J. DeMott^a, Arlin B. Super^b, Gerhard Langer^c, David C. Rogers^a
and Jack T. McPartland^b

^a Department of Atmospheric Science
Colorado State University
Fort Collins, CO

^b U.S. Bureau of Reclamation
Denver, CO

^c Boulder, CO

Abstract. Three methods were used to assess the ice nucleating ability of different AgI-based aerosols produced using two solution combustion generators. The standard method employed was an isothermal cloud chamber which has been historically used for "calibrations" of ice nucleus aerosol generators. Comparisons with historical data showed consistency over a 20 year period for one generator, but not for another. Data on rates of ice crystal formation were used to infer operative ice formation mechanisms, and make inferences to the relative utility of the different aerosols in the atmosphere. Comparative measurements of ice nucleus effectiveness at -20°C were made using two NCAR counters that have been used operationally to trace the aerosols tested. Results showed that these devices can give self-consistent results and typically measure about 33% of the ice nuclei measured in the larger cloud chamber and 25% of the total AgI aerosols present. These results varied depending on the ice nucleus aerosol tested, presumably due to differences in particle size and chemistry. Measurements of the ice-forming ability of one aerosol ($\text{AgCl}_{0.22}\text{I}_{0.78}\text{-}0.125\text{NaCl}$) were also made with a continuous flow ice-thermal diffusion chamber. These measurements showed that the water supersaturation dependence of the ice formation rate by condensation-freezing for these aerosols varies by more than three orders of magnitude between 0 and 7% supersaturation. Ice formation was nearly instantaneous above 7% supersaturation for all aerosols capable of acting as ice nuclei. The various measurements taken will permit the quantitative transfer of laboratory results on ice nucleus ability to a range of expected atmospheric conditions.

1. INTRODUCTION

A laboratory characterization of the ice nucleating ability of aerosols produced from burning silver iodide (AgI) based solutions in two solution combustion cloud seeding generators used in the Utah/NOAA Atmospheric Modification Program (AMP) was made at the Colorado State University (CSU) Cloud Simulation and Aerosol Laboratory (hereafter referred to as Sim Lab). The primary characterization was made using historical procedures. Namely, the CSU vertical dilution wind tunnel was used as an aerosol generation plenum and the isothermal cloud chamber (ICC) as the basis for effectiveness determination. This testing program afforded the opportunity to examine the consistency of results of ice formation effectiveness made 13 and

22 years previously with the same or similar cloud seeding generators. An analysis of ice formation rates and mechanisms was also undertaken following the procedures of DeMott et al. (1983).

In association with the cloud chamber testing, comparative measurements were made of ice nucleating effectiveness using two NCAR ice nucleus (IN) counters that were previously deployed for tracking ice nucleus transport and dispersion over the Wasatch Plateau of central Utah. The purpose of these comparative measurements was to be able to relate the NCAR counter measurements in the field to a quantitative ice nucleus aerosol concentration and to a predicted ice nucleation effectiveness based on the cloud chamber calibrations (e.g., Super and Holroyd, 1994). A previous laboratory study of this

type (Sackiw et al., 1984) had stated that in addition to the factor of 10 correction for ice crystal detection efficiency (Langer, 1973), NCAR counter concentration values were as much as another factor of 10 lower than ICC-measured effectiveness for certain AgI aerosols and varied depending on the nucleant chemistry. This was presumably due to differences in ice formation mechanisms and residence times in the two measurement methods. The aerosols used in the earlier studies were AgI-0.5NaI aerosols produced by burning impregnated-coke and very small AgI aerosols produced by arcing electricity between solid AgI electrodes. These results may not be generally applicable to measuring other nucleant types, such as ones generated by combustion of solutions.

An additional comparative study of ice formation ability was made using the continuous flow diffusion chamber (CFD) described by Rogers (1988; 1994). This instrument may be of great utility for tracing ice nucleus aerosols in the atmosphere. It permits the independent control of both temperature and humidity. This allowed for a preliminary study of the effects of saturation ratio on ice formation by one AgI aerosol.

2. LABORATORY METHODS

2.1 IN Aerosol Generation

Standard procedures for testing ice nucleus generators at the Sim Lab (see, e.g., Garvey, 1975) include the use of a vertical wind tunnel to simulate operational conditions of air flow rate and mixing for the generator being tested. A sample of the aerosol is taken from the tunnel at 8 m downstream of solution combustion generators using a 4.25 liter syringe. The mass concentration of nucleant in the syringe is calculated using the generator nucleant burn rate (g min^{-1}), and the tunnel air flow rate (l min^{-1}). The sample is sometimes diluted further by expelling a portion of the sample air from the syringe and replacing it with particle-free, dry air. Each dilution reduces the number of aerosols in the syringe by a factor of 8.64. This procedure reduces the number of nuclei to a level that will result in a ratio of ice crystals to cloud droplets (1:100 to 1:10) which will allow ice crystal growth to proceed without greatly depleting available cloud water in the ICC. This procedure also prevents the generation of transient supersaturations which can occur when warm, moist air is injected into the cloud. For conditions where ice nucleation activity is low (e.g., warmest supercooled

temperatures), it is necessary to inject undiluted samples.

The primary focus of this study involved the generation and characterization of the ice nucleating ability of aerosols produced from the combustion of acetone-water solutions consisting of 2% AgI by weight and 0.50 mole of NH_4I (ammonium iodide) with respect to AgI. The ground-based generators used were the Montana State University Skyfire-type generator (MSU) and the North American Weather Consultants (Salt Lake City, UT) ground generator (NAWC). In addition, some selected experiments were performed burning 3 weight % solutions of composition AgI-0.5 NH_4I -acetone-water in the MSU generator and 2% AgI solutions of composition AgI-0.385 NH_4I -0.125NaI-0.2175 $\text{C}_6\text{H}_4\text{Cl}_2$ -acetone-water in the NAWC generator. The former of these two solutions was burned in the past in the MSU generator and provides a check versus results obtained at CSU during 1972. The latter solution containing NaI (sodium iodide) and $\text{C}_6\text{H}_4\text{Cl}_2$ (paradichlorobenzene) is a means for producing condensation-freezing ice nuclei of expected composition AgI-0.125NaI. The speed of this condensation-freezing ice formation process was of particular interest.

The wind tunnel provides for aerosol generation with or without the use of a high capacity axial fan. Natural wind flow through air vents below the tunnel area and the heat of combustion was used to provide a "natural" draft for carrying effluent up the tunnel. The inability currently to define the exact flow in every natural draft situation is a potential source of the variability between tests at the same set of conditions. For these tests, as for past tests at the Sim Lab, a constant volume flow of 1×10^5 liters per minute is assumed for natural draft conditions (Garvey, 1975; DeMott et al., 1983). This represents a flow of $2\text{--}3 \text{ m s}^{-1}$ (measured by a hot wire anemometer) within the tunnel and essentially calm conditions at the generator heads. The 2% AgI solutions were also burned in both generators for conditions of maximum fan displacement. This resulted in a volume flow rate of 3.23×10^6 liters per minute in the tunnel, representing about 55 m s^{-1} wind velocity. In the burning area beneath the tunnel the wind velocity is about 10 m s^{-1} past the generator heads. While this was intended to simulate aerosol generation during strong surface wind conditions during storm episodes, the flow past the generator heads was more vertically-oriented rather than horizontally-oriented. Nevertheless, the expected

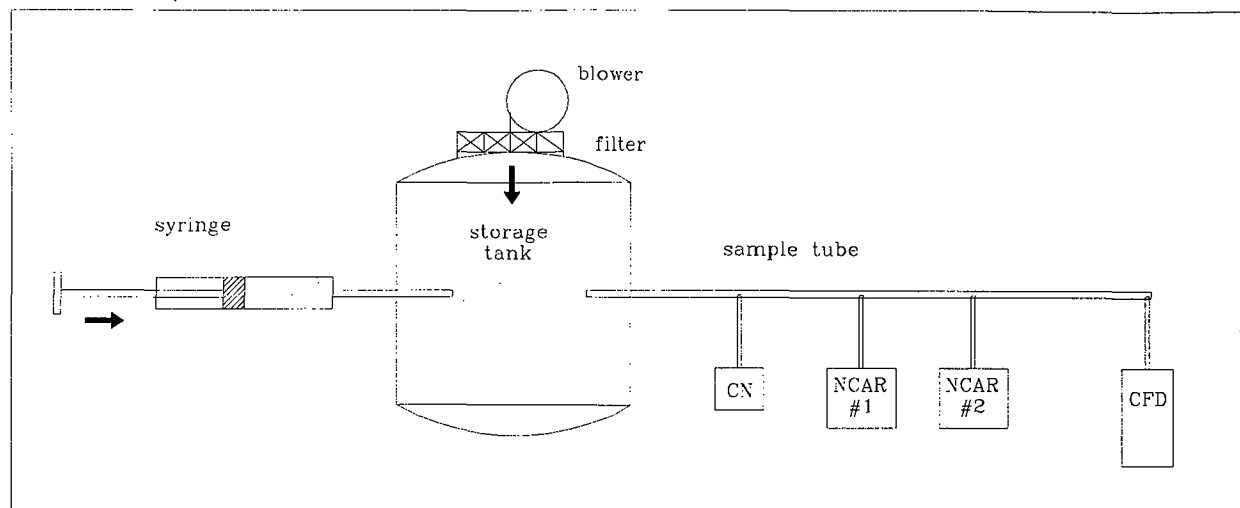


Figure 1. Schematic of aerosol sampling system.

quenching of the burn was simulated and the effect on ice formation was investigated. Both generators were operated with their wind shields in place.

Solution flow rates were characterized prior to testing at CSU. The burn rates for 2% AgI-0.5NH₄I solutions were 0.33 g min⁻¹ for the MSU generator and 0.13 g AgI min⁻¹ for the NAWC generator. The burn rate for the 3% AgI solution in the MSU generator was 0.50 g min⁻¹. The burn rate in the NAWC generator for the solution producing aerosol containing NaCl was assumed to be the same as for the standard 2% AgI solution. Propane was used both for pressurization (at 5 psi) and as a combustion source in the generators.

The procedures for storing aerosols for comparison between the ICC and other ice nucleus counting devices was similar to those used by Sackiw et al. (1984). A schematic of the system used is shown in Figure 1. For part of the testing program, two 4.25 liter syringe samples of aerosols were removed from the wind tunnel within a matter of seconds apart. One syringe was for use in the cloud chamber, while one was injected into a precleaned 770 liter holding tank in the laboratory. The holding tank was precleaned by blowing air into the tank through a HEPA filter. Total particle concentrations were monitored using a condensation nucleus counter (TSI Model 3010) sampling at 1 liter per minute. Immediately prior to injection of aerosols from the syringe, the blower was turned off. Residual turbulence aided in mixing particles throughout the

tank. The NCAR counters, CFD and CN counter were connected to the holding tank through a 1 inch diameter copper manifold. As they drew air from the storage vessel, the air was replaced by air which flowed through the HEPA filter. This also helped to relatively quickly mix the aerosol in the tank and continually deplete concentrations in the vessel at an expected first order decay rate with rate constant 0.0273 min⁻¹ (21 L min⁻¹/770L).

2.2 Isothermal Cloud Chamber

The characteristics of the isothermal cloud chamber are described in detail elsewhere (Garvey, 1975), but are briefly summarized here. The 0.96 m³ chamber can be controlled to contain a supercooled cloud within 0.3°C a test temperature between 0 and -25°C). The liquid water content (LWC) of the cloud can be set to any value between 0.2 and 3.0 g m⁻³ by controlling the rate at which cloud droplets are continuously introduced. After aerosol injection into the cloud, the number of ice crystals collected onto a tray of microscope slides is used to determine the total number settled from the chamber. The slides are successively pulled from the bottom of the chamber at 3 to 5 minute intervals until all ice crystals are nucleated and settle out. Crystals are counted manually using a cold-stage microscope. Yield (effectiveness) is calculated as the ratio of the total number of ice crystals formed to the mass of nucleating material in the sample injected.

Ice crystal formation and fallout times can vary from 1 to 50 minutes or more depending on a number of factors, including nucleus aerosol chemistry, ice formation mechanism, humidity in excess of water saturation and temperature (DeMott et al., 1983). Rates of ice crystal formation in the isothermal cloud chamber are presented as a means of displaying the time necessary for a given percentage of the effective ice nuclei to form ice crystals. The rates presented apply only for the cloud conditions simulated. These measured rates can only be given meaning for the conditions present in natural clouds if it is possible to infer the operative mechanism(s) for ice formation. Additional details of particle size and chemistry can influence the rate at which these processes occur. Utilizing the capability to vary cloud droplet concentrations in the ICC, and simple principles of chemical kinetics (DeMott et al., 1983), it is possible to distinguish whether ice formation results primarily from a collision-dependent or collision-independent process at water saturation. If the rate at which ice appears is found to predictably depend on cloud droplet concentrations (for the same droplet mean size), it can be deduced that contact-freezing nucleation is a dominant ice formation mode. The rate of ice crystal formation in real clouds by this mode will depend on time and the droplet sizes and concentrations present. Similarly, if the rate of ice crystal formation is not found to depend on droplet concentration in the ICC, it can be presumed that nucleation is dependent on a vapor to ice or a condensation-freezing process. In this case, both activity and ice formation rate in real clouds will probably depend on both temperature and water vapor saturation ratio. Ice crystal formation kinetics were examined in this study, but a definitive statement of the mechanisms of ice crystal formation can only be made by further testing at varied temperatures and LWC.

In all, 44 experiments were conducted in the isothermal cloud chamber, spanning a number of temperatures between -6 and -20°C. LWC was set to 0.5 g m⁻³ for all experiments. This value represents about 2100 droplets cm⁻³ in the cloud chamber. This high value of droplet concentration results from the small modal diameter (~7 μm) of cloud droplets generated by the ultrasonic humidifier used. It should be remembered that the cloud produced is only intended to reproduce a supercooled cloud

environment and is not a true simulation of a wintertime orographic cloud.

2.3 NCAR Ice Nucleus Counters

Two NCAR ice nucleus counters used to track the transport and dispersion of AgI aerosols in the 1994 Utah program were operated for comparison to the isothermal cloud chamber results. One counter had been deployed in an instrumented van driven on plateau-top highways, and the other was used in an aircraft. The fundamental operating characteristics of these devices are as described by Langer (1973). The two units used were built in 1976 at NCAR. The counters were tested in the same condition that they returned from the field season, except that the electronic sensitivity of the counters was reset for the Fort Collins elevation (4860 ft.). The mobile ground unit operated at about 10000 ft. and the aircraft unit was pressurized to 8000 ft. during the field program.

The NCAR counters were operated at -20°C, so comparisons to the isothermal chamber results were made at this temperature for as many of the aerosol types generated as possible. In addition, the counters were operated when testing was being conducted at -16 and -12°C in the ICC. In these cases, the ICC values were normalized to the values at -20°C for comparison to the NCAR counter. The cloud in the counters has been previously estimated to have a droplet concentration of 15000 to 20000 cm⁻³ with an average diameter of about 5 μm.

The NCAR counters sampled from the storage vessel at 10 liters per minute. The standard correction factor of 10 for ice crystals which do not make it into the NCAR counter detection section (Langer, 1973) was made to the raw data. In addition, a correction was made for coincidence losses caused by count integrators using an approximate 0.0075 s delay during each second in order to process the signal. This correction is described by the equation,

$$x_{\text{true}} = x_{\text{obs}} / (1 - (x_{\text{obs}} y / 60000)) \quad (1)$$

where x_{obs} is the counter concentration value (L⁻¹), x_{true} is the corrected value and y is the counter-specific delay in milliseconds. This equation is valid for x_{obs} less than about 8000 (depends on y). No data retrieval is possible for higher count values. Concentration data were integrated and recorded at

Table 1: Yield (Effectiveness) Data for MSU Generator

Temperature (°C)	Yield		
	(#/g ⁻¹ AgI) AgI (2%) Natural Draft	(#/g ⁻¹ AgI) AgI (2%) Maximum Draft	(#/g ⁻¹ AgI) AgI (3%) Natural Draft
-6	3.60X10 ¹⁰	7.60X10 ¹¹	8.60X10 ¹⁰
-6	8.60X10 ¹⁰	2.50X10 ¹¹	5.50X10 ¹⁰
-8	7.40X10 ¹³		
-8	2.00X10 ¹³		
-12	3.70X10 ¹⁴	1.10X10 ¹⁵	3.90X10 ¹⁴
-12	4.90X10 ¹⁴	1.00X10 ¹⁵	2.30X10 ¹⁴
-16	8.50X10 ¹⁴		
-16	4.90X10 ¹⁴		
-20	7.80X10 ¹⁴	1.20X10 ¹⁶	3.80X10 ¹⁴
-20	6.00X10 ¹⁴	4.80X10 ¹⁵	3.00X10 ¹⁴
-20	6.20X10 ¹⁴		

Table 2: Yield (Effectiveness) Data for NAWC Generator

Temperature (°C)	Yield		
	(#/g ⁻¹ AgI) AgI(2%) Natural draft	(#/g ⁻¹ AgI) AgI (2%) Maximum Draft	(#/g ⁻¹ AgI) AgICI-0.125NaCl Natural draft
-6	3.80X10 ¹²	7.30X10 ¹¹	8.30X10 ¹²
-6	4.80X10 ¹²	2.50X10 ¹¹	1.30X10 ¹³
-8	9.30X10 ¹³		9.80X10 ¹³
-8	1.80X10 ¹⁴		8.00X10 ¹³
-12	1.20X10 ¹⁵	2.20X10 ¹⁵	8.30X10 ¹⁴
-12	1.50X10 ¹⁵	2.90X10 ¹⁵	1.00X10 ¹⁵
-16	1.60X10 ¹⁵		
-16	1.90X10 ¹⁵		
-20	1.90X10 ¹⁵	2.30X10 ¹⁶	
-20	1.70X10 ¹⁵	2.40X10 ¹⁶	

one minute intervals during sampling. The 15 liter volume of the flow-through processing chamber also causes some lag-time measurement effects, as discussed by Heimbach et al. (1977), which may lead to an underestimate of the transient peak ice nucleus concentration in the tank. Because the IN concentration changed slowly in the tank, this factor was considered minor and no correction was made. It is also possible that the short residence time (~1.5 min) in the counter leads to an underestimate of ice nuclei which require longer times for activation.

2.4 Continuous Flow Diffusion Chamber

A continuous flow ice-thermal diffusion chamber (CFD) for ice nuclei measurement was also connected to the manifold for a few selected experiments during the program. This chamber is the unit described by Rogers (1988; 1994) with some minor changes. A brief description is given here. The chamber consists of an annular gap between two ice-coated cylinders. The cylinders are held at different temperatures, and a supersaturation forms between them. The aerosol sample, ~15% of the total air flow, is smoothly injected into this space, between two equal layers of particle-free sheath air. Droplets and

crystals nucleate in the supersaturated region and grow as they pass through the first $\sim 2/3$ of the chamber. The last $1/3$ has no ice on the warm cylinder; instead, it has a thin layer of dry insulation, and this change in boundary conditions creates a region that is below water saturation, so water droplets evaporate. This evaporation region helps to exaggerate the size difference between ice crystals ($\sim 5\text{--}15\text{ }\mu\text{m}$) that formed on ice nuclei from the much smaller residues of cloud droplets ($<1\text{ }\mu\text{m}$). At the chamber's outlet, the particles are counted with an optical particle counter (OPC); the amplitude of the OPC voltage pulses correspond to particle size. The pulses are digitized and accumulated in a multichannel analyzer (MCA) and recorded by computer. The detection of ice crystals, or ice nuclei, is based on particle size ($>4\text{ }\mu\text{m}$). To avoid erroneously including large non-IN aerosols, they are removed at the CFD inlet by an impactor which removes all particles larger than $\sim 3\text{ }\mu\text{m}$.

The sample temperature and supersaturation are independently controllable. Generally speaking, the sample temperature corresponds to the average temperature of the two walls, whereas the supersaturation corresponds to their difference. In these experiments, the maximum water supersaturation (SSw) was deliberately chosen to be very high, $+10\%$. This was done to ensure that water saturation was exceeded, so that all CCN activated, and droplets grew quickly before reaching the evaporation section. It is a unique capability of the CFD technique to produce well defined high SSw. The existence of water supersaturation was confirmed by looking through a window in the CFD just upstream of the droplet evaporation section and seeing cloud droplets illuminated by a laser beam.

3. RESULTS AND DISCUSSION

3.1 ICC Yields (Effectivities)

Yield computations for both generators and the different solution compositions are summarized in Tables 1 and 2. The use of 2% instead of the historical 3% AgI solutions in the MSU generator leads to no degradation of ice nucleus aerosol yield at the warmest temperature tested (-6°C) and an enhanced yield at colder temperatures. The latter fact is probably due to decreased average particle size and increased total numbers of particles generated per gram of AgI burned. Yield decreases a little more than an order of magnitude as temperature increases

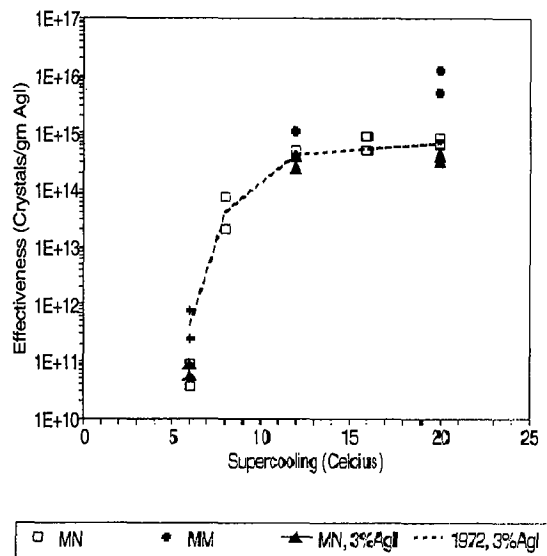


Figure 2. Yield (effectiveness) for different aerosols generated using the MSU ground generator (MN: natural draft; MM: maximum fan) as a function of cloud ($\text{LWC} = 0.5\text{ g m}^{-3}$) supercooling. Measurements for natural draft 3% AgI aerosols made in $\text{LWC} = 1.5\text{ g m}^{-3}$ clouds in 1972 are also presented.

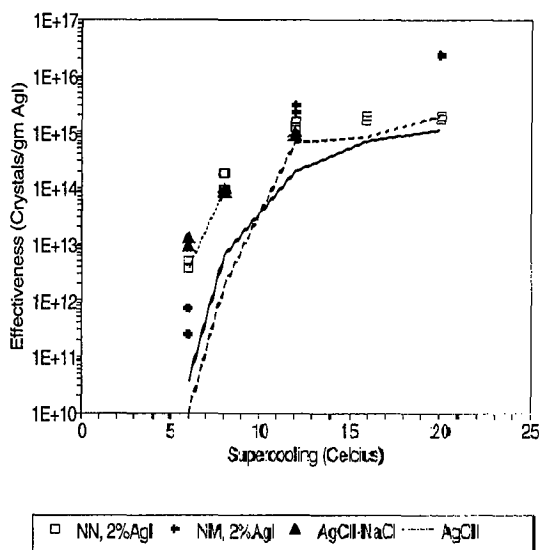


Figure 3. Yield for different aerosols generated using the NAWC ground generator (NN: natural draft; NM: maximum fan) as a function of cloud supercooling. Presented for comparison are natural draft results for 2% AgI aerosols tested in 1978 (solid line) and 1981 (dashed line), and average data points for $\text{AgCl}_{0.22}\text{I}_{0.78}$ aerosols tested in 1981.

from -20 to -8°C, but falls three more orders of magnitude lower at -6°C. Stronger ventilation of the burner leads to more rapid quenching of the flame and yet smaller and more numerous particles generated. The yield for maximum draft conditions is higher at all temperatures compared to natural draft (calm) conditions. The yield results for the MSU generator are displayed in Figure 2. The 3% AgI data from 1972 are presented for comparison. Within uncertainties which characterize ICC calibrations, the results are consistent over greater than 20 years.

Yield data for the NAWC generator tests are shown in Table 2 and Figure 3. This generator shows a slightly higher efficiency for IN generation at most temperatures compared to the MSU generator. In comparing the two generators it should be noted that the operational AgI output rate of the NAWC generator is lower by a factor of 2.5. As for the MSU generator, yield from burning 2% AgI solution decreases by about 1 order of magnitude as cloud temperature warms from -20 to -8°C. Unlike the

Table 3. Rates of Ice Crystal Formation

MSU Generator

Temp (°C)	k_{exp} (min ⁻¹)	k_{dil} (min ⁻¹)	k_{act} (min ⁻¹)	$t_{1/e}$ (min)	$t_{90\%}$ (min)	Yield Correction
2%AgI-0.5 NH ₄ I Natural Draft						
-8	0.1162	0.0365	0.0797	12.5	28.9	1.46
-12	0.1269	0.0542	0.0727	13.8	31.7	1.75
-16	0.1696	0.0854	0.0842	11.9	27.3	2.01
-20	0.2485	0.1020	0.1465	6.8	15.7	1.70
2%AgI-0.5 NH ₄ I Maximum Draft						
-12	0.2302	0.0542	0.1760	5.7	13.1	1.31
-20	0.4964	0.1020	0.3944	2.5	5.8	1.26
3%AgI-0.5 NH ₄ I Natural Draft						
-12	0.1276	0.0542	0.0734	13.6	31.4	1.74
-20	0.2086	0.1031	0.1055	9.5	21.8	1.98

NAWC Generator

Temp (°C)	k_{exp} (min ⁻¹)	k_{dil} (min ⁻¹)	k_{act} (min ⁻¹)	$t_{1/e}$ (min)	$t_{90\%}$ (min)	Yield Correction
2%AgI-0.5 NH ₄ I Natural Draft						
-6	0.1140	0.0302	0.0838	11.9	27.5	1.36
-8	0.1211	0.0346	0.0865	11.6	26.6	1.40
-12	0.1268	0.0474	0.0794	12.6	29.0	1.60
-16	0.1715	0.0854	0.0861	11.6	26.7	1.99
-20	0.1875	0.1057	0.0818	12.2	28.1	2.29
2%AgI-0.5 NH ₄ I Maximum Draft						
-12	0.2163	0.0474	0.1689	5.9	13.6	1.28
-20	0.3219	0.1057	0.2162	4.6	10.6	1.49
2%AgI-0.36 NH ₄ I-0.14NaI-0.15 C ₆ H ₄ Cl ₂ Natural Draft						
-6	0.1007	0.0289	0.0718	13.9	32.1	1.40
-8	0.1373	0.0339	0.1034	9.7	22.3	1.33
-12	0.1450	0.0469	0.0981	10.2	23.5	1.48

MSU generator, yield only falls about 1.5 orders of magnitude further between -8 and -6°C, rather than 3 orders of magnitude. This result is unexpected and inconsistent with previous results obtained at CSU for this generator. Comparison of yield under natural draft generation conditions versus temperature in test series performed in different years are also compared in Figure 3. It is apparent that the generator is now producing much more efficient ice nucleus aerosols from 2% AgI solutions at -8 and -6°C. In fact, the yields at these temperatures are almost exactly those determined for AgI-AgCl ($\text{AgCl}_{0.22}\text{I}_{0.78}$) aerosols produced by adding ammonium perchlorate to the standard solution in 1981. The yield under maximum draft conditions is higher at all temperatures except -6°C compared to natural draft (calm) conditions.

The generation of $\text{AgI} \cdot 0.125\text{NaCl}$ aerosols using the NAWC generator had very little effect on yield, showing an increase of only a factor of 2 at -6°C, while not changing yield very much at colder temperatures. The data do suggest that measurable activity might exist for these nuclei at temperatures warmer than -6°C. The yield values obtained are consistent with values previously obtained for $\text{AgCl}_{0.22}\text{I}_{0.78}$ aerosols from the NAWC generator.

The values reported in this section are "raw" yield, as have been reported in all past calibrations. These values should be corrected for losses which are a consequence of nuclei dilution (from cloud introduction air) during the extended ice formation process. This correction requires knowledge of the rates of ice crystal formation.

3.2 ICC Rates of Ice Crystal Formation

The presentation of rates of ice crystal formation follows the conventions of DeMott et al. (1983). The plots presented in Figures 4 and 5 provide graphical depictions of the raw ice nucleation kinetics (characteristic times for effective ice nuclei depletion) for two aerosols produced by the MSU generator as observed at -12°C. The plots present the natural logarithm of [100 - % (total ice crystals formed)] versus time for two experiments. A uniform 1 minute time for ice crystal growth and sedimentation is removed from the data account for this factor which can vary from 30 to 90 s depending on temperature. A linear regression fit is drawn through the points in each case. The high linear correlation in these and all other tests suggests that the underlying process creating ice crystals is pseudo-first order and probably singular (see, DeMott et al.,

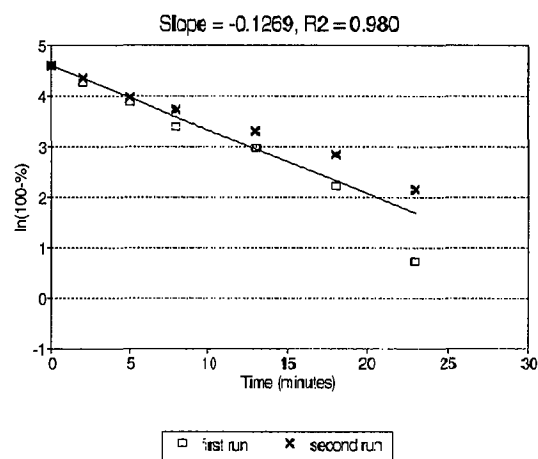


Figure 4. Ice crystal formation kinetics plot for AgI aerosols produced from combusting 2% AgI solutions in the MSU generator operating under natural draft conditions. ICC temperature was -12°C. The % in the ordinate is the percent of ice crystals formed at a given time.

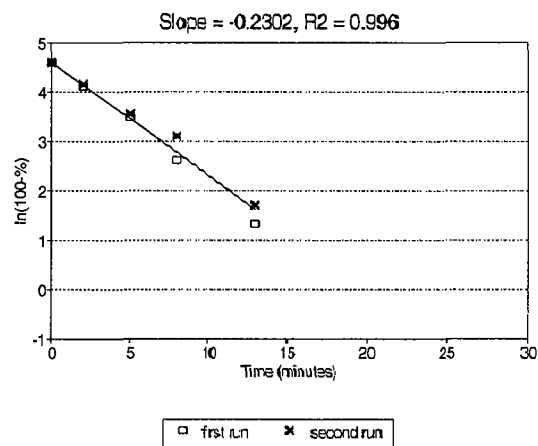


Figure 5. As in Figure 4, but for aerosols produced from combusting 2% AgI solutions under maximum draft generating conditions.

1983). The slope of the fits represents the apparent rate constant (k_{app}) for ice formation in the chamber. These slopes are listed in Table 3 for all aerosols tested and all temperature conditions. Not enough data (ice crystal counts) were available at -6°C to reliably apply the graphical technique at this temperature in all cases. Superimposed on the ice formation process is the first-order dilution of aerosols due to air flowing into and out of the chamber to continuously supply cloud droplets. This causes nucleation rates to appear faster and nucleation yield to appear lower. The rate constant

(min^{-1}) for cloud dilution (k_{dil}), predetermined by airflow through the cloud precooling and injection pipe in particular experiments (DeMott et al., 1983), is subtracted from the apparent rate constant to obtain the true rate constants (k_{act}) in Table 3. The resultant characteristic ice formation time ($t_{1/e}$ or time to use up 63.2% of active nuclei) and the time for using up 90% of the nuclei for the cloud conditions simulated are also given in Table 3. Figure 6 shows plots of the graphically-determined characteristic times versus temperature for the different solutions tested in the two ground generators. Several points can be made regarding the rate data for each generator. For the MSU generator aerosols,

1) Ice formation times in ICC conditions were nearly independent of temperature and quite slow for natural draft aerosol generation conditions at -16°C and warmer. Rates nearly doubled at -20°C for all three solution/generation variations (Table 3 and Figure 6).

2) Strong ventilation of the generator increased rates and decreased ice formation times by a factor of 2 to 3. This is apparent on comparing the raw data in Figures 4 and 5 and the dilution corrected rate constants in Table 3 (Figure 6).

3) The use of a 3% AgI solution had little effect on ice formation rate except to slow ice formation slightly at -20°C (Table 3 and Figure 6).

These points support a conclusion of the dominance of a contact-freezing process operating for the AgI aerosols in the ICC cloud conditions, at least for temperatures of -16°C and warmer. The only obvious physical effect of increasing ventilation would be to produce more and smaller particles. An increase in ice formation rate for smaller particles within a cloud of the same droplet concentration and humidity implies a rate process limited by collisions between droplets and ice nucleus aerosols. Two additional factors support this conclusion. First, the extrapolated (versus temperature) maximum activity of the natural draft and maximum fan aerosols imply average particle diameters of 0.062 and $0.020\ \mu\text{m}$, respectively. For a collision process controlled by Brownian diffusion, calculations presented in DeMott (1990; 1995) show that the collision rate of the maximum draft aerosols with the $0.5\ \text{g m}^{-3}$ ICC cloud should be 3.0 times faster than for natural draft aerosols. The observed value was about 3, in exact agreement. Secondly, rate results obtained for 3% AgI aerosols in 1972 (not shown) indicate that the ice formation rates in $\text{LWC} = 1.5\ \text{g m}^{-3}$ clouds

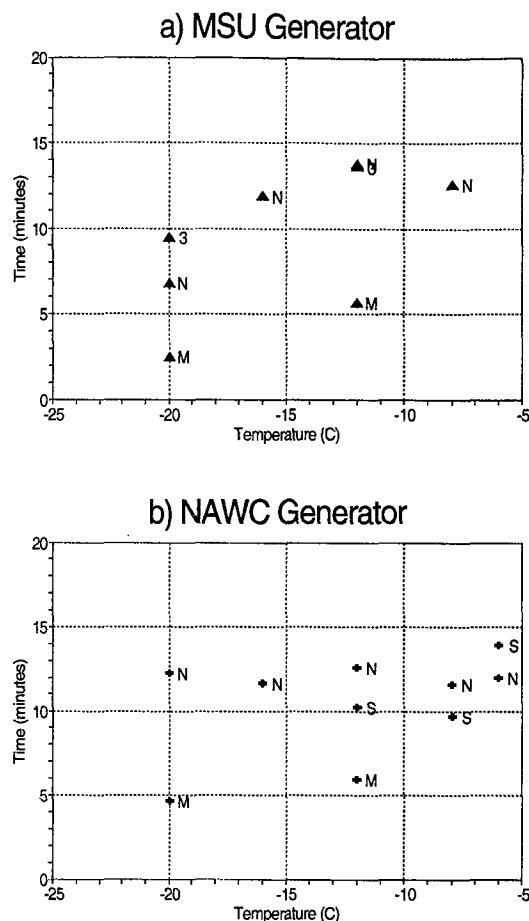


Figure 6. Characteristic ($1/e$) times for ice formation at different ICC cloud temperatures for different aerosols generated. Results for AgI aerosols produced from combusting 2%AgI solutions under natural draft (N) and maximum fan draft (M) conditions, AgI aerosols produced from combusting 3%AgI solutions under natural draft conditions (3), and AgICl-0.125NaCl aerosols (S) are indicated by interior labels.

containing ~ 4300 droplets cm^{-3} are about 2.3 times faster than for the $0.5\ \text{g m}^{-3}$ (~ 2100 droplets cm^{-3}) clouds in the recent tests. Calculations estimate that the rate in the higher LWC cloud would be 2.1 times faster for a collision-controlled process, as this value should be the ratio of droplet concentration values in the respective clouds. The observations are in good agreement with calculations in both instances, considering the 30% uncertainty in droplet concentrations. Faster rates at -20°C cannot be explained in a straightforward manner for the MSU generator aerosols. It is inferred that a different or additional ice formation mechanism was operative at

this colder temperature, but it was not possible to discern what this process was.

For the aerosols produced with the NAWC generator, the following points regarding ice formation rates can be made from an analysis of Table 3 and Figure 6:

- 1) Ice formation rates were nearly constant and quite slow across the ICC cloud temperature range tested.
- 2) Strong ventilation increased rates and decreased ice formation times by a factor of 2 to 3.
- 3) AgICI-0.125NaCl aerosols have about 15% shorter ice formation times at temperatures colder than -8°C.

The NAWC results suggest that a contact-freezing process was also a predominant mechanism in the ICC for AgI aerosols produced from burning the standard AgI-NH₄I-acetone-water solution. Data from previous tests in 1.5 g m⁻³ clouds at CSU supports this conclusion. Previous data indicate that ice formation rates were about 2.2 times faster in the higher concentration clouds. Again, a 2.1 factor is expected for a collision-dependent process. The average particle sizes inferred from the extrapolated maximum yield in the current tests are 0.041 and 0.016 μm, respectively, for natural draft and maximum fan generation conditions. Theoretically, the collision rates of the smaller particles should be about 2 times faster than the larger ones. The maximum fan ice formation rates were observed to be 2.4 times faster than for natural draft aerosols. Thus, the data are consistent with the predominance of contact-freezing nucleation across the temperature range tested.

Inference to ice formation mechanisms by AgICI-0.125NaCl aerosols produced from the NAWC generator is difficult to make without additional information, such as varied droplet concentration tests. It was presumed that the addition of the NaI would lead to a condensation freezing process. It clearly did not result in the activation of a rapid condensation-freezing process at water saturation. As a check on the relative condensation behavior of this nucleant, some aerosols were collected and processed for CCN activity using a thermal gradient diffusion chamber (Mee Industries Model 230). The results indicated very poor CCN activity; 0.5, 2 and 5% of aerosols active as CCN, respectively, at 1, 2, and 2.5% water supersaturation. These percentage activities as CCN are almost exactly as measured for similar-sized AgI-AgCl aerosols which did not

contain any NaCl (DeMott, 1990; 1995). Therefore, it is questionable whether or not the small amount of sodium chloride introduced will have any added effect toward promoting the rapid condensation-freezing process which can occur when generators are operated in ice supersaturated and subcooled wintertime situations (Finnegan and Pitter, 1988). DeMott (1991) has shown that hydrophobic AgI-AgCl aerosols will respond quite readily to the supersaturations which might occur in these situations. Nevertheless, the observation that the ice formation rate is about 15% faster than AgI aerosols at temperatures colder than -6°C suggests that the ice formation mechanism changed to condensation-freezing simply due to the slight water uptake by the AgI_{0.78}Cl_{0.22}-0.125NaCl aerosols. This observation is consistent with those of Finnegan et al. (1994) based on past testing at CSU using a different generator.

The rate data presented also permit correction of yield data. Since the aerosols require some time for the process of ice formation to occur, the actual yield is always somewhat higher than that given by the initial calculations presented in Section 3.1. Again, this follows from the fact that some nucleating aerosols are diluted from the chamber over time (through unsealed places) by cloud introduction air. The faster the nucleation rate, the less the correction needed. The magnitude of the correction is equal to the ratio k_{exp}/k_{act} (see, DeMott et al., 1983). This factor, given as Yield Correction in Table 3, affects one's interpretation of the effect of LWC on yield if other values of LWC are used for testing because, for a contact freezing process, the ratio is inversely dependent on LWC in the ICC. Therefore, for example, the slightly lower activity of the 3% AgI aerosols from the MSU generator in the current tests compared to the 1972 results is erased if the rate correction factors are applied.

3.3 Comparisons to NCAR Counters

Since the cross-calibration research effort was conducted in an exploratory manner, only a limited number of comparative data are considered here. A number of initial experiments were deemed to have been affected by contamination around the storage tank due to the generation of high concentrations of AgI aerosols in the nearby laboratory wind tunnel. This problem does not affect ICC calibrations because the cloud chamber room is overpressured by particle-free air, but use of the storage vessel in that room would have potentially contaminated those results. Special efforts were later taken to isolate the storage vessel from outside contamination. It was

more difficult to isolate leaks into the CN counter from around its sample inlet. Consequently, in only 3 of the tests represented in summary Table 4 were reliable CN concentrations deemed to have been recorded. Knowledge of syringe dilution conditions, generator consumption rate of AgI, and the maximum activity of the different aerosols generated as extrapolated from the ICC results were used to obtain a best estimate of initial aerosol concentration in the storage vessel. These values were used to compare to the NCAR counter and to the ICC results at -20°C . These estimated initial aerosol concentrations in the storage vessel showed good agreement with the few CN measurements which were deemed to be reliable.

Figure 7 shows an example of the response of the two NCAR counters following an injection of aerosols into the storage vessel and depicts the procedure used to calculate the initial mixed concentration value. The values presented in this figure are not corrected for coincidence losses. It can be seen that both NCAR counter records show excellent agreement after a few minutes with an exponential decay factor of 0.027 min^{-1} (represented by the solid line drawn through the data). This value of the decay constant represents the 21 L min^{-1} being drawn from the 770 liter storage vessel and replaced with clean air. Fitting this decay curve to the data (by eye) permitted determination of the NCAR counter ice nucleus concentration at the point of injection and rejection of higher initial concentrations measured before the aerosol was completely mixed through the tank. This initial peak is exaggerated by the $\sim 2\text{ min.}$ residence time of a unit sample within the counters. The two NCAR counters showed linear correlation coefficients mostly above 0.90 during the experiments, with differences generally being less than 15%.

Table 4 compares the coincidence-corrected NCAR counter ice nucleus number (NCAR in Table 4) measured for different aerosols in specific experiments with the values measured in concurrent ICC tests and with the estimated (CNEST) and measured initial CN concentration in each case. Where a different dilution factor was used in the ICC test than for the storage tank injection, the ICC value (ICC in Table 4) is corrected to be in accordance with the tank syringe dilution. The ICC value is also normalized to activity at -20°C when test temperature was different than -20°C . The correction to ICC yield for ICC airflow dilution (Tables 1 and 2) has been

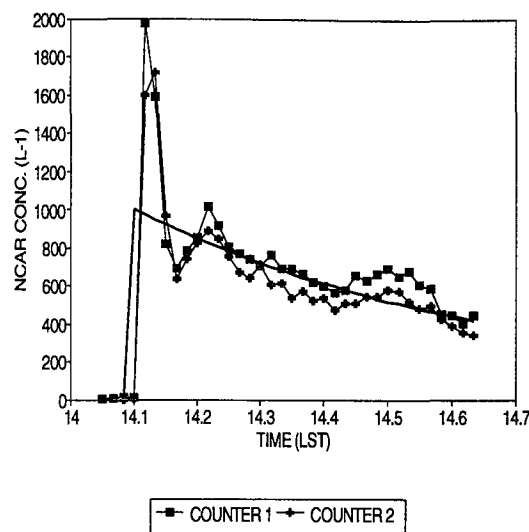


Figure 7. NCAR counter IN concentration versus time in hours local time after aerosol injection into storage vessel in one test. The decay rate caused by the 21 L min^{-1} sampling rate (solid line) is superimposed on the concentration values. The initial burst was an artifact of the mixing process.

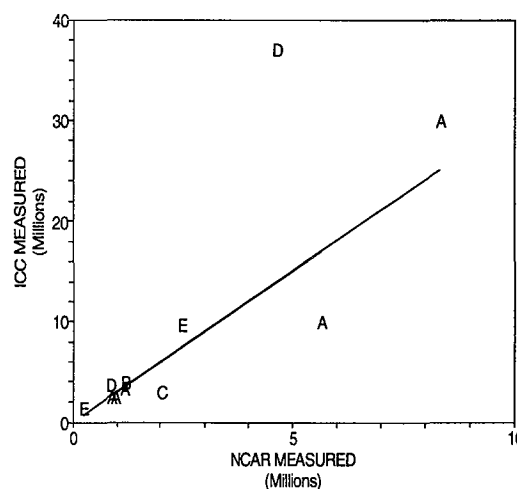


Figure 8. Dilution-corrected ICC versus NCAR counter total ice nucleus number for coordinated measurements. Following the key in Table 4, samples indicated A are the MN aerosols. The linear regression fit is for these samples. Points indicated as B, C, D, and E are for MM, MN3, NN, and NM aerosols, respectively.

Table 4. NCAR Counter/Isothermal Cloud Chamber Cross-calibration Data

CNEST	CN	NCAR	ICC	ICCC	TYPE	ICCT	NCAR/ ICCC	NCAR/ CNEST	ICCC/ CNEST
(est.)	(meas.)					(°C)			
2.7x10 ⁷		1.2X10 ⁶	3.2X10 ⁶	4.0X10 ⁶	MM	-20	0.30	0.04	0.15
4.2x10 ⁷		4.6X10 ⁶	1.6X10 ⁷	3.7X10 ⁷	NN	-20	0.13	0.11	0.88
2.1X10 ⁷		2.5X10 ⁶	6.5X10 ⁶	9.7X10 ⁶	NM	-20	0.25	0.12	0.46
1.4X10 ⁷	1.3X10 ⁷	5.6X10 ⁶	6.0X10 ⁶	1.0X10 ⁷	MN	-20	0.56	0.40	0.71
3.5X10 ⁶		9.8X10 ⁵	1.5X10 ⁶	2.5X10 ⁶	MN	-20	0.39	0.28	0.71
3.0X10 ⁷	1.5X10 ⁷	8.3X10 ⁶	1.8X10 ⁷	3.0X10 ⁷	MN	-16	0.28	0.28	1.00
3.5X10 ⁶		8.7X10 ⁵	1.5X10 ⁶	2.5X10 ⁶	MN	-12	0.35	0.25	0.71
3.5X10 ⁶		1.2X10 ⁶	2.0X10 ⁶	3.4X10 ⁶	MN	-12	0.35	0.34	0.97
3.5X10 ⁶		2.0X10 ⁶	1.7X10 ⁶	3.0X10 ⁶	MN3	-12	0.68	0.58	0.86
4.8X10 ⁶		8.6X10 ⁵	1.6X10 ⁶	3.7X10 ⁶	NN	-20	0.23	0.18	0.77
2.5X10 ⁶		2.4X10 ⁶	6.9X10 ⁶	1.4X10 ⁷	NM	-20	0.17	0.10	0.56
4.8X10 ⁶			1.6X10 ⁶	2.6X10 ⁶	NN	-12			0.54
3.0X10 ⁷	2.7X10 ⁷	1.2X10 ⁷			MN	-20		0.41	
					All:		0.34	0.26	0.69

Key:

MN: MSU generator natural draft, 2% AgI
 MN3: MSU generator natural draft, 3% AgI
 MM: MSU generator maximum draft, 2% AgI
 NN: NAWC generator natural draft, 2% AgI
 NM: NAWC generator maximum draft, 2% AgI

applied to the values listed as ICC in Table 4. Ratios between the various quantities are also indicated in Table 4. Figure 8 presents the comparison between ICC and NCAR for the various aerosols tested while the devices were operating concurrently. A linear regression on the data for the MSU generator aerosols generated in natural draft airflow conditions (A:MN) is given by the solid line in the figure. This fit is described by $ICCC = 3.02 (NCAR)$ with a correlation coefficient squared of 0.87. The good correlation provides a measure of confidence in the validity of the calibration. R^2 values of 0.94 and 0.97, respectively, for linear regressions of NCAR and ICC on CNEST for the MN data (not shown here) also validate that the two methods for measuring ice nuclei responded in kind to changes in ice nucleus concentration. The regression between the two methods suggests that the NCAR counter saw only about 33% of the MN nuclei measured by the ICC (corrected) at -20°C. A simple average of the MN NCAR/ICCC ratios gave a value of 39%. Compared to the total number of aerosols present (CNEST), the NCAR counter measured 31% on average. Compared to raw ICC values, which is

the way that they are typically reported, the NCAR counters saw about 65% of the ICC-measured nuclei.

Not enough data were obtained for other aerosol types to perform complete analyses as done for the MN data. Only a single data point exists for each of the cases of a change in the wind speed or a change to 3% AgI in solutions for the MSU generator aerosols. The changes noted are an increase in the efficiency of the NCAR counters for detecting the 3% AgI aerosols and a slight decrease for detecting the 2% AgI maximum draft aerosols. It is tempting to interpret this as an effect of the differences in particle sizes in each case, but much more data would be required to confirm such an assertion. Results in Table 4 and Figure 8 also suggest that the NCAR counters are less efficient in detecting the ice nucleus aerosols from the NAWC generator. It is not clear why this should be so, but it must relate either to the inferred smaller size of the NAWC aerosols compared to the MSU aerosols or the relative efficiency of different ice formation mechanisms in the NCAR counters versus the ICC for the different aerosols.

3.4 Exploratory Studies of Ice Nucleus Behavior Using a Continuous Flow Diffusion Chamber

The CFD method has not been used before to characterize cloud seeding aerosols. These experiments provided an opportunity to explore the potential use of the instrument in this way. Only results from studies of the AgICl-0.125NaCl aerosols will be presented here. The CFD sampled during a period of simultaneous measurements with the ICC, but not while the NCAR counters were operating. The CFD sampled from the tank while the temperature and supersaturation varied continuously. Figure 9 shows the history of temperature, SSw, and SSi. Total air flow through the CFD was ~ 9 LPM; sample flow was ~ 1.5 LPM. Sample residence time within the CFD was about 5 s. The time history of IN and CN measurements are shown in Figure 10. The CN trace shows that the particle concentration in the tank was fairly steady near $1.5 \times 10^5 \text{ L}^{-1}$ during this test. It decayed much slower than during the NCAR counter experiments because the airflow demand was less, 2.5 LPM instead of ~ 21 LPM. At the time of coldest temperatures and highest supersaturation, IN reached values of $\sim 5 \times 10^4 \text{ L}^{-1}$. Notice that the initial rise of IN was very rapid and was associated with SSw exceeding 0%. IN concentration increased by approximately three orders of magnitude as the temperature dropped 2°C and SSw rose to 4%. For these exploratory experiments, temperature and SSw were changed together, so these data do not clearly separate the two effects on ice formation. The ICC data indicate that at most a factor of about 2 increase in ice formation should have been expected based on temperature change alone.

The fraction of AgI aerosols that are active as ice nuclei in the CFD can be calculated by combining the IN and CN measurements. That is, the fraction active is the concentration of IN divided by the total particle concentration (CN) at each point in time. This fraction is shown in Figure 11. It is seen that more particles were activated during transit through the CFD at higher SSw, reaching maximum values of about 0.4 at 7% water supersaturation at about -16°C . IN fraction did not increase for higher supersaturations, implying that total activation was achieved for this temperature. Although this aerosol was not tested at -16°C in the ICC, the 40% activation value is about the expected aerosol fraction which can activate under any conditions at -16°C .

The CFD results for AgICl-0.125NaCl aerosols are better understood by considering ice

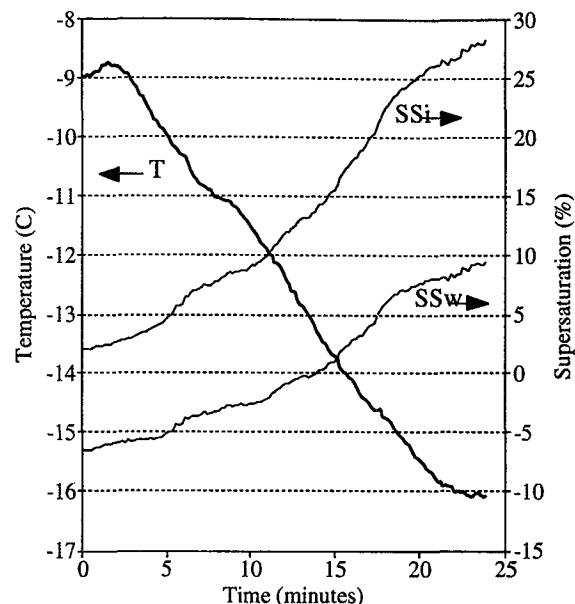


Figure 9. History of temperature, SSw, and SSi at the location of the AgI aerosol in the CFD.

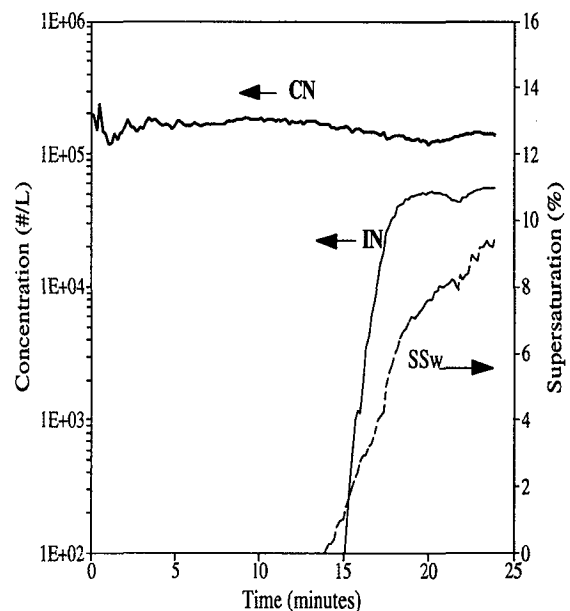


Figure 10. History of particle concentrations and water supersaturation in CFD experiment. Note that IN and SSw traces are in phase.

formation mechanisms. Since residence times are very short and droplet concentrations too small for contact-freezing to occur in the CFD; the primary

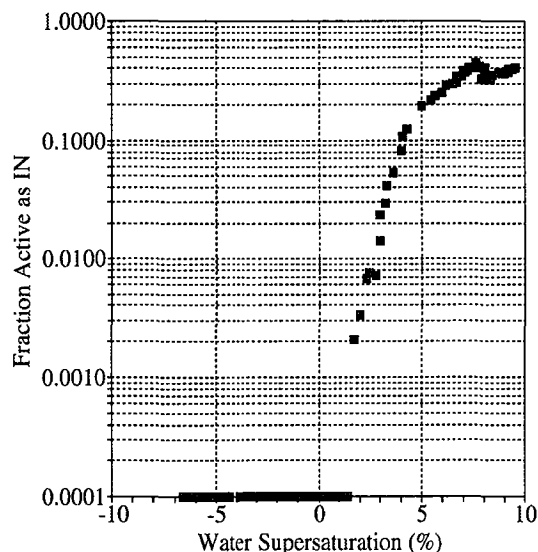


Figure 11. Fraction of aerosols active as ice nuclei versus water supersaturation. Temperature decreased from -13.6°C to -16.2°C as SSW rose from 0 to 9%. Fractions of 0 are plotted at 0.001.

mechanisms analyzed for are condensation-freezing, sorption and deposition. Since the CFD found very little activity at SSW $<0\%$, we conclude that condensation-freezing was the primary ice formation mode measured in the CFD. The results observed are then reasonably consistent with isothermal cloud chamber results and with considerations based on the CCN characteristics of the aerosols tested. The ICC tests suggested that a condensation-freezing process predominated. The rate constant for this process measured at -12°C in the ICC was 0.00167 s^{-1} . This implies that the fraction of total aerosol number capable of forming ice in the CFD at near water saturation should have been $0.4(1-\exp(-0.00167(5)))$ or 0.003. Here we have used 0.4 as the maximum aerosol fraction active at -16°C and a transit time through the CFD of 5 s. The expected fractional activation did not occur until SSW reached 2% in the CFD test. Nevertheless, considering that both temperature and supersaturation were changing fairly rapidly at the time of the measurement, the agreement is not bad. As SSW rose further, the ice formation rate by condensation-freezing increased until the activation was complete within the CFD transit time. That a fairly high supersaturation was required for this to occur is consistent with the high SSW required for these aerosols to act as CCN. Thus, the rate of ice formation by condensation freezing is related to the ease of formation of dilute solution droplets. This is

in agreement with the observations of Feng and Finnegan (1989) that AgI-Cl-NaCl aerosols with higher molar ratios of NaCl showed faster rates of ice crystal formation by condensation-freezing. DeMott (1990) found that AgI-4NaCl aerosols act extremely efficiently as CCN.

Further quantitative insight into the rates and yield of ice formation as a function of both humidity and temperature could be obtained in the future by operating the CFD in a different manner than was done for this exploratory study. In particular, by varying residence time within the CFD at one temperature by changing flow rate and/or chamber length, both the rate constant and yield of ice formation could be estimated.

4. SUMMARY AND CONCLUSIONS

Yield values in the CSU isothermal cloud chamber were obtained for aerosols produced from combusting 2 and 3 weight % AgI solutions using the MSU Skyfire generator. The yields for aerosols from the 2% AgI solutions were not substantially different than for 3% AgI solutions, indicating that no added benefit exists for using 3% AgI solutions in warmer supercooled cloud conditions. Comparison of 3% AgI solution aerosols in the current tests with those tested in the MSU generator in 1972 gave excellent agreement. Ventilation of the generator at higher wind speeds increased the generator yield across the temperature spectrum tested by a factor of 2 to 10 times. This is an unusual result for most generators at the warmest temperatures since the typical effect of ventilation is more rapid quenching of the burn and production of smaller particle sizes which usually are less efficient at warmer temperatures. This may merit further investigation.

Yield values obtained using the NAWC generator indicated greatly enhanced ice formation activity warmer than -10°C for AgI-NH₄I-acetone-water solutions (2% AgI) compared to earlier tests in 1978 and 1981. Apparently, some changes to generator combustion design have been made. As a consequence, a chemical change to the solution to produce very efficient AgI_{0.78}Cl_{0.22}-0.125NaCl composite nuclei, produced only a slight enhancement in yield at the warmest temperature tested (-6°C). Nevertheless, these aerosols do appear to offer the potential for enhanced yield at even warmer temperatures. This would have to be verified by further testing. Ventilation of the NAWC generator at higher wind speeds was found to increase

yield by about 10 times at -20°C , but decrease the yield by 10 times at -6°C . This was consistent with results obtained in previous calibrations and is believed to reflect the dependence of activation on particle size (smaller during ventilation).

Examination of ice formation rates in the isothermal cloud chamber indicated that the 2% AgI aerosols produced by both the MSU and NAWC generators functioned by contact-freezing at temperatures warmer than -16°C in the ICC. Previous tests of the 3% AgI MSU generator aerosols for higher LWC and higher droplet concentrations in the ICC indicated faster ice formation rates in proportion to droplet concentration, quantitatively supporting this conclusion. Ice formation rates were faster at temperatures below -16°C . The ice formation mechanisms in this temperature regime could not be discerned.

Use of the solution containing ammonium iodide and paradichlorobenzene in the NAWC generator did not force a rapid condensation-freezing nucleation process at water saturation in the ICC. Nevertheless, evidence does indicate that a slower condensation-freezing process did occur. This ice formation process could provide substantial advantages in natural clouds over aerosols which realize their greatest activity as contact-freezing nuclei. This is because the ice formation rates by contact-freezing are dependent on the droplet concentration at water saturation, while the ice formation rates by condensation-freezing are not. Consider, for example, a natural orographic cloud with 100 droplets cm^{-3} of similar sizes to those in the ICC tests. In this case, the contact-freezing rate constants expected in the natural cloud for MSU and NAWC natural draft AgI aerosols are obtained by multiplying the k_{act} values in Table 3 ($\sim 0.08 \text{ min}^{-1}$ at $T \geq -16^{\circ}\text{C}$) by the ratio of in the ICC versus natural droplet concentrations ($100 \text{ cm}^{-3}/2100 \text{ cm}^{-3}$). For a 20 minute transit time at a constant temperature through the natural cloud, this implies that only about 7% of the potential yield (Tables 1 and 2) would be realized. For NAWC AgICI-0.125NaCl aerosols, the rate constant would be 0.1 min^{-1} regardless of droplet concentrations. Thus, in 20 minutes transit at one temperature, 86% of the potential yield (Table 2) would occur. An order of magnitude difference in ice crystal formation is inferred to be possible by switching aerosols from AgI to AgICI-0.125NaCl. Future studies of these and other aerosols tested for this paper would benefit from analysis of dependence of ice formation rate on varied cloud droplet

concentrations and humidities, in order to validate mechanisms.

The measurements made with two NCAR counters coordinated to sample the same aerosols used in ICC tests indicated that the NCAR counters sampled ice nucleus aerosols at about one-third of the efficiency of the ICC at -20°C after dilution airflow corrections are applied to the ICC data. In comparison to raw ICC results, such as are commonly reported from the CSU laboratory, the NCAR counters detected closer to two-thirds of the ice nuclei. There appeared to be differences in this counting efficiency factor as a function of the aerosol tested, but not enough data were collected to confirm this. Nevertheless, the counting efficiency noted is a factor of about ten higher than measured for two other NCAR counters sampling different AgI aerosols by Sackiw et al. (1984). This could be related to differences in the operating characteristics of the units tested in the earlier experiments compared to the units used in the present study. It could also relate to basic differences in the counter response to the different aerosols tested in the two studies. Although the ice formation mechanism operating within the NCAR counters is unknown for the aerosols tested, the amount of ice crystals formed compared to the ICC are reasonable if one assumes that a contact-freezing process dominated, but was limited by the shorter residence time within the counters compared to the cloud chamber.

The results of the ICC/NCAR counter cross-calibration should be extremely useful for quantifying the NCAR data in field experiment studies of cloud seeding using the aerosols tested. The excellent consistency noted between the two units tested was another positive result in this regard. We recommend cross-calibrations of the type performed here for NCAR counters before use in field operations.

The CFD experiments on AgICI-0.125NaCl aerosols from the NAWC generator yielded several interesting results which demonstrate the utility of this technique alone or in concert with other measurements of ice nuclei. The results, which by their nature did not permit contact-freezing nucleation to be observed to any degree, indicated that these aerosols required greater than 4% water supersaturation to achieve 10% instantaneous activation by condensation-freezing at -16°C . These conditions are probably met on some occasions during field generation due to the moisture released during combustion (Finnegan and Pitter, 1988). Combined with the ICC results, the CFD results also

give vital information permitting calculations of ice formation rates in real clouds. This will be the subject of future analyses and experimentation. The CFD results also show that it will be readily possible to easily and quantitatively describe differences in chemically different (e.g., more hygroscopic or more hydrophobic) ice nuclei in future experiments. Concerning the practical matter of using such an instrument simply for tracking the transport of manmade ice nuclei by aircraft, the results imply that the device should be operated at a high supersaturation to facilitate efficient detection.

Acknowledgments: The research discussed in this paper was primarily supported by the NOAA Atmospheric Modification Program in cooperation with the Utah Division of Water Resources. The NCAR counters and MSU AgI generator were supplied by the Bureau of Reclamation. CFD studies were made possible through support from NSF Grant ATM-9311606.

5. REFERENCES

- DeMott, P.J., W.G. Finnegan and L.O. Grant, 1983: An application of chemical kinetic theory and methodology to characterize the ice nucleating properties of aerosols used in weather modification. *J. Clim. Appl. Meteor.*, **22**, 1190-1203.
- DeMott, P.J., 1990: Quantifying ice nucleation by silver iodide aerosols. Ph.D. Dissertation. Department of Atmospheric Science, Colorado State University, Fort Collins, CO, 253 pp.
- DeMott, P.J., 1991: Comments on 'The persistence of seeding effects in an orographic cloud seeded with silver iodide burned in acetone.' *J. Appl. Meteor.*, **30**, 1376-1380.
- DeMott, P.J., 1995: Quantitative descriptions of ice formation mechanisms of silver iodide-type aerosols. *Atmospheric Research* [in Press].
- Feng, D., and W.G. Finnegan, 1989: An efficient, fast-functioning nucleating agent -- AgI-AgCl-4NaCl. *J. Wea. Mod.*, **21**, 41-45.
- Finnegan, W.G., and R.L. Pitter, 1988: Rapid ice nucleation by acetone-silver iodide generator aerosols. *J. Wea. Mod.*, **20**, 51-53.
- Finnegan, W.G., A.B. Long and R.L. Pitter, 1994: Specific applications of ice nucleus aerosols in weather modification. Preprints, 6th WMO Scientific Conference on Weather Modification, Paestum, Italy, 247-250.
- Garvey, D.M., 1975: Testing of cloud seeding materials at the Cloud Simulation and Aerosol Laboratory, 1971-1973. *J. Appl. Meteor.*, **14**, 883-890.
- Heimbach, J.A., Jr., A.B. Super and J.T. McPartland, 1977: A suggested technique for the analysis of airborne continuous ice nucleus data, *J. Appl. Meteor.*, **16**, 255-261.
- Langer, G., 1973: Evaluation of NCAR ice nucleus counter. Part I: Basic operation. *J. Appl. Meteor.*, **12**, 1000-1011.
- Rogers, D.C., 1988: Development of a continuous flow thermal gradient diffusion chamber for ice nucleation studies. *Atmospheric Research*, **22**, 149-181.
- Rogers, D.C., 1994: Detecting ice nuclei with a continuous-flow diffusion chamber - some exploratory tests of instrument response. *J. Atmos. Oceanic Tech.*, **11**, 1042-1047.
- Sackiw, C.M., F.E. Robaitaille, J.W. Mason, F.D. Barlow, W.G. Finnegan, R.D. Horn and J.A. Heimbach, Jr., 1984: Comparison tests of NCAR ice nucleus counters. Ext. Abstracts of 9th Conf. on Weather Modification, 21-23 May, Park City, UT, Amer. Met. Soc., 12-13.
- Super A.B., and E.W. Holroyd, 1994: Estimation of effective AgI nuclei by two methods compared with measured ice particle concentrations in seeded orographic cloud. *J. Wea. Mod.*, **26**, 33-40.

ON THE CONSUMPTION OF AgI SEEDING AGENT: DEPENDENCE ON THE LIQUID WATER CONTENT IN THE SEEDING ZONE

Mladjen Ćurić and Dejan Janc

Institute of Meteorology, University of Belgrade, Belgrade, Serbia, Yugoslavia

Abstract. A one-dimensional kinematic model of Lagrangian type is applied to investigate some hail suppression efficiency parameters dependence on the liquid water mixing ratio in the seeding zone. The silver iodide seeding agents are injected at the bottom of the seeding zone (a level of -8°C). Their interaction with cloud is simulated by a microphysical model. It calculates the maximum seeding agent mixing ratio at the bottom of the seeding zone needed to produce the critical number concentration of graupel at its top. This ratio is expressed through the number of hail rockets fired (N). The value of N strongly depends on the type of agent especially for lower values of liquid water mixing ratio.

1. INTRODUCTION

Extensive field measurements and numerical modeling efforts have been made during the last three decades to examine the physical and dynamic processes taking place in hailstorms and also to develop the reliable hail suppression technology. One of the concepts for reducing the sizes and concentrations of hailstones falling from convective storms is beneficial competition (Sulakvelidze, 1967). Many hail suppression projects all over the world have been organized (Federer, 1977; Miller and Fuchs, 1987). One of them is the operational hail suppression project based on the beneficial competition concept which has been in operation in Serbia twenty-seven years, where the hail suppression system covers about $40,000\text{ km}^2$ of agricultural surface. This is one of the largest areas in the world protected by such a system (Ćurić, 1990; Radinović, 1972). Now, it will be expanded by an additional $20,000\text{ km}^2$ in the agricultural area of Vojvodina. The hail suppression technology used is that of injecting the silver iodide by rockets into the zone between isotherm levels of -8°C and -12°C , when the radar reflectivity is greater than 25 dBz .

Measuring technology has increased the amount and quality of data available from hail suppression programs. Nevertheless, improvement of the measurements to the required degree is likely to be slow because of the technical difficulty of obtaining data which are at once comprehensive, accurate, representative and without temporal and spatial limitations. Numerical modeling offers the opportunity to supplement the measurements. It may be possible to obtain useful insight into the cloud seeding zone by studying it through numerical

modeling (Ćurić and Janc, 1990; 1993; Farley *et al.*, 1994 a,b).

The choice of seeding material and its efficiency when it is injected into the cloud has not been subjected to rigorous examination until now, largely due to the lack of quantitative knowledge of the dynamical and microphysical characteristics of the atmosphere in the seeding zone. This paper will attempt to examine the dependence of seeding agent's residence time in the seeding zone and the final graupel production at its top upon the liquid water mixing ratio inside it. A 1-D kinematic model will be used to access the utility of seeding material used.

2. MODEL DESCRIPTION

A 1-D kinematic model of Lagrangian type (Ćurić and Janc, 1993) is applied to investigate the seeding agent's residence time and the final graupel production in the seeding zone. It is assumed that the vertical velocity depends on the graupel production resulting from seeding.

The number concentration of the produced graupel is calculated by microphysical model described by Ćurić and Janc (1990, 1993). The microphysical scheme of the model is shown in Ćurić and Janc (1990). The seeding agent may produce cloud ice by several mechanisms. Among them, the contact and deposition nucleation mechanisms are the most important.

The main assumptions for the model parameters inside the seeding zone are as follows. The lapse rate of temperature is taken to be

7 K km^{-1} . The mean climatological value at the base of the seeding zone is 570 hPa. The depth of the seeding zone in all calculations is 571 m. The liquid water content is assumed to be fixed; we use the liquid water mixing ratio of 3, 4 and $5 \times 10^{-3} \text{ kg kg}^{-1}$ in our calculations. The Khragian-Mazin size distribution for the all drop spectrum is assumed. The mean droplet radius takes the value of $60 \text{ }\mu\text{m}$. The value of the reference vertical velocity is taken to be fixed (in our case 20 ms^{-1}). The entrainment rate, μ , is given the fixed value of 10^{-3} s^{-1} .

In the operative Hail Suppression Project in Serbia, four principal types of agents are applied (TG-10, TG-5, SAKO-6 and PP-6). Their maximum values of the seeding agent mixing ratio and particle masses are presented in Ćurić and Janc (1993). They are based on the results of Hsie *et al.* (1980). The modal radius of the seeding agent size distribution is supposed to be $R_g = 0.03 \text{ }\mu\text{m}$.

The continuity equation for the silver iodide mixing ratio is the same as in Ćurić and Janc (1993), except that the immersion freezing term is omitted. So, the main sink terms are caused by the turbulent diffusion process (described over the entrainment rate) as well as the Brownian and inertial collection rates due to cloud droplets and raindrops, phoretic processes, and deposition nucleation. The analyzed mixing ratio is related to the maximum seeding agent mixing ratio.

3. MODEL RESULTS

In order to investigate the effectivity of each particular seeding agent in producing graupel, the final graupel production (N_{gf}) as a function of the liquid water mixing ratio is presented in Fig. 1. This production is a result of the aerosols released per m^3 from one rocket fired at the bottom of the seeding zone. It is clearly shown that the PP-6 and the SAKO-6 aerosols are much more effective in producing graupel compared to the TG-10 and TG-5 aerosols. Also, the slopes of curves for PP-6 and SAKO-6 are larger than for the other two agents. For the TG-10 agent this production is practically independent of liquid water mixing ratio.

The time evolution of different microphysical mechanisms responsible for final graupel production is shown in Fig. 2 for a liquid water mixing ratio of $3 \times 10^{-3} \text{ kg kg}^{-1}$.

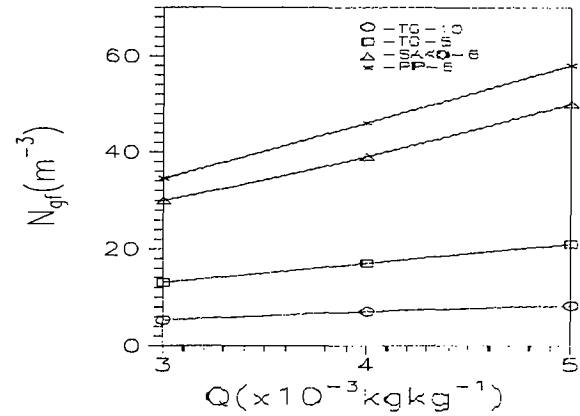


Fig. 1: The final graupel production, $N_{gf} (\text{m}^{-3})$, as a function of the liquid water mixing ratio, $Q (\times 10^{-3} \text{ kg kg}^{-1})$, for four types of the seeding agents.

The rates of change in number concentration of cloud ice or graupel particles are designated by J_x . The subscript x takes values: bc, ic, br and ir for the Brownian and inertial collection rates due to the cloud droplets and raindrops, while rcn and rd are related to accretion rates caused by collecting the cloud ice generated by contact and deposition nucleation mechanisms, respectively, by raindrops.

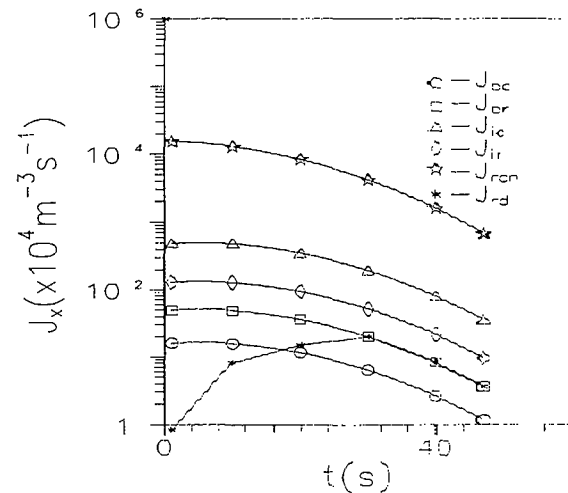


Fig. 2: The rate of change in number concentration, $J_x (\times 10^4 \text{ m}^{-3} \text{ s}^{-1})$, caused by: Brownian and inertial collection rates due to cloud droplets and raindrops ($J_{bc}, J_{ic}, J_{br}, J_{ir}$), accretion rates between cloud ice formed by contact or deposition nucleation and raindrops (J_{rcn}, J_{rd}), as a function of time for the PP-6 aerosol and $Q = 3 \times 10^{-3} \text{ kg kg}^{-1}$.

All mechanisms except J_{rd} decrease with time. The greatest values are for contact nucleation (J_{ren}). The mechanisms analyzed provide higher values for a fixed time as the liquid water content increases.

The values of terms J_x at any time depend on the number concentration of droplets and raindrops. In order to illustrate the dependence of values of J_x on the liquid water mixing ratio (Q), the initial cloud droplet, $N_c(m^{-3})$, and raindrop, $N_r(m^{-3})$, number concentrations as functions of Q are shown in Table 1. It can be seen that both N_c and N_r increase with liquid water content.

Table 1. The initial cloud droplet, $N_c(m^{-3})$, and raindrop, $N_r(m^{-3})$, number concentrations, as functions of the liquid water mixing ratio, $Q(x10^{-3} kg kg^{-1})$, for $R_M = 60 \mu m$.

	$Q(x10^{-3} kg kg^{-1})$		
	3	4	5
$N_c(m^{-3})$	5×10^5	7×10^5	8×10^5
$N_r(m^{-3})$	6×10^5	8×10^5	10^6

The aerosol residence time (t_R) as a function of the liquid water mixing ratio for four seeding agents used is shown in Table 2. It may be observed that values of the residence time for $Q = 3 \times 10^{-3} kg kg^{-1}$ differ more significantly than those for $Q = 5 \times 10^{-3} kg kg^{-1}$. The residence time as well as the final graupel production are the greatest for PP-6.

Table 2. The agent residence time $t_R(s)$, as a function of the liquid water mixing ratio, $Q(x10^{-3} kg kg^{-1})$, for four agents used under condition when $w = 20 ms^{-1}$, $\mu = 10^{-3} s^{-1}$, and $R_M = 60 \mu m$.

	$Q(x10^{-3} kg kg^{-1})$		
	3	4	5
	$t_R(s)$	$t_R(s)$	$t_R(s)$
TG-10	110	103	102
TG-5	96	124	89
SAKO-6	94	80	115
PP-6	122	97	161

The primary parameter in an operational hail suppression project is the maximum seeding agent mixing ratio at the bottom of the seeding zone needed to generate the critical number concentration of graupel ($100 m^{-3}$) at its top (Srivastava, 1967). It can be expressed through the number of hail rockets fired (N).

The relationship between the number of rockets (N) and liquid water mixing ratio (Q) is illustrated in Fig. 3. It is seen in this figure that rockets with PP-6 and SAKO-6 chemical formulations follow the same trend. N is nearly independent of Q for the aerosols produced by these two types of rocket compositions. For the other two agents this interdependence is stronger, especially for TG-10. The number of rockets N is always greater for TG-10 in comparison to those for PP-6 and SAKO-6, especially for smaller values of Q .

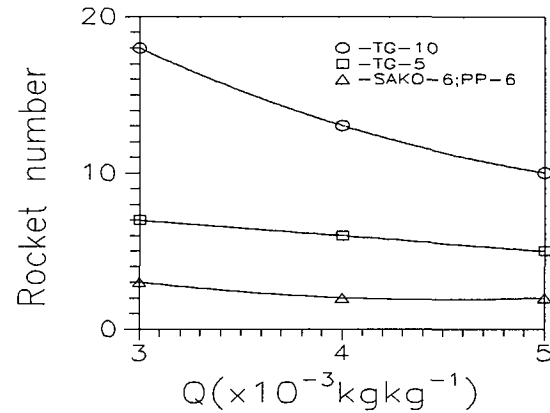


Fig. 3: The number of rockets required for four agent types as a function of the liquid water mixing ratio (Q).

By comparing the differences in N for each four aerosols it is obvious that the number of rockets fired in order to produce the critical number concentration of graupel strongly depends on the type of seeding materials which they contained. For lower values of liquid water mixing ratio, this difference becomes a factor of six. Because the price of one rocket is practically independent of the seeding agent, the cost of hail suppression can be significantly reduced by using the most efficient graupel producing seeding agent, especially for lower liquid water mixing ratios in the seeding zone.

4. CONCLUSIONS

Results presented in this paper show that the seeding agent residence time in the seeding zone, the final graupel production at the top of the seeding zone, and the number of hail rockets fired (N) needed to produce the critical number concentration of graupel strongly depends on the values of the liquid water mixing ratio in the seeding zone, especially for the TG-10 seeding agent.

It has been found that consumption of hail rockets (N) can be six times smaller for lower liquid water mixing ratio clouds if it is a PP-6 or SAKO-6, instead of a TG-10. This means that the cost of hail suppression can be significantly reduced by using the appropriate seeding agent, especially for clouds with lower liquid water mixing ratios.

These types of numerical calculations improve our understanding of hail suppression activity based on the beneficial competition concept.

Acknowledgments. This research is partly supported by the Union of Science of Serbia.

REFERENCES

- Ćurić, M., 1990: One evidence of the hail suppression efficiency derived from radar measurements. *J. Wea. Mod.*, **22**, 79-81.
- Ćurić, M., and D. Janc, 1990: Numerical study of the cloud seeding effects. *Meteorol. Atmos. Phys.*, **42**, 145-164.
- Ćurić, M., and D. Janc, 1993: Dependence of the simulated seeding effects of Cb cloud on the types of the AgI agents. *Meteorol. Atmos. Phys.*, **52**, 91-100.
- Farley, R. D., P. Nguyen, and H. D. Orville, 1994a: Numerical simulation of cloud seeding using a three-dimensional cloud model. *J. Wea. Mod.*, **26**, 113-124.
- Farley, R. D., T. Wu, H. D. Orville, and H. Chen, 1994b: The numerical simulation of hail suppression experiments. *Proc. Sixth WMO Sci. Conf. on Wea. Mod. WMO WMP*, **22**, 161-166.
- Federer, B., 1977: Methods and results of hail suppression in Europe and in the USSR. *Meteor. Monogr.*, **38**, 215-223.
- Hsie, E.-Y., R. D. Farley, and H. D. Orville, 1980: Numerical simulation of ice-phase convective cloud seeding. *J. Appl. Meteor.*, **19**, 950-977.
- Miller, J. R., and M. J. Fuchs, 1987: Results of hail suppression efforts in North Dakota as shown by crop hail insurance data. *J. Wea. Mod.*, **19**, 45-49.
- Radinović, D. J., 1972: *Hail Control*. 124 pp. (NTIS, Springfield, VA 22151).
- Sulakvelidze, G. K., 1967: Showers and hail. [In Russian] Leningrad, Gidrometeoizdat. 412 pp.

OPERATIONAL EFFICIENCY ASSESSMENT OF HAIL SUPPRESSION FOR AGRICULTURE IN GREECE

N. R. Dalezios
Department of Agriculture
University of Thessaly, 38334 Volos, Greece

and

S. I. Spanos
Hellenic Agricultural Insurance Organization
Macedonia Airport, Thessaloniki, Greece

Abstract. The National Hail Suppression Program (NHSP) in Greece has been basically designed as an operational cloud seeding program with a small research component at its initial stages. During the 9-year history of the NHSP, significant experience and knowledge have been gained. The paper aims at assessing the operational efficiency of the NHSP with the objective of possibly improving operations. The paper focuses on topics such as hail forecasting and nowcasting, radar controlling and siting, flight operations, optimum length of the operational period, systems efficiency, available and required resources and infrastructure, seeding hypothesis and launch criteria. Finally, applied research findings and the incorporation of new technological advancements into the NHSP are discussed in an effort to draw conclusions and inferences towards optimum operation and gradual reduction of the overall program's cost.

1. INTRODUCTION

Hail is internationally considered as a severe threat to agriculture. In Greece, on the average about 4.6 billion drachmas (in constant 1991 values) are spent annually for hail insurance payouts. These payouts could be much larger, but the Hellenic Agricultural Insurance Organization's (ELGA) policy does not cover hail damages of the order of less than 20% in crop production

losses, which are the majority of the cases in Greece. The National Hail Suppression Program (NHSP) in Greece was established in 1984 under the auspices of ELGA. The NHSP has been mainly designed as an operational cloud seeding program to reduce hail damage over three distinct agricultural areas, namely two areas: A1 (2,340 km²) and A2 (1,306 km²) in northern Greece and one area A3 (2,400 km²) in central Greece (Fig. 1). The program has been

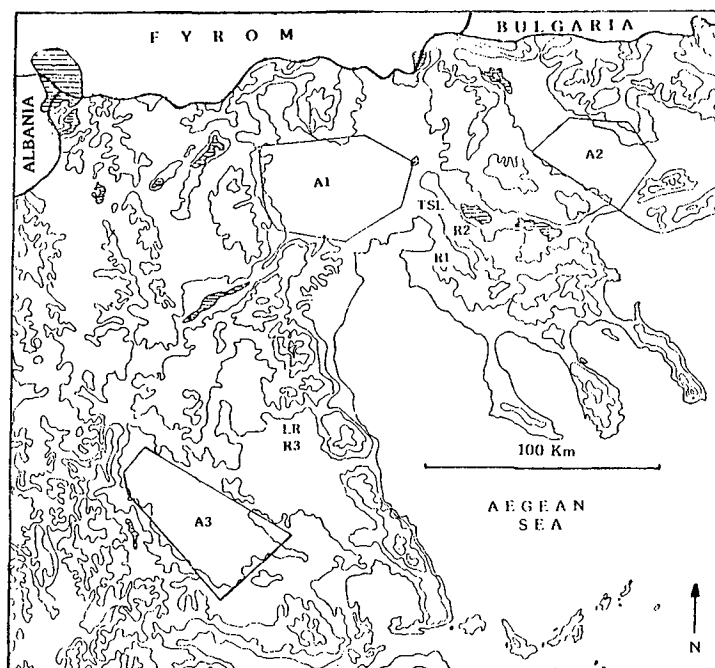


FIGURE 1: Map of the protected areas in the NHSP. Elevation contours are 200, 600, 1200, and 1800 m.

operational continuously until 1993 with the exception of 1991. At the beginning there was a 5-year (1984-88) randomized experiment in one of the areas (A1), but the NHSP has been mainly run as a commercial program. The NHSP is currently at a stage of overall evaluation due to its high operational cost, significance for national agriculture, as well as drastic expected changes in international agriculture.

The objective of this paper consists of assessing the operational efficiency of the NHSP with the goal of possibly improving operations and reducing the program's cost. The assessment is based on the annual reports submitted to ELGA by the contractors (Alberta Ltd., 1990 and 1991; Atmospheric, Inc., 1985; C.I.C-3 Delta-Avionic, 1993 and 1994; Intera Technologies Ltd., 1987, 1988 and 1989). Within this framework the various components of the program are analyzed and the upgrading as well as the current structure of the program is thoroughly examined. Specifically, hail forecasting and nowcasting, radar controlling and monitoring, flight operations, systems efficiency, as well as available resources and infrastructure are examined on the basis of 9-year statistics and experience gained. The problem of the optimum length of the operational period is also addressed as well as the technological advancements and the number of the required aircraft and resources. The paper is organized as follows: Section 2 covers a description of the program including design and operations; Section 3 comprises a presentation of how each component performed during the operations based on the available statistics; and Section 4 consists of a discussion of the impact of each component to each other and to the program's efficiency.

2. DESCRIPTION OF THE NHSP

2.1 Design

The adopted seeding hypothesis is based on the conceptual model of the beneficial competition theory (Foote and Knight, 1977). Limited observations in convective clouds in northern Greece support the ice phase or graupel embryo precipitation process and are consistent with the beneficial competition theory (Krauss and Papamanolis, 1989). These observations include the presence of conical graupel embryos, average summertime cloud base temperatures near 10°C

and a continental drop size distribution (Krauss and Papamanolis, 1989). Furthermore clouds with tops warmer than -10°C have not been observed to produce precipitation.

Seeding operations were carried out in three agricultural areas (Fig. 1) ranked among the first in the list of annual hail damage insurance payouts. Based on payout statistics for the decade 1970-1980, area A1 covers on the average 15%; area A2, 4%; and area A3, 12% of the annual hail damage payouts, respectively. The three protected areas are orographically similar, since they are mostly surrounded by complex mountain terrain (Fig. 1). This characteristic has a major effect on storm forecast, radar monitoring, and seeding techniques. Five aircraft were employed in the seeding operations lasting from mid-April till the end of September every year.

Seeding was conducted either at cloud base or at cloud top when the following two criteria were met: a cell existed over area A1 or it was within 20 minutes of entering the area; and the cell was exhibiting a radar reflectivity factor of >35 dBz at an altitude between -5°C and -30°C in the cloud. In practice, seeding was begun on storms when the leading edge of the 35 dBz contour first entered the buffer zone, which was defined as a 20 minute upwind boundary (Karacostas, 1984). Frequently, storms reached seeding criteria within the area and were seeded as soon as possible thereafter. Cloud top seeding was conducted within the layer between -8°C and -15°C by penetrating the upshear sides of the tops of the daughter clouds of multicell storms, whereas in single-cells the penetrations were conducted at the upshear edges. The nominal seeding rate for penetrations near -10°C was one to two 20-gr AgI droppable flares every five seconds resulting in a seeding rate of 240 gr/min. Weak to moderate updrafts of 10 m/s were assumed. In practice, these rates were adjusted either upwards or downwards by up to a factor of two depending on conditions.

Cloud base seeding was conducted by seeder aircraft flying at the upshear side of multicell storms within the secondary flow area or within the main inflow area of a single-cell storm. Seeding at cloud base was conducted by burning one or two 150-gr wing flares over a four-minute period, or by burning one or two 75-gr wing flares over a two-minute period. Both

methods have resulted in a seeding rate of 40 to 80 gr/min. Side-skim seeding was used when there were no clearly defined feeder turrets. Seeding was conducted by the seeding aircraft making cloud penetration on the upshear side of the storm edge between -5° and -10°C , while burning a wing flare and dropping pencil flares when updrafts were encountered.

Besides operations, a research component was also designed to study the dynamic and microphysical characteristics of the potential hail producing clouds and to permit credible scientific evaluation of the effects of cloud seeding. The research part included a 5-year (1984-1988) statistical evaluation experiment with exploratory and confirmatory stages in area A1 using a cross-over randomization scheme (Karacostas, 1984 and 1989). Area A1 was divided in two sub-areas (north and south), namely the target and control areas, which were randomized and not the experimental unit. The experimental unit was determined to be any declared hail day when the above mentioned seeding criteria were met. Certain procedures were followed during the experiment concerning the designation of target and control areas. When radar reflectivities first reached seeding criteria, one half of area A1 was randomly designated as target and the other half as control. Seeding was conducted in the target only. Data from a hailpad network (Dalezios *et al.*, 1991) were collected after each operational day. Additional sources of data have included surface reports and soundings, synoptic information from weather maps, manually tabulated radar readings and airborne collected micro-physical data from one properly instrumented aircraft.

Since the NHSP was initially designed and run as an operational program, the evaluation experiment included a limited number of response variables out of which only a few were processed due to lack of the appropriate infrastructure and lack of advanced technology into the NHSP. The first three years of the NHSP (1984-86) were designated as an exploratory phase wherein various hailpad parameters were identified and examined with respect to their ability to detect differences between target and control hailpad data (Table 1). The specification and bases for selection of the evaluation parameters and statistical testing methodology have been described in Rudolph *et al.* (1987).

Based on the data analysis in the exploratory phase, one response variable was selected as primary estimator, namely total hail impact energy, which is defined as the total stone kinetic energy normalized by the number of exposed pads. It is known that this variable is sensitive to hailstone size (diameter to the fourth power) and that it is relatively insensitive to uncertainties in hailpad threshold response. The following two years (1987-88) comprised the confirmatory phase during which the selected hailpad parameter in the exploratory phase was further examined to determine the success of the NHSP from a statistical standpoint. The results of the statistical evaluation of the five year program are summarized in Table 1, where several response variables are presented, along with the selected primary response variable.

Based on the results of this statistical analysis the appropriate modifications in the program were implemented in the subsequent years. In particular, by 1989 the randomization factor was reduced to one seeding unit for three hail days and by 1990 randomization was abandoned. Hailpad network continued to provide data in the years 1992 to 1993.

2.2 The Operational Component

Cloud seeding operations for hail suppression require a forecast of hail/no hail for the protected areas and, if possible, a prediction of the maximum hail size. The primary role of convective forecasting for seeding operations is to assess the operational readiness and efficiency and to set launch criteria for aircraft and the appropriate crew status depending upon the likelihood and probable growth rate of storms, as well as the preferred timing for aircraft maintenance.

During 1984 and 1985, an operational period forecast was issued at 0800 UTC (1100 local time) and a daily status of "GO", "STANDBY", or "NO-GO" was posted. During all "GO" and "STANDBY" situations, a second weather forecast was issued at approximately 1600 UTC (1900 local time). By 1986, the adopted hail forecasting procedure in the NHSP was an objective prediction pattern, in the form of a multiple linear regression model, based on modification of a synoptic index of convection (Strong and Wilson, 1983). This procedure was further

TABLE 1: List of Hailpad Evaluation Parameters with Estimated Treatment Effect ($A_T/A_C - 1$) % and Wilcoxon Signed-Rank, Two-Tailed P-Values.

Year Parameter	1984	1985	1986	1987	1988	84-88
Number of Pads Hit	-12 .834	-40 .281	-74 .208	-11 .715	+04 .379	-19 .392
Total Number of Stones	-44 .208	-68 .178	-92 .094	-45 .361	-39 .551	-52 .006
Median Diameter	-71 .059	+25 .590	-68 .094	-39 .361	+20 .650	-24 .109
Maximum Diameter	-74 .059	-08 .787	-64 .173	-36 .584	+09 .733	-34 .046
Total Volume	-66 .208	-80 .178	-96 .059	-58 .361	-59 .551	-68 .003
Total Impact Energy	-76 .208	-85 .178	-97 .059	-59 .361	-66 .551	-74 .003

improved in 1989 (Riley, 1991). Model input consisted of various meteorological parameters from Thessaloniki soundings. Among others were the 24-hour height and temperature change at 500 hPa, the relative humidity change at 700 hPa, stability indices and other thermodynamic parameters (Riley, 1991). The model was not designed as a forecaster's substitute, but as a valuable aid to accurate forecasting. The predictant was the Convective Day Category (CDC). The CDC for a day was defined as the maximum degree of convective intensity for a region in a number of discrete classes (Table 2). Several indices of atmospheric instability were also incorporated in the forecasting methodologies and were used complementarily to the CDC with satisfactory results (Dalezios and Papamanolis, 1991).

Weather surveillance for the project areas was provided by three radars. Two were S-band, and the third was a C-band. The two S-band radars were tower-mounted at the Thessaloniki (TS) and Larisa (LR) airports and covered areas A1 and A3, respectively (Fig. 1). The C-band radar, which was provided by the contractor, was truck-mounted and located near Nigrita in area A2 during 1984 and 1985 seasons and at Filiron (FL), approximately 20 km north of Thessaloniki, thereafter (Fig. 1). Radar 2 provided an unobstructed view of area A2 and also

acted as a backup for radar 1 (TS). In 1988, a continuous 20-hour radar watch was maintained daily by ELGA meteorologists at radars 2 and 3.

The establishment and maintenance of a reliable communication system became a key factor not only for the response time, but also for conducting effective management and coordination during and in between operations. Three radio channels (FM band) were licensed for operational needs. Each was dedicated to radar communications with seeding aircraft when concurrently flying. Aircraft were launched when storms were in the "launch buffer," i.e., storms could enter the project areas within 80 minutes with tops above 6 km and radar reflectivity of at least 25 dBz, or when thunderstorms were forecast regardless of the actual intensity.

In the 1984 and 1985 operational periods, radar watch was decided during the morning briefing by the coordinator on the basis of the daily issued forecast. Radar operators were gradually involved in radar watch. By 1989, radar operators became radar controllers. Launch decision, however, remained the coordinator's responsibility. The project coordinator was following a regular shift and was also available 24 hours per day when needed. Figure 2 is a flow chart of established daily routine in the NHSP since the 1989 operational season.

TABLE 2: Verification Criteria for Convective Day Categories (CDC).

Category (CDC)	Definition	Verification Criteria
-2	TCU,ACC,CC, Virga possible. No precip.	Visual observation. Possible detectable radar echoes.
-1	CB, Isol. RW. No TSTMS	Radar activity below 35 dBz. Brief radar activity between 35 and 40 dBz do not "Bust" the forecast. Visual observation.
0	Sctd RW, TSTMS. No Hail	Radar activity in the range 35-50 dBz at or above -5 C level. Cloud tops extend to -40 C level. Visual observation.
1	TSTMS, Hail "pea" sized up to -1.3 cm	Confirmed hail observation. Hailpad strikes. Verifiable minor crop damage. Radar reflectivity values exceed 50 dBz at or above -5 C level.
2	TSTMS, Hail "grape" sized 1.3-2.0 cm.	Confirmed hail observation. Hailpad strikes. Verifiable crop damage. Persistent radar activity exceeding 55 dBz at or above -5 C level. Tops reach to the tropopause.
3	TSTMS, Hail "walnut" sized 2.1-3.2 cm.	Confirmed hail observation. Hailpad strikes. Verifiable crop damage. Radar reflectivity exceeds 60 dBz at or above -5 dBz C level. Tops penetrate tropopause.
4	Severe TSTMS "golfball" sized 3.3-5.2 cm.	Confirmed hail observation. Hailpad strikes. Verifiable crop damage. Radar reflectivity exceeds 65 dBz at or above -5 dBz C level. Tops penetrate tropopause 1.5 km.

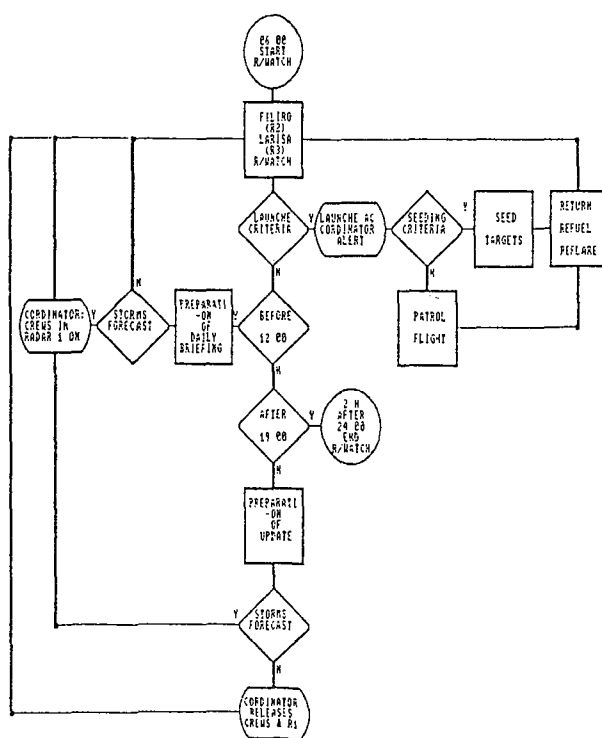


FIGURE 2. Flow chart of daily operations in the NHSP.

Cloud seeding operations in areas A1 and A2 were conducted by three aircraft based at Thessaloniki operational center (airport), whereas area A3 was supported by two aircraft based at Larisa airport. This allocation of aircraft has changed since 1990, where four aircraft were based at Thessaloniki and one at Larisa.

3. EFFICIENCY ASSESSMENT OF THE NHSP

3.1 Hail Forecasting

Hailstorms in the protected areas of the NHSP have been characterized as short-lived, moderate to severe and occur mainly during early afternoon (Foris, 1992a; Karacostas, 1991). Thus, reliable and efficient forecast of hail/no hail or even the maximum hail size is very important and can positively affect hail suppression operations in the NHSP. Convective day category (CDC) and flight levels were issued to the radar operators by radio communications. Figure 3 is a diagram showing the average

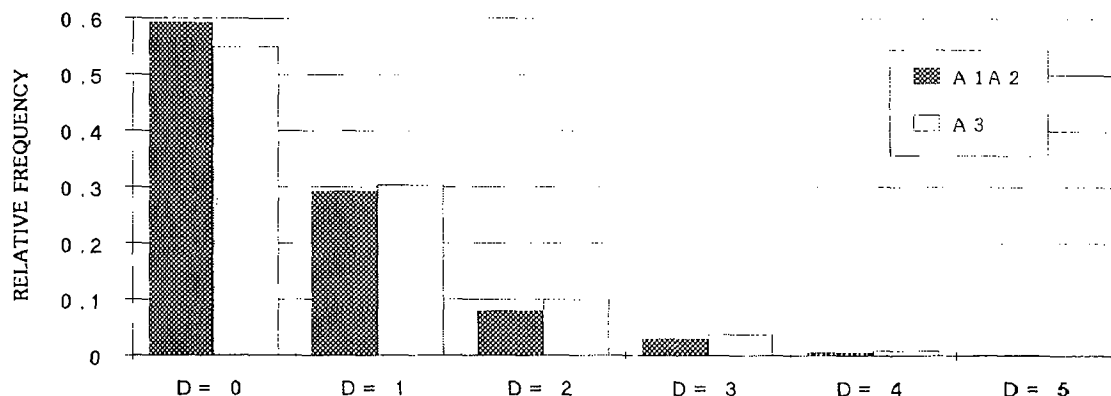


FIGURE 3: *Frequency occurrence of deviation between forecast and observed CDC.*

forecast accuracy in four operational seasons (1988, 1989, 1990, 1992). The forecast that was out by two or more categories (Table 2) was considered as "busts" and never exceeded 20% of the cases (Foris, 1992b). Within this sample (CDC greater or equal to +1) hail was correctly forecasted 70% to 80% of the cases for the three areas.

Update briefings, given at 1600 UTC, were also included in the daily routine by 1986. The need for a detailed update became apparent among the personnel not only in cases of forecast "busts," but also when the duration of convective activity was affecting the staff schedule. The access of forecast office to satellite imagery, which was added by 1990, also contributed towards that direction. Finally, a continuous weather watch was established in the forecast office along with the radar watch.

3.2 Radar Monitoring and Controlling

Only radar 1 has had the data digitized during the 1988 operational season. Radar logs were recorded routinely and showed that most convective cells were observed within the time interval of 1200 to 1800 local time (Karacostas, 1991). After 2000 local time, only 16% of convective cells were observed. Figure 4 illustrates the diurnal variation of total occurrences of convective cells in percent of seasonal values. The examination of reflectivity values within this sample also showed that on active days the weakest activity occurs between 0300 and 1100 local time (Foris, 1992a). Radar 2 was designated as the primary radar watch site for areas A1 and A2, due to the unobstructed view in both areas. During operations the radar 2 controller was responsible only for area A2. Operations in area A1 were conducted from

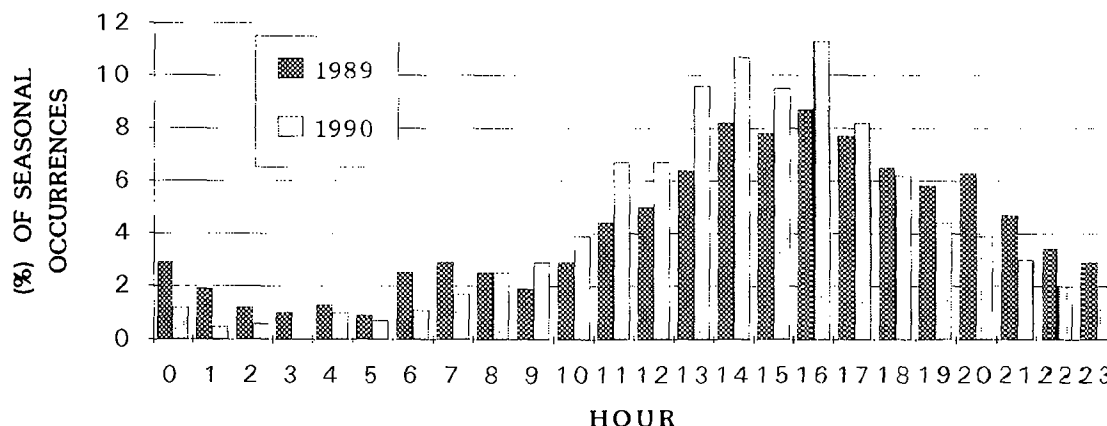


FIGURE 4: *Diurnal variation of convective cell occurrences in (%) of total number of occurrences for two operational seasons (1989, 1990).*

TABLE 3: Number and Hours of Operational Flights (Patrol and Seeding) in Each Month and Year for Areas A1 and A2 (Patrol and Seeding/Seeding).

YEAR	APRIL		MAY		JUNE		JULY		AUGUST		SEPTEMBER	
	FL	HR	FL	HR	FL	HR	FL	HR	FL	HR	FL	HR
1984					21/14	50.2/40.1	4/3	7.1/5.7	44/27	86.3/63.4	13/7	26.2/15
1985			35/20	77.1/49.6	9/2	14.3/5.6	3/0	3.4/0	12/10	25.4/22.2	0/0	0/0
1986	5/2	9.4/4.2	13/4	24.3/10.4	18/11	32.8/22.1	6/4	11.4/8.3	12/7	27.6/17.2	0/0	0/0
1987	5/3	8.3/6.1	14/7	30.3/19.0	9/3	19.7/9.8	25/19	51.1/40.2	25/22	56.2/50.0	11/4	19.3/10
1988	9/4	19.6/10	41/23	88.4/60.0	37/25	81.6/60.8	14/8	33.1/22.1	9/5	18.1/11.4	2/0	3.9/0
1989			12/10	24.6/21.7	39/22	67.9/49.0	23/14	53.4/37.3	10/5	19.6/12.6	9/4	16.1/7.8
1990	5/3	11.5/8.4	21/11	44.2/28.6	16/12	36.2/30.5	20/14	53.9/42.2	12/4	25.9/11.5	3/0	4.7/0
1992					29/22	70.1/56.1	21/16	51.1/42.9	5/2	13.1/5.7	5/4	9.0/7.9
1993	8/6	17.8/14.1	58/44	129.4/119	14/9	31.2/22.5	7/2	14.3/6.4	10/2	16.6/4.6	2/0	4.0/0

radar 1 after being alerted by radar 2. Radar 1 controller was assisting in the forecast preparation when no storms were threatening area A1.

3.3 Flight Operations

The number of flights and flight hours per month during nine years of operations for areas A1 and A2, and area A3 are provided in Tables 3

and 4, respectively, where the numbers in April represent only the operational part of the month. The number of flights and flight hours with two concurrent aircraft and the cases with three concurrent aircraft are also presented in Tables 5 and 6, respectively. It is obvious that the number of cases with three concurrent flights in areas A1 and A2 is considerably low (Table 6). Moreover, in the 9-year operational history only five cases existed with three or more aircrafts concurrently

TABLE 4: Number and Hours of Operational Flights (Patrol and Seeding) in Each Month and Year for Area A3 (Patrol and Seeding/Seeding).

YEAR	APRIL		MAY		JUNE		JULY		AUGUST		SEPTEMBER	
	FL	HR	FL	HR	FL	HR	FL	HR	FL	HR	FL	HR
1984					8/2	12/6.2	0/0	0/0	4/4	6.9/6.9	1/0	2.6/0
1985			11/5	17/11.2	5/3	11.2/7.7	3/1	6.2/3.0	1/0	1.2/0	2/0	3.7/0
1986	2/0	3.8/0	11/4	17.9/9.4	12/5	22.8/11.8	9/4	11.9/6.0	3/1	6.1/1.8	0/0	0/0
1987	6/0	5.9/0	3/0	4.7/0	1/0	1.3/0	8/5	10.9/8.2	6/3	13.5/7.8	3/0	1.5/0
1988	2/1	2.5/1.6	11/7	21.2/14.6	6/3	9.7/5.9	3/2	5.4/4.3	2/0	2.4/0	4/0	3.9/0
1989			1/0	2.3/0	4/2	6.9/4.3	7/2	12.4/4.6	4/2	8.6/4.8	5/3	7.9/6.1
1990	0/0	0/0	2/1	4.9/3.5	1/1	3.1/3.1	0/0	0/0	0/0	0/0	0/0	0/0
1992					8/6	18.8/16.0	10/5	21.3/11.3	2/1	3.9/1.3	0/0	0/0
1993	9/6	18.3/13.3	32/26	77.7/67.3	12/10	25.5/24.0	1/1	2.3/2.3	6/2	12.1/5.3	1/0	2.2/0

TABLE 5: Number of Cases with Two Aircraft Concurrently Flying and the Corresponding Flight Hours for Areas A1 and A2.

YEAR	APRIL		MAY		JUNE		JULY		AUGUST		SEPTEMBER	
	FL	HR	FL	HR	FL	HR	FL	HR	FL	HR	FL	HR
1984					11	19.4	2	3	20	25.3	4	5.5
1985			0		3	3.5	0	0	4	3.2	0	0
1986	1	0.8	2	1.4	4	4.1	6	5.9	7	4.5	3	1.5
1987	0	0	1	0.9	4	3.3	1	0.7	1	1	0	0
1988	1	1.3	20	24.9	14	19.4	5	5.9	0	0	0	0
1989			2	4.9	4	4.1	3	2.7	2	2.9	1	3.2
1990	2	1.6	5	5.3	5	5.4	5	6.1	0	0	0	0
1992					5	3.5	4	4.8	0	0	1	0.9
1993	1	1.3	17	24.7	2	1.1	0	0	0	0	0	0

TABLE 6: Number of Cases with Three Aircraft Concurrently Flying in the 9-year Operational History for Areas A1 and A2.

APRIL	MAY	JUNE	JULY	AUGUST	SEPTEMBER
0	5	2	1	1	0

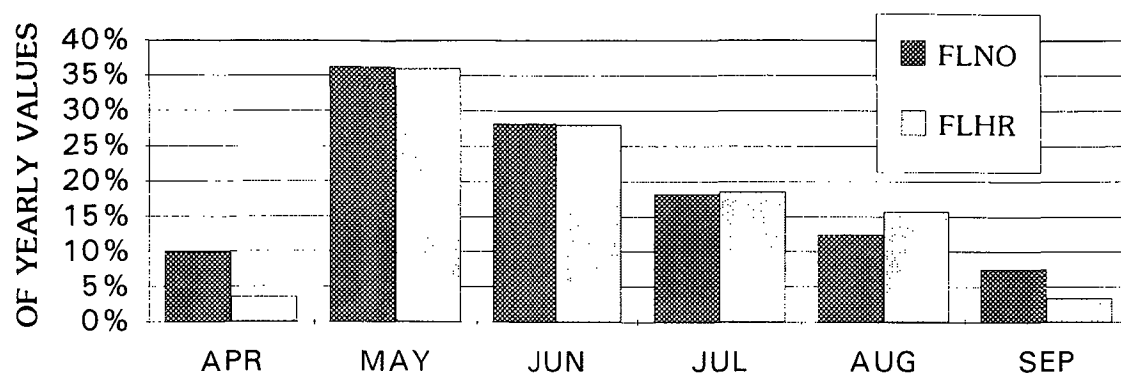
flying during May, which is the most active month. Furthermore, during the months of April and September no cases were reported.

The number of aircraft needed in the operations is further examined. To investigate the actual aircraft needs, the number of two concurrent flights as percentage of total monthly flights for north areas was calculated from Tables 3 and 5. The highest mean ratio of two concurrent flights to total flights occurs in June and it consists of only about 30%.

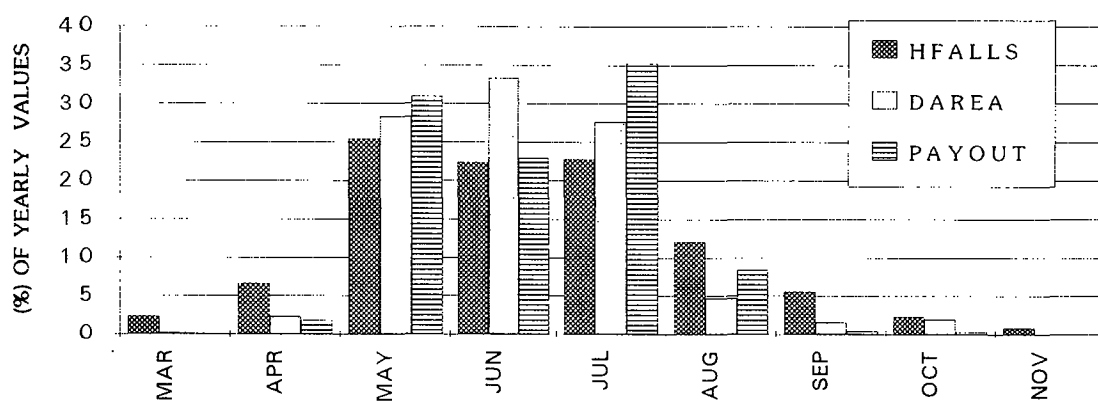
The length of the operational season is investigated in Fig. 5 for areas A1 and A2 and in Fig. 6 for area A3, respectively. Insurance data were obtained from a 13-year (1971-1983) monthly record provided by ELGA. Mean payout values were normalized by annual values to account for inflation. Damaged areas and hail occurrences were similarly normalized. The same approach was also followed in the presentation of flight data. Separate data sets for

flights (1984-1993) and crop insurance data (1971-1983) were used. The independent data periods provided the basis for an objective comparison. If the same data period were selected, the seeding effect would be present in the distribution of hail damages.

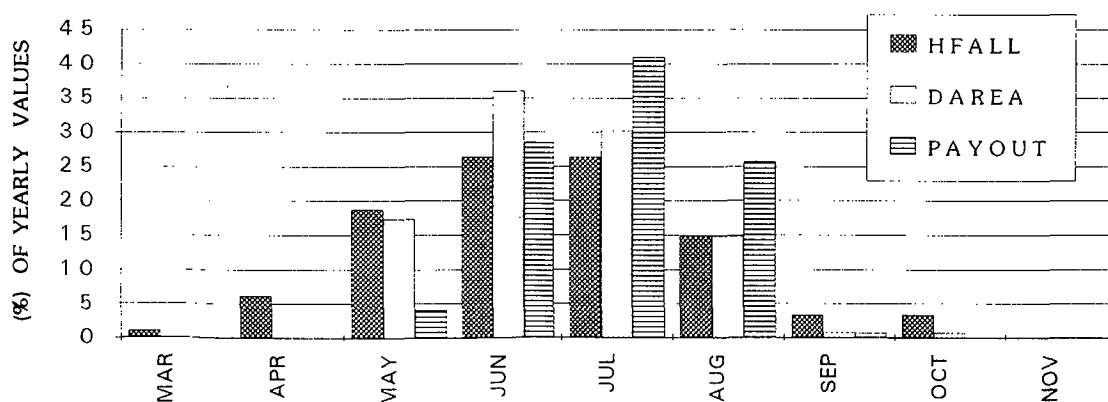
The comparison showed that the percentage of flights and flight hours regularly followed the same pattern with values similar to the percentage of hailfall for all the months. Major differences, however, existed between flight data and payouts, especially for the months of April and September. In areas A1 and A2 during April, while the number of flights and flight hours constituted on the average 7% of the seasonal values, the crop damage payouts were only 2% for area A1 and less than 1% for area A2, respectively (Fig. 6). Similar values were observed in September. The variation of insurance data in the two northern areas showed that hailfall statistics were similar (Figures 5a, 5b). Significant differences existed in the variation of



(a)



(b)



(c)

FIGURE 5: Monthly variation of flight and insurance data for the northern areas A1 and A2: (a) mean flight number (FLNO) and flight hours (FLHR) (%) of yearly values; (b) mean hailfalls, damaged area and payouts (%) of mean yearly values for area A1; (c) as in (b) but for area A2.

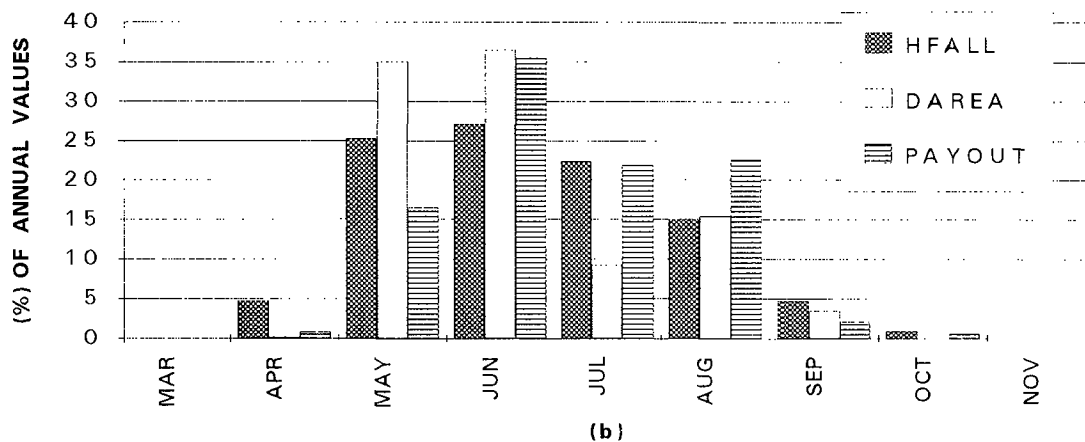
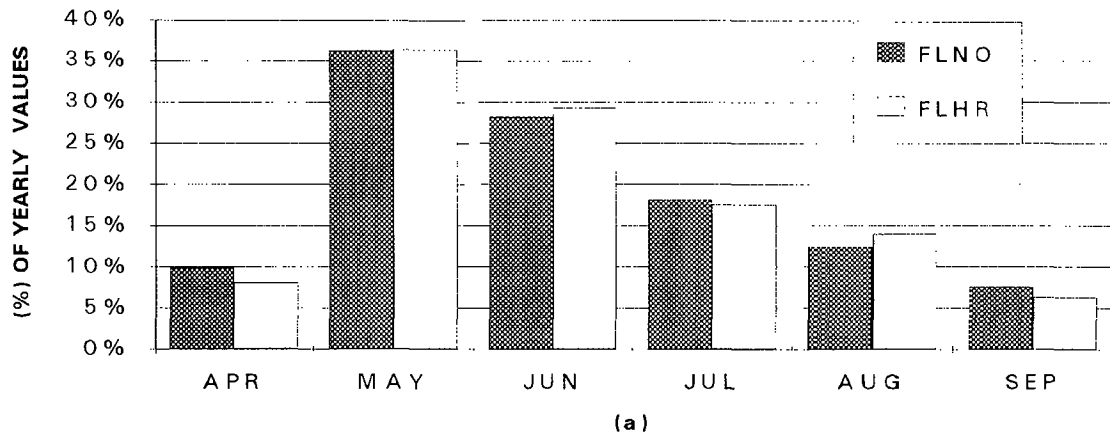


FIGURE 6: Monthly variation of flight and insurance data for area A3: (a) mean flight number (FLNO) and flight hours (FLHR) (%) of annual values; (b) mean hailfalls, damaged area and payouts (%) of mean annual values for area A3.

the areal extent of damages, as well as in the payouts. This can be probably attributed to the different crop types in the two areas. Area 1 is cultivated by fruit trees, while area A2 is dominated by wheat, corn, cotton and barley. Areas A2 and A3 are dominated by the same type of crops. In area A3, while the number of flights and flight hours for April constituted 10% and 8% of the annual values, respectively, the crop damage payouts consisted of only 1% (Fig. 6). Similar values were observed in September.

The observed differences in April and September between flight and payout normalized values are further investigated in Fig. 7. Figure 7 shows the variation of the ratio monthly seeding flights to monthly total operational flights and the same ratio for the flight hours. The ratios

were low in September (10%) and April (30%) in area A3. However, for areas A1 and A2, the problem existed only in September, which showed a ratio of 30%. The increased number of patrol flights was the main reason for the small ratios in April and September.

3.4 Human Resources and Administration

The lack of advanced technologies in the operational part of the NHSP such as radar digitization, aircraft tracking, centralization of services and similar topics had a significant impact on human resources requirements for operations. The annually involved personnel in the NHSP varied in number, ethnic background and degree of education/training. The variation followed changes in project requirements and the

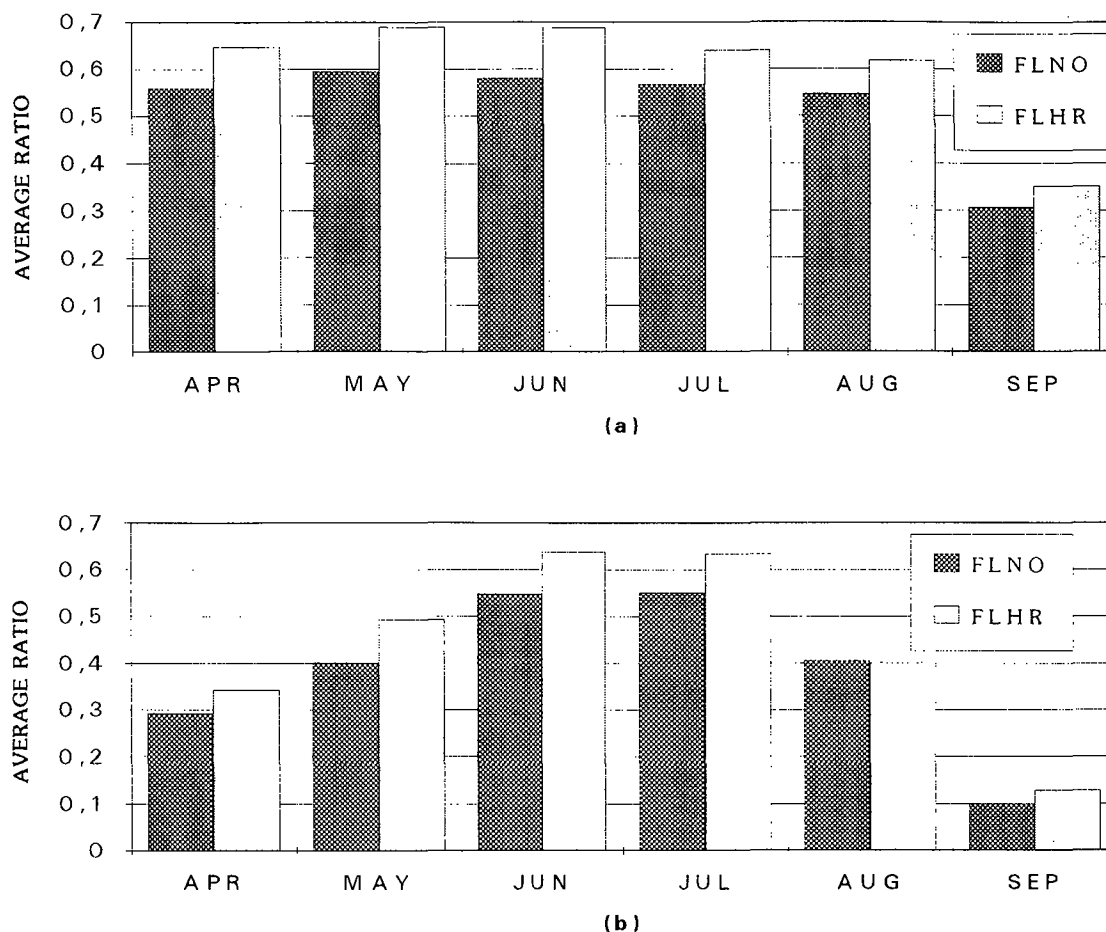


FIGURE 7: Monthly variation of the mean ratios, seeding flights to total flights and seeding flight hours to total flight hours: (a) for northern areas A1 and A2; (b) for area A3.

expansion of the protected areas from 3000 to 6000 km² in 1989, as well as the adopted technology-transfer policy. This is summarized in Table 7. Furthermore, the personnel distribution during 1992-93 seasons is given in Table 8.

A general assessment of program's efficiency from an administrative point of view can be attempted on the basis of the flow chart shown in Fig. 2, where the primary circuit covers actions and decisions concerning the seeding and patrol flights. The other three circuits are supporting the flight operations and cover forecasting and radar controlling and monitoring. The coordinator's involvement in every decision taken must be noticed. The three sources of information available during briefing, which were used by the coordinator in the decisions procedure were: the condition and operational status of the means from the technical point of view, the personnel

schedule, the forecasted weather and the radar information. The 24-hour readiness and availability of the project coordinator had a positive effect on management and administration.

4. DISCUSSION

The seeding effect on hail parameters was investigated by several researchers on the basis of the randomized crossover experiment (Flueck *et al.*, 1986). Studies on crop damage payouts were conducted by comparing target and control values in the same period (Rudolph and Papageorgiou, 1991). The discussion on the operational efficiency of the NHSP that follows also involves various comments on cost assessment. The mean total annual cost in the period 1984-1988 was estimated to be 375 million drachmas (CIC- 3 Delta- Avionic, 1993). At the same time the average annual payouts for the three protected

TABLE 7: Employed Personnel in NHSP.

Year Company	1984-85	1986	1987	1988	1989	1990	1992-93
Contractor	20	26	23	19	22	21	21
ELGA	0	9	16	27	28	31	16

TABLE 8: Personnel Distribution During 1992-93 Seasons.

Specialization Company	Meteorologists	Pilots	Technicians	Secretary
Contractor	4	13	4	0
ELGA	12	3	0	1

areas were 310 million drachmas in constant 1988 values. In current values, the program's annual cost was over 600 million drachmas in 1989-93.

As already mentioned, there are considerable differences in the frequency and variation of convective activity between the northern areas A1 and A2 and area A3. During the warm season there is a transition zone with synoptic disturbances usually affecting only the northern areas. Shallow cold fronts that occur during summer rarely penetrate the mountain chains north of area A3. Moreover, area A3 is more than 60 km away from the sea and surrounded by mountains. The unique landscape probably creates boundary layer conditions significantly different from the north areas. Thus, forecasting convection in area A3 on the basis of Thessaloniki 0900 and 1200 soundings is subject to great uncertainty. The forecast success rates for area A3 were usually lower than for the northern areas (Foris, 1992b). A boundary layer study should be conducted for area A3 to provide guidelines and improve the forecast.

There are always limitations in the forecast accuracy (Fig. 3) that even in the northern areas cannot be exceeded. During the last two operational years of the NHSP a different approach was attempted and steps were taken towards nowcasting. Nowcasting seems to be the appropriate direction, since storms in these three areas appear to be short-lived, fast evolving and intense. The continuous weather watch, digital

radar monitoring, and the access to satellite images could be major contributions. A very important step, however, seems to be the transfer of radar control and images to the Thessaloniki office. The integration of surface meteorological data, digital satellite and radar images into one unit could strengthen the operational efficiency of the program. Nowcasting procedures based on the above requirements should have a direct effect on personnel for hail forecasting, radar controlling and flight operations.

Once a continuous and detailed weather watch is established, radar shifts can be easily reduced by at least 50%. Radar controllers at Filiron and Larisa should not need to cover two 10-hour shifts per day. Continuous radar watch will be held only at the "Nowcasting Center," which in case of an emergency should alert radar controllers to carry out the operations. The operational needs for radar coverage of northern areas should also be reassessed. The Thessaloniki radar can be removed and sited at Filiron or elsewhere in the vicinity. The new radar site should be selected to meet the requirement of unobstructed coverage for both areas (Dalezios *et al.*, 1989). The effectiveness of controlling two or more operating aircraft from the same radar should be considered. Following the last arrangement, no extra radar provided by the contractor is needed. This will result in a significant reduction of the operational cost.

Flight statistics revealed that the number of aircraft involved in the NHSP can probably be

reduced by at least one to two for all operational months and by two in September. The risk taken with such a decision is minimal. Cases of three concurrent flights rarely occur in operational months. It is believed that during September two aircraft for the north areas and one for area A3 are more than sufficient. The policy of keeping one aircraft at the Larisa airport was proven acceptable, but in some cases a second aircraft had to be provided in area A3 by the Thessaloniki air base, although the number of these cases was very limited.

The optimum length of the operational season deserves further investigation. The approach followed in Section 3 was based on a comparison of flight and insurance data on a monthly basis. A more detailed examination is needed on the first and last dates of hail occurrence and the corresponding probabilities. However, some preliminary results about the transitional months of April and September can be discussed. Operational activity during these two months was on the average observed at the same percentage that hailfalls occur, but when a comparison is attempted between the number of flights or flight hours and damaged area or payouts considerable differences exist. The small percentages of payouts during September and April are probably related to the phenological stages of the associated crops, since hailfalls produce less damage per unit area in the early or late stages of plant growth. The areal extent of damages or the dimensions of the hailswaths depend on the development of convection in complexes, as well as on its life cycle. It was evident that in the transitional months organized convection and long-lived cells were rare. Compared to the amount spent for hail damage payouts during the two months, too much effort in terms of the number of flights and flight hours was spent for hail suppression. Hail climatology suggests that hailfalls do occur in March, October and November, but the probabilities are low and the damages are not significant enough to support the need for hail - suppression operations. The evidence presented supports the notion to restrict the operations between the months of May and August inclusive. To finalize the result and specify more about the dates, a detailed study of probability of occurrence should be conducted. For area A3, the ratio of seeding flights to total monthly flights has pointed out the increased number of patrol flights. Launch

criteria were usually met during transitional months in situations of embedded convection, but seeding criteria were rarely exceeded. The modification of launch criteria to reduce the number of patrol flights especially for the months of April and September deserves further investigation. Digital radar data should also be analyzed to establish a firm relationship between measured reflectivity and probability of hail on the ground.

There is an obvious need for applied research and technological development and advancement in the NHSP, which is expected to improve operations and gradually reduce operational cost. One area of research seems to be nowcasting and quantitative hail forecasting. The study of the protected areas and development of the appropriate boundary-layer models, instability indices and synoptic convective indices could be helpful in this direction. This effort needs to be supported by studies on cloud physics and dynamics with an overall impact on launch criteria and seeding hypothesis, which influence flight operations and the associated costs. Another area of required research and development is weather radars. Needless to say, radar is the core in hail suppression programs and can assist in forecasting and nowcasting, controlling and monitoring, as well as in the evaluation of such programs. Radar digitization seems to be the first step in the NHSP, which is expected to assist in optimum radar siting, hailstorm tracking and forecasting, identification, structure and thresholding of hailstorms and rainstorms, timing of hailstorm occurrence, program evaluation parameters, required personnel scheduling and associated cost of the NHSP. Flight operations is another area for research with an impact on the length of the program, number of required aircraft, seeding rates and material and associated cost. Finally, a study on alternative hail suppression techniques such as canons, and pledge (networks), among others, needs to be investigated.

5. SUMMARY AND CONCLUSIONS

The operational efficiency of the NHSP in Greece was assessed in order to possibly improve operations and lead to gradual reduction of the operational cost. Several components of the NHSP were investigated and the results were summarized. It seems that the incorporation of

applied research findings and technological advancement into the NHSP would improve operations. Specifically, since hailstorms in Greece are, in general, short-lived and intense, nowcasting and quantitative hail forecasting could be very helpful for improving efficiency. The incorporation of digital satellite and radar images along with conventional meteorological information into a "nowcasting unit" could strengthen the operational efficiency of the program. Furthermore, radar digitization and optimum radar siting should provide efficient monitoring and radar controlling, as well as a gradual reduction of the operational cost. Moreover, additional research in cloud physics and mesoscale modeling could improve seeding hypothesis and launch criteria with an impact on operations. Finally, the analysis supports an adjustment on the length of the operational period and the number of the necessary aircraft with an overall impact on the required human resources for operations.

Acknowledgments. The authors would like to express their gratitude to the program's personnel, as well as ELGA's administration for their support throughout this study. The authors are also grateful to the anonymous reviewers for their valuable comments.

REFERENCES

- Alberta Ltd., 1990: *NHSP Annual Report of 1989*. Prepared for Hellenic Agricultural Insurance Organization (ELGA), Athens. 164 pp.
- Alberta Ltd., 1991: *NHSP Annual Report of 1990*. Prepared for Hellenic Agricultural Insurance Organization (ELGA), Athens, 224 pp.
- Atmospherics Inc., 1985: *The 1984-1985 National Hail Suppression Program in Greece*. Prepared for Hellenic Agricultural Insurance Organization (ELGA), Athens. 201 pp.
- C.I.C.-3 Delta-Avionic, 1993: *NHSP Annual Report of 1992*. Prepared for Hellenic Agricultural Insurance Organization (ELGA), Athens. 300 pp.
- C.I.C.-3 Delta-Avionic, 1994: *NHSP Annual Report of 1993*. Prepared for Hellenic Agricultural Insurance Organization (ELGA), Athens. 380 pp.
- Dalezios, N.R., N.K. Papamanolis and P. Linardis, 1989: Siting of a weather radar network for operational hail suppression in Greece. *Proc., COST-73, Intern. Seminar on Weather Radar Networking*, Brussels, Belgium, Sep. 4-8, 242-247.
- Dalezios, N.R., and N.K. Papamanolis, 1991: Objective assessment of instability indices for operational hail forecasting in Greece. *Meteorol. Atmos. Phys.*, **45**, 87-100.
- Dalezios, N.R., M.V. Sioutas and T.S. Karacostas, 1991: A systematic hailpad calibration procedure for operational hail suppression in Greece. *Meteorol. Atmos. Phys.*, **45**, 101-111.
- Flueck, J.A., M.E. Solak and T.S. Karacostas, 1986: Results of an exploratory experiment within the Greek National Hail Suppression Program. *J. Wea. Mod.*, **18**, 1, 57-63.
- Foote, G.B., and C.A. Knight, ed., 1977: Hail: A review of hail science and hail suppression. *Meteor. Monogr.* **16**, No. 38, Amer. Meteor. Soc. 277 pp.
- Foris, D.V., 1992a: Χρονική Εξάπλωση του Ουράνιου Ηλεκτρισμού στην Βόρεια Ελλάδα (Temporal distribution of convective activity in northern Greece). *Proc. 1st Hellenic Conference on Meteorology, Climatology and Atmospheric Physics*, Univ. of Thessaloniki, 23-25 May, 331-338.
- Foris, D.V., 1992b: *Evaluation of Forecast Accuracy*. In NHSP prepared for Hellenic Agricultural Insurance Organization, Athens, Feb. 1993. 2.8 - 2.15.
- Intera Technologies Ltd., 1987: *NHSP Annual Report of 1986*. Prepared for Hellenic Agricultural Insurance Organization (ELGA), Athens. 165 pp.

- Intera Technologies Ltd., 1988: *NHSP Annual Report of 1987*. Prepared for Hellenic Agricultural Insurance Organization (ELGA), Athens. 209 pp.
- Intera Technologies Ltd., 1989: *NHSP Annual Report of 1988*. Prepared for Hellenic Agricultural Insurance Organization (ELGA), Athens. 280 pp.
- Karacostas, T.S., 1984: The design of the Greek National Hail Suppression Program. *Proc. 9th Conf. on Weather Modif.*, Amer. Meteor. Soc., Park City, Utah, 26-27.
- Karacostas, T.S., 1989: The Greek National Hail Suppression Program: Design and conduct of the experiment. *Proc. 5th Conf. Weather Modif. and Appl. Cloud Physics*, Beijing, China, 5-8 May, 605-608.
- Karacostas, T.S., 1991: Some characteristics of cells in the Greek National Hail Suppression Program. *Proc. 2nd Yugoslav Conf. Wea. Modif.*, Mavrovo, Yugoslavia, Vol. I, 274-283.
- Krauss, T.W., and N. Papamanolis, 1989: Precipitation formation processes within hailstorms of northern Greece. *Proc. Fifth WMO Sci. Conf. Wea. Modif. and Applied Cloud Phys.*, Beijing, China, 321-324.
- Riley, G., 1991: A simple objective forecasting program for northern and central Greece. *Proc. 2nd Yugoslav Conf. on Wea. Modif.* Mavrovo Yugoslavia, Vol. II, 1-7.
- Rudolph, R.C., D.S. Davison, C.M. Sackiw and T.J. Spoering, 1987: Identification of a primary evaluation parameter based on hailpad data. INTERA Technologies Ltd., Report No M86-215, for ELGA, Calgary Canada.
- Rudolph, R., and C. Papageorgiou, 1991: Effects of cloud seeding on hail insurance statistics in northern Greece. *Proc. 2nd Yugoslav Conf. Wea. Modif.*, Mavrovo, Yugoslavia, Vol. I, 202-209.
- Strong, G.S., and W.D. Wilson, 1983: The synoptic index of convection. Part I: Evaluation of the single-valued index, 1978-1982. *Proc. 17th Annual Canadian Meteorological and Oceanic Society Conf.*, Alberta Research Council Report, Banff, 23-37.

OBSERVATIONS AND MODEL SIMULATION OF AgI SEEDING WITHIN A WINTER STORM OVER UTAH'S WASATCH PLATEAU

Edmond W. Holroyd III^a, James A. Heimbach^b and Arlin B. Super^a

^a Bureau of Reclamation, Denver CO

^b University of North Carolina at Asheville NC

Abstract. Observations from a cloud seeding experiment conducted over the Wasatch Plateau of central Utah were analyzed for treatment effect and were modeled. The day was characterized by weak surface winds, light snowfall and weak convection embedded in a thin orographic cloud during the final stages of a storm. Silver iodide was released from a generator well up the windward (west) slope of the Plateau. Seeded periods and locations were defined using measurements of co-released SF₆ tracer gas and a drifting frame of reference. Seeded and nonseeded periods and domains were defined using the derived plume history. A strong seeding signal was found in the occurrence of ice particles, both on the Plateau top and at aircraft levels. Calculations based on van-mounted 2D-C probe observations along the Plateau top's west edge indicated increased snowfall rates in the silver iodide plume, primarily due to aggregates. While some precipitation gauge observations farther downwind suggested possible increased snowfall, the evidence was not definitive and any seeding-caused snowfall was quite limited in amount. Application of the Clark mesoscale numerical model suggested the case was characterized by weak and shallow clouds principally driven by orographic influences with little buoyant contribution. The simulated tracer and cloud patterns were associated with orographic lifting and gravity waves. The model correctly predicted plume transport from the release point over the target area, but at a slower rate than indicated by field measurements. The plume core was predicted to be transported over the Radar-Radiometer site and somewhat south of the Target site to a height of about 1 km above the Plateau in good agreement with observations.

1. INTRODUCTION

The National Oceanic and Atmospheric Administration (NOAA) administers the Atmospheric Modification Program (AMP) in cooperation with the States of Arizona, Illinois, Nevada, North Dakota, Texas and Utah. The overall goals of the Utah/NOAA AMP are to physically evaluate the operational seeding program that has been conducted in Utah for over two decades (Griffith et al. 1991), and to suggest ways of improving the program's effectiveness. Toward those objectives, the Utah/NOAA AMP conducted a field program on the Wasatch Plateau (hereafter Plateau) of central Utah from mid-January to mid-March 1994. A similar field program was conducted at the same place in early 1991. Papers describing results from the 1991 program include Griffith et al. (1992), Heimbach and Hall (1994), Super (1994), Super and Holroyd (1994), Huggins (1995), and Super (1995).

This paper examines a silver iodide (AgI) seeding experiment conducted on 21 February 1994 during a period with thin (1 km thick) orographic cloud and weak embedded convection in flow from the southwest near the end of a storm episode. This experiment was selected for a detailed case study because a good observational data set was obtained and obvious microphysical changes resulted from the AgI seeding. However, it will be shown that both supercooled liquid water (SLW) and snowfall were limited during the experiment. Similar low SLW amounts and precipitation rates are typical of many winter storm hours (Super 1994). Microphysical effects of seeding were pronounced both on the Plateau top and at aircraft levels. Ground-released plumes were well observed and good supporting data were obtained. Consequently, the experiment was selected for intensive case study analysis and simulation by numerical modeling. The combination of a high quality observational set and sophisticated modeling offers a powerful approach toward improved understanding of seeding plume transport and dispersion and associated microphysical effects within orographic clouds.

Silver iodide and sulfur hexafluoride (SF_6) tracer gas were released from the Aspen Hills Site (AHS) located well up the west (windward) slope of the Plateau at an elevation of 2340 m (all elevation and altitude references will be above mean sea level). The valley floor was at about 1800 m and the Plateau was at about 2900 m. Various instrument sites used in early 1994 are shown on Fig. 1. Aircraft sampling was done with the NOAA Beechcraft King Air C-90 along the two flight tracks ("west track" and "east track") shown on Fig. 1, and also along a line connecting the radar-radiometer site (RRS, elevation 2980 m) and target site (TAR, elevation 2900 m). Instrumented van sampling of AgI ice nuclei (IN), SF_6 , and ice particles was done primarily along the "upwind highway", a section of Highway 31 from its intersection with Highway 264 to southeast (SE) of RRS. The upwind highway north of RRS is essentially under the west flight track. Some van sampling was done from the same intersection to near TAR and back along Highway 264.

The main observations to be discussed include AgI IN measured by four NCAR acoustical IN counters (hereafter NCAR IN counters) (Langer, 1973) in the aircraft, van, RRS and TAR. A recent comparison has shown reasonable agreement between the van and aircraft NCAR IN counters and the Colorado State University isothermal cloud chamber (DeMott et al., 1995). Concentrations of SF_6 were measured with fast-response detectors (Benner and Lamb, 1985) in the aircraft and van. Ice particles were detected by Particle Measuring Systems (PMS) 2D-C imaging probes on the aircraft and van, and at TAR. The latter two probes were vane-mounted which kept them pointed into the resultant wind.

Rawinsonde observations were obtained from site RAW in the valley west of the Plateau. Wind speed and direction, temperature, relative humidity (or dewpoint temperature) and precipitation were measured at several surface locations shown on Fig. 1. Winds, positioning and state variables were measured by the aircraft. Supercooled liquid water was monitored by a vertical-pointed microwave radiometer (Hogg et al. 1983) at RRS, by Rosemount icing rate meters at HAS, RRS and TAR, and by a King liquid water probe on the aircraft. K_a -band radar volume scans were made from RRS. A Doppler acoustic sounder (sodar) observed half-hourly averaged horizontal winds over DAS.

2. SYNOPTIC CONDITIONS

There was a long wave trough over the western continental United States. One of several short wave troughs embedded within this feature passed over Utah in the early morning of 21 February. A stationary front extended from northern Idaho through southern Wyoming, through eastern Colorado and northern New Mexico. In the early morning, a fast-moving storm system associated with the upper short wave trough passed to the south of the Plateau. Most sections of Utah received some snow with the heaviest snowfalls over the mountains and higher southeast valleys. Some mountainous areas received 15 to 25 cm of snow during the night. The experiment was conducted in the morning after the passage of the surface trough. During the experiment the target area had weak convective precipitation stimulated by orography while the valleys had broken clouds.

3. THERMODYNAMICS

Vertical profiles of potential and equivalent potential temperature were made from rawinsonde, aircraft, and surface data. From the valley floor at 1800 m to 4000 m the potential temperature increased from about 287°K to about 292°K, though the range at surface sites was 285 to 297°K caused in part by solar heating. The profile indicates that the air was somewhat stable with respect to the dry adiabatic lapse rate, though solar heating could easily create local instabilities. Such instabilities may have helped the seeding plumes rise more rapidly on thermally driven updrafts than would have been the case with purely mechanical mixing as was simulated by the model described later. Studies on the Grand Mesa, Colorado, (Holroyd et al. 1988) showed that surface air could rise (bringing nuclei with it) in otherwise stable air to the level at which the ambient potential temperature equalled the peak found at the surface.

Profiles of equivalent potential temperature decreased slightly from about 296.5°K in the valley to about 293.5°K aloft. Surface stations ranged from 287 to 306°K. The air was therefore slightly conditionally unstable, mostly because dew points decreased with altitude. Convective elements could rise easily but mixing would dry and dissipate them. Broken convective cloudiness was in fact observed over the Sanpete Valley throughout the experiment. Cloud cover was generally solid over

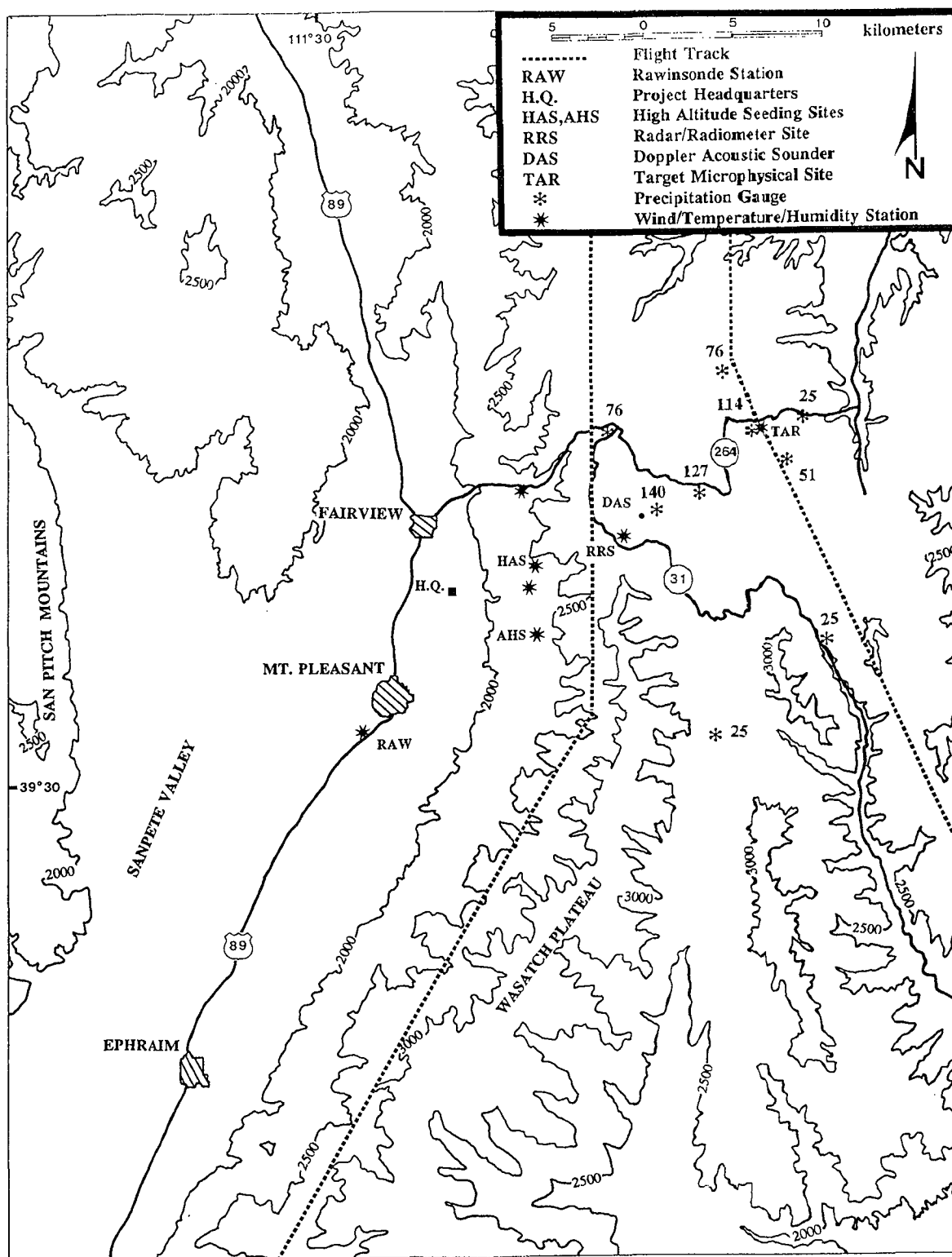


*Fig. 1. Map of the Wasatch Plateau experimental area showing equipment siting and highways used for the early 1994 field program. The two dashed lines are aircraft sampling tracks over the west and east edges of the Plateau top. Contours are in meters above mean sea level. Numbers by the nine gauges represent total precipitation (mm * 100) received after estimated AgI plume arrival (see text).*

the Plateau at the beginning of the experiment, but was becoming broken by the end.

4. PLUME DETERMINATION

Silver iodide was released from AHS from 0800 to 1215 (all times local standard) at 22.5 g h^{-1} (a typical ground release rate) with a Desert Research Institute radio-controlled generator. Sulfur hexafluoride was released from 0830 to 1212. The stated times, together with wind speed and direction, determined the extents of the plumes along the wind direction axis. Diffusion, deflection, and wind variability determined the transverse extents relative to the mean wind direction axis. Wind directions over the Plateau were generally from the southwest. Wind speeds over the Plateau were faster than over the valley at the same pressure altitude.

4.1 Drift Speed

A distinct but small wind shift to more southerly directions was detected in the data from the AHS and HAS (0950-1020), RRS (1012-1036), and TAR (1055-1115) sites. The wind shift was accompanied by an marked increase in detected IN at the RRS and TAR sites and warmer air temperatures. A restoration of original wind directions followed. A drift speed of $4.5 \pm 1 \text{ m s}^{-1}$ was calculated by tracking the fluctuations of IN, temperature, and winds between all four sites. This abnormally slow speed is within or near the scatter of those calculated from aircraft straight-and-level flight segments ($6 \pm 3 \text{ m s}^{-1}$) and from well-exposed Plateau top surface instruments ($3.7 \pm .9$ at RRS to $5.8 \pm 1.1 \text{ m s}^{-1}$ at TAR). Wind speeds at RAW, in the up-wind canyons, and at the two west slope seeding sites (AHS and the unused HAS) were slower.

4.2 Drift Direction

The plume positions were readily determined by the boundaries of enhanced concentrations of SF_6 , AgI , and ice particles, as recorded by the aircraft, van, and surface instruments at RRS and TAR. The angle from the plume center back to the AHS release site was calculated to give the drift direction of the plume. Aircraft observations showed plume orientations near 235 degrees for the first passes along the west track, 235 degrees for the lower passes along the east track, 244 and 253 degrees for the top two east track passes, and 243 degrees for the last west track passes. Vertical shear exist-

ed over the east track but not the west track. The winds were becoming more westerly with time along the west track. The van found plume orientations of about 240 degrees before and after the more southerly wind shift and 227 degrees during it.

These directions of plume transport are close to the winds determined by the 0900 RAW rawinsonde for the same altitudes but with the expected more southerly shift caused by friction over the Plateau. The constriction of the air flow caused by the height of the Plateau was responsible for the increased wind speeds there. The lack of wind shear over the west track may indicate that most of the air at the levels of the experiment came from a common source (Sanpete Valley) and had a common momentum. Its forced rise dominated wind speed and direction near the RRS. Farther downwind, near TAR, the air had time to respond to normal pressure gradients and showed angular shear.

4.3 Drifting Frame of Reference

A rotated coordinate system drifting with the plume was designed to refine examinations of the plume behavior. The new frame of reference was used to coordinate the time and space differences among the many observations. The observations are thereby related to positions relative to the plume itself. The origin was defined to be at RRS at 0800 and drifting with respect to the ground at 4.44 m s^{-1} (16 km h^{-1}) from 235 degrees. The abscissa was oriented parallel to 235 degrees and is representative of time in a steady state flow. The ordinate was therefore perpendicular to the plume axis and measures diffusion and fluctuations transverse to the mean axis. The slight change in speed from the actual value of 4.5 m s^{-1} was for ease in plotting graphics and is insignificant; it amounts to a discrepancy of less than 1 km over the 4.25 hour experiment.

Figure 2 shows the plume in the rotated and drifting (new) frame of reference. The long figure is split into two pieces, a. start and b. end, with repeated center, for ease of display. Earlier times are to the right and later to the left. The AHS site ordinate was -0.94 km and the TAR ordinate was 0.97 km . The AgI IN concentrations (light shading) are plotted on a compact logarithmic scale above the drift track of the RRS and TAR sites through the figure. SF_6 concentrations are hand

sketched on a similar compact logarithmic scale to the right of the tracks (thin lines) of the aircraft (medium shading) and van (dark shading). Some approximate SF_6 plume edges are suggested by the thick lines. The plume concentrations are obviously variable with position. Similar concentration graphs could have been plotted from ice particle data from the aircraft and van and from IN data from the van. Slight concentrations of IN and ice particles were measured by the east van pass at abscissa -57 and stronger concentrations on the return pass at -63, though no SF_6 was indicated in the final data (contrary to field notes). The last pass of the van (abscissa -77) found no SF_6 , AgI IN, or significant ice particle concentrations, confirming the shutdown of the generators and the rapid flushing of IN from the study region.

The AgI plume length in the new frame of reference was 68 km, starting at abscissa -6.7 km (0800 release start at AHS) and ending at -74.7 km (1215 end of release). The SF_6 plume length was 59 km, starting at -14.7 km (0830 release start at AHS) and ending at -73.7 km (1112 end of release). The AgI was detected at RRS (1 km away from AHS in the new frame) as soon as the instrument was turned on at 0900, about a half hour after expected for a transport speed of 4.5 m s^{-1} . Only traces of AgI were detected at the RRS during the final hour of its expected presence.

The presence of AgI IN at TAR was detected at low levels ($1\text{--}4 \text{ counts s}^{-1}$, equivalent to about $60\text{--}240 \text{ IN L}^{-1}$ effective at -20°C) as soon as the data system was started at 1000. (Background IN levels in the absence of AgI, as measured with an NCAR IN counter on the Plateau, were typically $1\text{--}4 \text{ counts min}^{-1}$.) Similar low levels of AgI were detected throughout the experiment with two exceptions. Levels decreased to near background after 1235, and much higher levels ($10\text{--}40 \text{ counts s}^{-1}$) were monitored between 1049 to 1111. The brief period of high AgI IN concentrations was associated with the southerly wind shift. At other times most of the plume was south of TAR.

Van and aircraft sampling of the plume did not occur until about abscissa -30 km. The SF_6 plume width then was 1.5 to 2.0 km on each of the first van (starting at 0954) and aircraft (starting at 0957) detections of the gas. Thereafter the SF_6 plume rapidly expanded to a width of 4.0 to 5.5 km with

numerous internal peaks in concentrations. Those peaks appear to be associated with the positions of the canyon heads upwind. The widening of the plume was associated with the wind shift. The plume top on the east track was laterally sheared to a width of 7 km at a more southerly position. Starting with a van penetration (1058) at abscissa -46 km, the plume width along the western track shrank to a steady 2 km until the end of the experiment when plumes were no longer found along the upwind highway.

Initial examination of K_a -band radar volume scan data from the RRS did not provide definite evidence of plume position. Apparently radar returns from widespread natural snowfall obscured any returns from presumably smaller seeded ice particles because of the strong dependence of radar reflectivity on ice particle size and mass.

The typical transverse plume spread of 2 km at about the RRS site is equivalent to an angular spread of about 15 degrees. That value is comparable to seeding plumes on the Grand Mesa, Colorado, (Holroyd et al. 1988) released under similar conditions. The wider plume during the wind shift had an angle from AHS of about 50 degrees. There was no indication of additional transverse spreading between the west and east flight tracks, which matches some, but not all, earlier results from the Grand Mesa.

4.4 Vertical Cross Section-cross wind

Vertical cross sections were constructed through RRS at the 235 and 305 degree azimuths. They serve as bases for Figures 3 and 4. Terrain elevations within 4 km of the 235 degree axis were plotted as the scatter of dots. In Figure 3 the view is downwind and the terrain is restricted to the slopes between the seeding site, AHS, and the Plateau crest near RRS. The location of those sites are indicated by the white circles and enclosed crosses. In order to show possible channeling effects of the terrain, Figure 3 shows terrain departures from a plane that generally follows the western slope of the Plateau. The zeroing is arbitrary. This terrain cross section shows a major canyon head (between the major peaks), having about a 6 km width, and three or four minor canyon heads within having about 1.5 km widths.

At the top of Figure 3 are plotted SF_6 concentrations on compressed logarithmic scales for the first

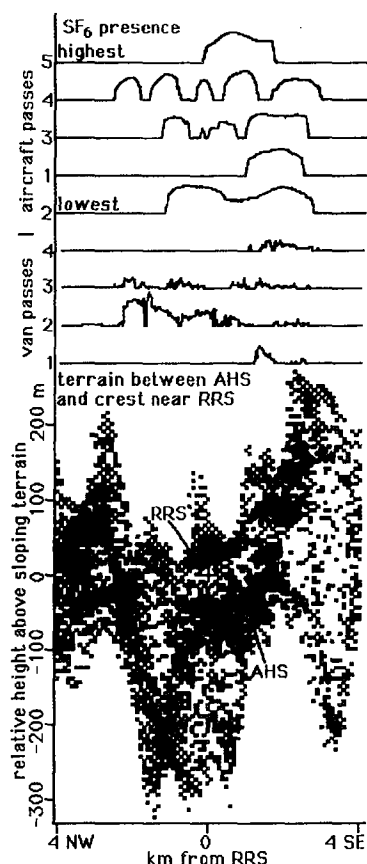


Fig. 3. A vertical cross section, looking downwind, of the terrain on the west slope of the Plateau between the seeding site, AHS, and the crest near RRS. Above are graphs of SF_6 presence as measured on some of the first passes by the van and aircraft. The canyon heads appear to affect the locations of plume maxima and extents.

Table 1. Peak SF_6 concentrations (ppt) for the aircraft and van passes of Fig. 3.

passes	peaks, left to right
aircraft-5	214
aircraft-4	25, 58, 14, 129, 18
aircraft-3	17, 5, 33
aircraft-1	65
aircraft-2	83, 56
van-4	17
van-3	17
van-2	301
van-1	40

4 van passes and the first 5 aircraft passes along the crest. Peak concentrations, in parts per trillion (ppt) by volume are given in Table 1. The scales differ somewhat between the van and the aircraft,

but the graphs are intended to show mainly the plume position and structure with respect to the ground. The aircraft passes are plotted in order of their elevation.

It appears that the plume positioning and lateral spreading of the lower parts of the plume were largely controlled by the interaction of the wind direction with the topography of the canyon heads. The transverse structure of the plumes appeared to have higher concentrations aligned with the positions at which the rising air exited the minor canyons and crossed the Plateau top. For the van passes and lower aircraft passes there is a consistent plume presence on the southeast side, bounded by the higher terrain to the right of the plume. That plume width is comparable to the size of the minor canyon head in that location. Van passes 2 and 3, affected by the wind shift, appear to be bounded on the left by the other peak of higher terrain. Aircraft pass 3 appears to be partitioned by three minor canyon heads.

4.5 Vertical Cross Section-along wind

The six parts of Fig. 4 show cross sections aligned with the wind, as viewed towards the NW. Surface and aircraft observation locations are indicated by a larger symbol. Aircraft pass numbers are given as integers in Fig. 4a only. Passes 13 and 14 were parallel to the axis of the figure and are not indicated. Van passes in the plume were near RRS and from TARSW to TAR. (All 4 and 5 letter names used in this report are for precipitation gauge locations described in section 6.) An approximate edge of the plume top is indicated for reference. Data values on aircraft passes 3, 9, and 15 were appreciably low, possibly from clear subsiding air between cloud elements, for most parameters in the six parts of this figure. Values from those passes were generally ignored in the contouring but the actual values are indicated.

Fig. 4a shows the distribution of liquid water content (LWC) as determined by the aircraft passes. The data, shown as two-place decimals, were averaged throughout the plume and to about 3 km to both sides. LWC values were slightly lower within the plume, probably from greater consumption by the enhanced ice particle concentrations there. The wettest parts of the cloud were the lower layers over the western track (crest line). The cloud dried appreciably to the east. Visual observations at TAR consistently indicated a broken cloud deck

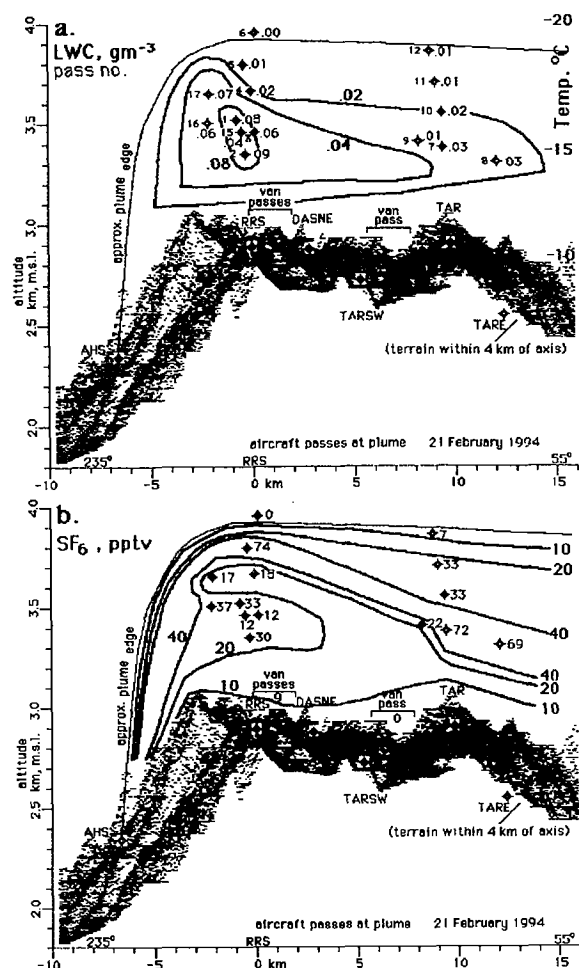


Fig. 4. Vertical cross sections, looking cross wind to the NW, of plume and microphysics parameters. The panels are a. LWC, temperature and pass number; b. SF₆, c. IN, d. ice concentration, e. nonseeded IWC, and f. seeded IWC and particle trajectories.

based well above the site from 0948 (first observation) through the experiment's end. In contrast, the RRS was in cloud until after 1200. This is further evidence of subsiding air over the Plateau top's east edge.

Temperatures, shown at the right of Fig. 4a, are generally from -11°C at the Plateau top to -19°C at cloud top. AgI is active in this temperature range, especially at the colder end. A recent calibration of a Desert Research Institute (DRI) remote-controlled AgI generator using AgI-NH₄I-acetone solution (Huggins, 1994) indicated about 10^{15} IN per gram of AgI at -12°C , the coldest temperature

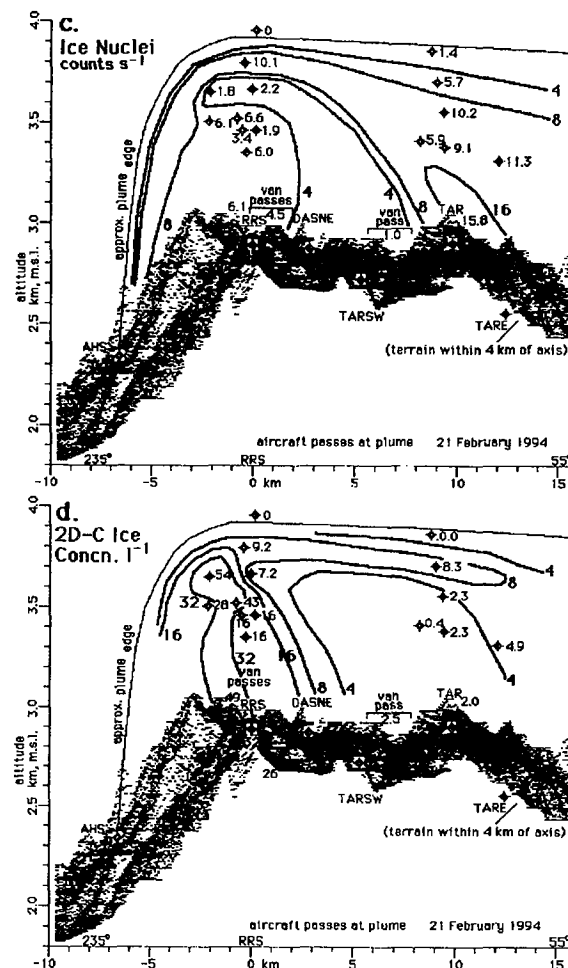


Fig. 4. (cont.), c. IN, d. ice concentration

tested, for natural draft conditions. The same type of generator and solution were used at AHS. This solution was chosen because it is used in the Utah operational seeding program.

Figures 4b, 4c, and 4d show the observed concentrations of SF₆, IN, and ice particles, respectively, averaged over the width of the SF₆ plume. NCAR IN counts were shifted by 60 s because of hold-up time in unit's cloud chamber. The SF₆ and AgI IN contours have the same basic pattern. The highest concentrations on the west flight track are at the plume top with a secondary peak at the middle levels. The highest concentrations are at the lower levels on the east track, suggesting that the plume core descended while crossing the Plateau.

At RRS (at which data were collected for 6-min periods) the IN varied considerably. They were

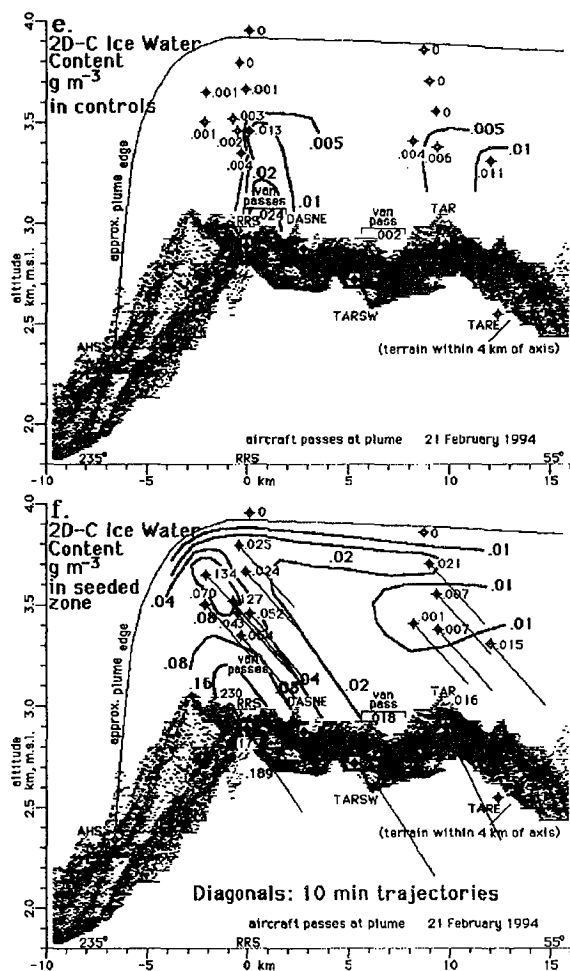


Fig. 4. (cont.), e. nonseeded IWC, and f. seeded IWC and particle trajectories.

detected in abundance from as soon as the counter was turned on at 0900 until about 0936. The wind direction was 220 to 243 degrees during this IN maximum with count rates typically near 6 counts s^{-1} . The wind shifted to between 250 to 266 degrees from 0936 until 1006 and IN levels dropped below 1 count s^{-1} . Winds at the RRS were again more southerly (226 to 241 degrees) from 1012 to 1036 and count rates showed a second maxima with values similar to the first. From 1036 through the end of the experiment the wind direction was never more southerly than 250 degrees and IN counts remained low. These observations indicate the AgI plume was generally south of the RRS except for the two periods with more southerly flow.

As a basis for comparison, for all RRS 6-min periods with IN averaging $>1 s^{-1}$ the average was 6 counts s^{-1} . The TAR IN for the 35 minutes with highest concentration averaged 16 counts s^{-1} . The first four van passes along the west track were combined to an average of 4.5 counts s^{-1} . For reference, 10 counts s^{-1} is equivalent to about 600 IN per liter at $-20^{\circ}C$, the temperature of the NCAR IN counter cloud chambers. This value results from the usual times 10 correction because of ice crystal losses to glycol-covered cloud chamber walls (Langer, 1973).

Surface IN concentrations are generally low compared to aircraft values shown in Fig. 4c. Because NCAR IN counter response times (about 60 s) are usually longer than within-plume sampling times by the aircraft, the aircraft values cited were calculated as the total counts per pass divided by the number of seconds in the SF_6 plume. In other 1991 (e.g. Super, 1995) and 1994 experiments the van values were usually much higher than aircraft values, indicating a plume core hugging the ground. This light wind case, in contrast, indicates that the SF_6 and AgI plumes were rapidly lifted to cloud top altitudes.

Fig. 4d shows a different pattern for the concentration of ice particles. The highest concentrations were observed in the middle cloud levels of the west track, particularly on the last pass. Similar high concentrations were also found by the van, plotted near RRS for three range intervals, 1 km wide, over which the four west track passes were averaged. To the east concentrations were much lower, with the greatest somewhat below cloud top. The general pattern is of rapid fallout of particles and an anvil type of remnant to the east.

Ice water contents (IWC), comparable to LWC in Fig. 4a, were calculated from the 2D-C data using concentration algorithms and masses in Holroyd (1987). They are plotted in Fig. 4e for plume nonseeded zones defined in the next section, and in Fig. 4f for measurements within the SF_6 plume (seeded zone). IWC for the nonseeded zones was everywhere less than LWC, indicating an inefficiency in the natural precipitation process. IWC for the seeded zones generally was comparable with LWC for the same intervals (the LWC in the seeded zones was somewhat reduced compared to nonseeded zones). IWC was in significant excess of LWC on passes 1 and 17 in the upper left part of

Table 2. Ice particle concentrations L^{-1} , in the seeded and nonseeded zones. (NN=north nonseeded, S=seeded, SN=south nonseeded, AN=average nonseeded, R=S/AN). Values between 0 and 0.1 indicated by >.0.

		Concentrations, L ⁻¹					Precip. Rates mm h ⁻¹ *100				
pass	track	NN	S	SN	AN	R	NN	S	SN	AN	R
Van											
1	W	2.2	27.8	3.1	2.6	10.5	2.1	47.2	5.9	4.0	11.8
2	W	4.1	60.0	5.4	4.7	12.7	3.8	58.5	10.5	7.2	8.1
3	W	3.9	24.2	2.6	3.3	7.4	4.5	34.2	2.8	3.7	9.4
4	W	6.3	21.1	3.3	4.8	4.3	6.1	38.4	4.5	5.3	7.3
6	E	0.3	2.5	-	0.3	9.1	0.3	4.1	-	0.3	13.4
TAR	E		2.0					4.7			
Aircraft											
1	W	0.5	42.8	1.3	0.9	47.9	0.2	20.6	0.8	0.5	44.7
2	W	0.9	16.1	1.1	1.0	15.8	0.5	8.7	0.8	0.6	13.6
3	W	7.1	15.9	0.2	3.6	4.4	3.8	9.7	0.1	2.0	4.9
4	W	0	7.2	0.4	0.2	36.2	0	3.6	0.3	0.1	28.3
5	W	0	9.2	0	0	INF	0	3.8	0	0	INF
6	W	0	0	0	0	-	0	0	0	0	-
7	E	1.3	2.3	2.2	1.8	1.3	0.7	1.0	1.3	1.0	1.0
8	E	2.3	4.9	4.0	3.2	1.6	1.4	2.2	1.9	1.6	1.4
9	E	>.0	0.4	2.3	1.1	0.3	>.0	0.1	1.4	0.7	0.2
10	E	0.2	2.3	0.2	0.2	10.3	0.1	1.1	0.1	0.1	16.8
11	E	0	8.3	0	0	INF	0	3.1	0	0	INF
12	E	0	>.0	0	0	INF	0	>.0	0	0	INF
13	NE	>.0	6.6	0	>.0	671.6	>.0	3.3	0	>.0	1257.
14	NE	0	3.0	1.0	0.5	6.2	0	1.5	0.5	0.2	6.1
15	W	0.7	16.2	0.3	0.5	33.1	0.5	6.4	0.2	0.4	17.1
16	W	0.2	27.9	0.5	0.4	74.9	0.1	10.6	0.2	0.2	58.0
17	W	0	54.1	0.8	0.4	139.9	0	19.4	0.3	0.2	119.7

the figure, where the greatest ice concentration was found.

Precipitation rate calculations (not shown) from the 2D-C data have a pattern similar to the IWC. The sizes and terminal velocities of the particles contributing median values to the precipitation rates were determined. Using those terminal velocities, the $4.5\ m\ s^{-1}$ drift speed, and ignoring vertical air motions, 10-minute subsequent trajectories were calculated for each pass and are shown as the diagonal lines in Fig. 4f. Half of the precipitation falls faster and half slower than indicated by these lines. The patterns along with IWC or ice particle concentrations indicate that the western track ice particles were precipitating rapidly, with much of the snowfall likely reaching the ground before the DASNE and TARSW gauges. The figures suggest that little snow would be left for the gauges near the east track.

5. ICE PARTICLE CHARACTERISTICS

5.1 Analysis of Observations

Following a procedure that has become standard for our studies, 2D-C ice particle data were analyzed

by the methods discussed in Holroyd (1987) and Super et al. (1988). Ice particles less than $100\ \mu m$ size (4 pixels) were ignored as were particles with estimated center of mass outside the 2D-C probe's field of view. For the van and aircraft data the seeded zone was usually defined by the entrance and exit times through the SF_6 plume. Buffer zones of 12 flight seconds for the aircraft (about 1 km) and 1 km NW or SE for the van were defined immediately adjacent to the seeded zone. Beyond that, on both sides, nonseeded (control) zones of 24 flight seconds and 2 km width were defined. Ice particle characteristics were thereby determined for five zones for each pass of the aircraft or van. The concentrations and precipitation rates from the 2D-C images are listed in Table 2 for the seeded and nonseeded zones. (Buffer zones are ignored.) Also listed are the seeded to nonseeded ratios.

The TAR site was potentially influenced by the AgI plume above it for all but the last 15 min of the 1000 to 1330 observation time period, though AgI nuclei were detected for only 35 min there. TAR data were therefore analyzed in 15 min increments and considered totally seeded. In fact, the TAR ice particle concentration showed no obvious change during the time of AgI presence.

Plume boundary exceptions are as follows: Aircraft pass 6 was in clear air; an arbitrary 1 minute period was chosen in the expected location for averaging other parameters. On the northeastward pass 13, lacking an SF_6 plume detection, the start was 44 seconds before the start of the IN detection, based on passes where both AgI and SF_6 were present. The exit time was where the ice particle concentration dropped below 1 L^{-1} . Van pass 6, returning from the target, did not have detectable SF_6 values in the processed data (contrary to field notes); the north edge plume entry was defined as 55 seconds before the average IN counts first reached 2 s^{-1} . The van penetrated further into the plume and then went back out (see Fig. 2b, abscissa -63) of the north side, which was then defined geographically. None of these variant plume edge definitions are critical to the conclusions.

It is seen that the seeded zones almost always had greatly enhanced ice particle concentrations (ratios $\gg 1.0$). That is the normal first effect of seeding shown in a number of past studies which include Holroyd et al. (1988), Super and Boe (1988), Super and Heimbach (1988), Deshler et al. (1990) and Deshler and Reynolds (1990). Precipitation rates calculated from the 2D-C images had a similar relationship. The aircraft precipitation rates are less than those measured by the van during the same time period. This is normal because ice particles have additional opportunity to grow as they fall to the ground. The rates for the van are comparable with the precipitation rates measured by gauges during the same general period shown in Table 3. The TAR 2D-C rate is much less than the average measured by the nearby TAR gauge. However, the TAR 2D-C was not operated until after 1000 and missed the more intense precipitation from 0900 to 1000. The TAR gauge detected no precipitation from 1000 until the 2D-C probe was turned off at 1330 except for 0.38 mm between 1100 to 1115. The latter interval matches a period of greater snowfall and concentrations from the TAR 2D-C from 1057 to 1127.

The ice particle size spectra for the four west track van passes were analyzed as presented in Fig. 5. Figure 5a shows the spectrum (thick lines) with respect to the particle contributions to the precipitation rate for both the seeded and nonseeded zones. Figure 5b shows the normal size spectrum of the particles with no mass or terminal velocity weighting. The basic sizes are slightly smaller for the

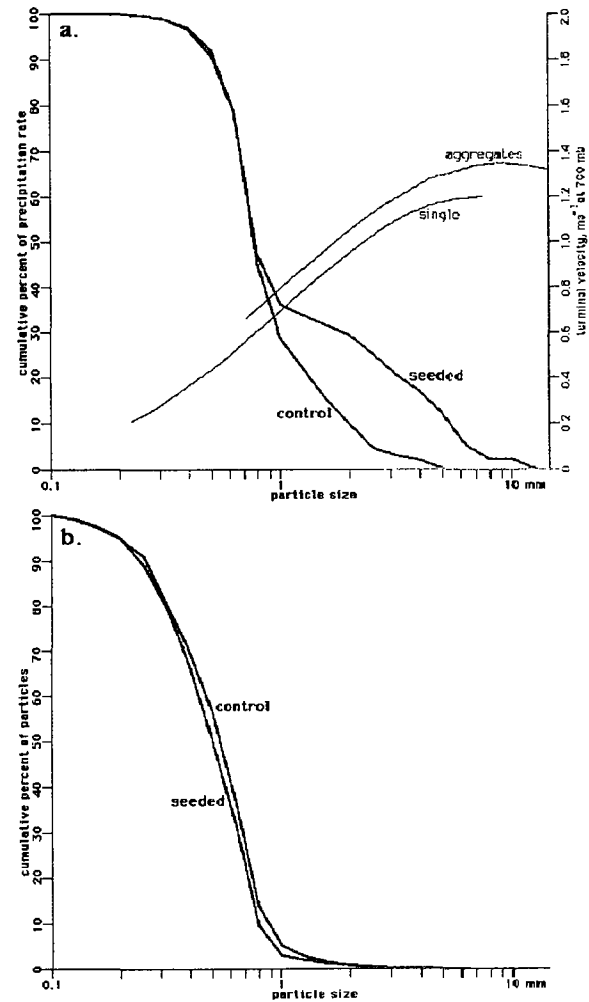


Fig. 5. Size spectra of van 2D-C particle data. *a.* with respect to precipitation rate. *b.* with respect to particle concentration. Particle terminal velocities used for various calculations are shown in *a.* Aggregation accounts for the separation between the seeded and nonseeded (control) spectra in *a.*

seeded zone than for the nonseeded zone except for the presence of large aggregates in the seeded zone. Those aggregates are not visible in Fig. 5b because there are about ten times as many particles (mostly small) in the seeded zone compared to the nonseeded (Table 2). Precipitation rates, however, are dominated by the large end of the particle spectrum. In the nonseeded zone the large particles are single. In the seeded zone they are aggregates of the numerous smaller particles, greatly affecting the separation of the two spectral curves in Fig. 5a. As an additional reference, the typical terminal velocities at 700 mb of the ice particles of the

single particles (mostly "tiny", "hexagonal", and "irregular" classes of Holroyd 1987) and "aggregates" are shown in Fig. 5a as the thin lines. Those velocities were used in Fig. 4f.

5.2 Physical Plausibility of Apparent Seeding Effects

It is reasonable to ask whether increased aggregational growth in the AgI plume observed along the upwind highway appears physically plausible. There are two separate issues: time for nucleation of ice crystals by the AgI and time for development of aggregates greater than 1 mm size as observed within the AgI plume.

Precise cloud base observations were not available during this experiment because of failure of a time-lapse camera system at RAW. Visual observations at the RRS, located at the canyon head above AHS, noted that RRS was in cloud until between 1200 and 1230. Relative humidity measurements at AHS were about 95 percent for the first two hours of AgI release, while temperatures were -6 to -7°C . Thereafter the temperature increased and the relative humidity decreased as the storm episode ended. By 1100 the AHS temperature was -4.5°C and the relative humidity was 90 percent. Although relative humidity sensors have only moderate accuracy near water saturation, it appears likely that AHS was in-cloud until at least 1000. With temperatures colder than -6°C and humidities of at least ice saturation, rapid production of high concentrations of ice crystals can be expected very near the generator as demonstrated by the field observations of Finnegan and Pitter (1988) for the same AgI solution. Therefore, it is reasonable to assume that rapid ice crystal nucleation occurred near the AHS generator until at least 1000, and that crystals had at least 7 km of upslope transport within cloudy air before reaching the upwind highway. Winds at AHS and HAS were near 2 m s^{-1} during the experiment. Assuming a mean transport speed of 3.5 m s^{-1} from AHS to the upwind highway translates into 33 min of travel, a considerable time for crystal growth. Much less rapid ice crystal formation by contact nucleation, and less within-cloud transport, probably occurred downwind of the AHS as the cloud base presumably ascended above the seeding site sometime after 1000.

The ice crystal aggregation process is not well understood, particularly in low liquid water clouds such as sampled during this experiment. However,

there is evidence in the literature to support the hypothesis that seeding can result in aggregation. For example, Holroyd and Jiusto (1971) reported that aggregation was the dominant precipitation form resulting from heavy seeding of a lake effect winter storm. Heimbach and Super (1988) presented results of observations during two storms within an AgI plume on top of the Bridger Range's main crest. These measurements, made only 3 km downwind (and upslope) from the AgI generator, showed pronounced aggregation of plates and/or linear particles. Snowcourse observations suggested marked seasonal snowpack increases only 5 km downwind of the AgI generator. Similar findings were reported for the earlier Bridger Range Experiment (Super and Heimbach 1983). Both Bridger Range studies suggested that aggregation may have produced the apparent snowpack increases within 5 km of the AgI generator.

Heymsfield (1986) reviewed evidence of aggregate development in seeded clouds and presented model calculations of the aggregation process. His views included, "The time required for the observed onset of aggregation in seeded clouds is 5 to 8 min." and "Most of the precipitation that develops in convective clouds that decay shortly after being seeded is apparently produced by aggregates." Such clouds may have limited liquid water contents typical of winter orographic clouds. Heymsfield (1986) noted that aggregation was most likely to occur at temperatures near -6 and -16°C but was unlikely between -10 and 12°C .

In view of the evidence presented, it is concluded that the van 2D-C probe observations of aggregates greater than 1 mm within the AgI plume is consistent with current physical understanding of expected seeding effects. There appears to have been adequate time for ice particle growth and aggregation in the plume of enhanced particle concentrations observed by the van along the upwind highway along the Plateau top's west edge. However, the average transport speed of 4.5 m s^{-1} on this day (Sec 4.1) was atypically slow. More typical wind speeds above the Plateau during winter storms are 2 to 3 times as fast.

6. PRECIPITATION GAUGE OBSERVATIONS

A network of precipitation gauges was operated as shown on Fig. 1. Belfort Universal weighing gauges were used with 24 h rotation chart drives

Table 3. Estimated AgI plume arrival times (HHMM), 3.5 hour precipitation totals (mm) and equivalent hourly rates (mm h⁻¹*100) at the nine precipitation gauges shown on Fig. 1. Gauges are noted as S=seeded or N=nonseeded according to whether they were under or crosswind of the AgI plume.

gauge	arrival	type	total	rate
RDJNC	0845	N	0.76	22.
TARNW	0905	N	0.76	22.
DASNE	0835	S	1.40	40.
TARSW	0845	S	1.27	36.
TAR	0900	S	1.14	33.
TARSE	0900	S	0.51	15.
TARE	0910	S	0.25	7.
FARS	0810	N	0.25	7.
FARSE	0840	N	0.25	7.

providing a time resolution of about 2 minutes. All gauges had 28.7 cm diameter orifices (twice standard area) which resulted in a snow water equivalent resolution of 0.13 mm (0.005 inch). All gauges were located in protected clearings in the conifer forest, and were equipped with Alter-type wind shields, both to minimize wind-related gauge undercatch. Even light winds can result in serious gauge undercatch of snowfall as demonstrated by Goodison (1978).

The 4.5 m s⁻¹ transport speed was used for estimating arrival times of the AgI plume leading edge at each gauge. For sites off the plume axis a line perpendicular to the plume was used to estimate arrival times which are listed in Table 3. It is seen that arrival times for seeded gauges ranged between 0835 to 0910, or 35 to 70 min after start of seeding. RDJNC is the gauge near the junction of Highways 31 and 264. FARS and FARSE are the two most southerly gauges where S=south and SE=southeast. Other gauges are named by direction relative to sites shown on Fig. 1. For example, TARNW is northwest of TAR and DASNE is northeast of DAS.

Gauges are noted as seeded or nonseeded based on the AgI plume positions from both observations and model results to be discussed in Sec. 7. Four gauges were clearly crosswind of the AgI plume throughout the experiment, two north of the plume and two far south of the plume.

The two most southerly gauges (FARS and FARSE in Table 3) were effectively in a different weather

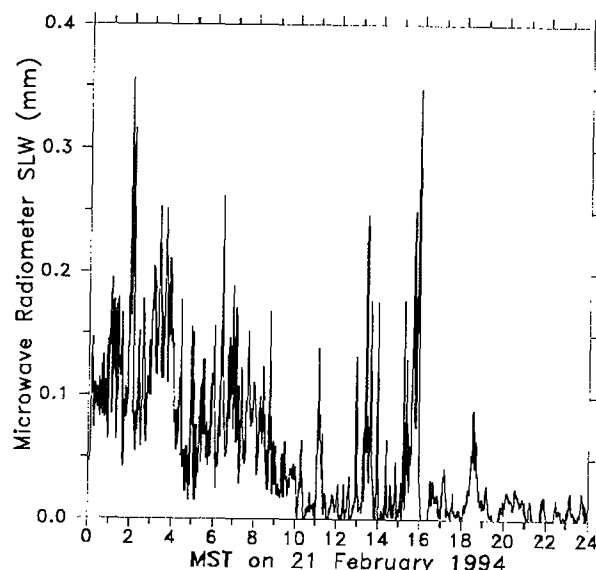


Fig. 6. Vertically-integrated SLW measured by the RRS microwave radiometer during 21 February 1994.

regime as they received significantly less snow than all other Plateau top gauges. The aircraft scientist noted that cloud cover was more broken about 15 km south of the RRS-TAR area in the vicinity of gauges FARS and FARSE.

The AgI generator was turned off at 1215 because the storm was obviously ending and the cloud deck over the Plateau was breaking up. By 1230 the aircraft was beginning its final pass before returning to base. The last reference to observed snow in the van was at 1142 as it crossed the Plateau heading toward TAR. Later, after leaving TAR and driving along the upwind highway, the van encountered, "no plumes, no cloud (at the van altitude), no precipitation". The last visual report of any snowfall at the RRS was at 1200. The RRS log reported at 1246, "bright sunshine here, several large convective elements around."

Figure 6 shows that the vertically-integrated SLW over RRS gradually decreased after 0400 until about 1030 and was at low levels thereafter, with the exception of a few short-lived peaks characteristic of convective cell passage. Amounts of SLW were markedly greater during the several hours prior to seeding than during seeding, and likely as a consequence, precipitation decreased with time.

Since the storm was clearly ending by about 1200, precipitation accumulations were carefully extracted

from the chart records with the aid of magnification for exactly 3.5 h after the estimated time of AgI plume arrival at (or crosswind of) each gauge. This placed the ending times between 1205 to 1240 and the resulting 3.5 h accumulations and equivalent hourly rates are listed in Table 3. In fact, snowfall had ended at all seeded gauges between 1100 to 1130. Nonseeded gauge TARNW again received snowfall from 1300 to 1320, with an accumulation of 0.38 mm. That brief episode likely was caused by a small convective shower as no other gauge detected snowfall at or near that time period.

Examination of the 3.5 h totals from Table 3, plotted on Fig. 1, suggests that seeding may have increased the snowfall at three of the four Plateau-top gauges under the AgI plume (DASNE, TARSW and TAR). These sites had somewhat more accumulation than RDJNC and TARNW, both north of the plume, each of which received 0.76 mm. Differences between these seeded and nonseeded gauges averaged 0.5 mm (0.02 inch), a limited amount over 3.5 h. Moreover, seeded gauges TARE and TARSE received less snowfall than DASNE or TARNW. The TARE observation might be anticipated because the gauge is on the Plateau's lee slope and so could be expected to be under subsiding, drying air. But there is no obvious reason why seeded gauge TARSE should have received so little snowfall. Consequently, it is possible but not certain that seeding increased the snowfall at a few gauges. However, any such increases were quite limited in magnitude in spite of the pronounced microphysical evidence of seeding from the aircraft and van 2D-C probes. Minor snowfall increases might be expected in view of the limited available SLW. The SW to NE gradient in total precipitation received by the seeded gauges is consistent with the indications of Fig. 4f. That gradient, and the 2D-C observations of aggregates along the upwind highway, suggest that most seeded snowfall reached the surface before the Plateau top's east edge, in agreement with the discussion of Sec. 5.

7. APPLICATION OF CLARK MESO-SCALE MODEL

7.1 The Model and its Configuration

Although field observations were diverse and of high quality, their horizontal density was limited. Moreover, an approximately 600 m vertical layer

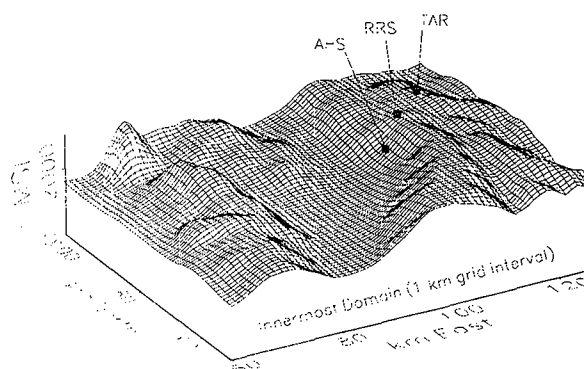


Fig. 7. Terrain for innermost domain used in the modeling. The vertical dimension has been exaggerated by a 9-to-1 factor.

above the Plateau top (300 m above highest terrain) could not be sampled because of aircraft safety considerations. Numerical modeling provides an opportunity to "fill in" the data sparse regions and to test application of treatment strategies.

The mesoscale model of Clark and associates of NCAR (Clark 1977, Clark and Farley 1984, Clark et al. 1994) was applied to this case study. The model is three dimensional and time dependent. The formulations are nonhydrostatic and anelastic, implying vertical accelerations are allowed, but the anelastic continuity equation is used to eliminate acoustic-scale waves. The model uses geo-spherical nonorthogonal coordinates with terrain following vertical coordinates such that the lowest grid points of the model are aligned with the terrain, and the top is at a constant level. For the application herein it was run in four dimensions, x , y , z and t , using three interactively nested domains to insure broader mesoscale patterns contributed to the fine-scale innermost resolution, while not exceeding computer resources. All the domains had a stretched vertical increment beginning with $\Delta z = 100$ m at the surface, increasing to $\Delta z = 1$ km by $z = 18$ km. The horizontal grids were 18 by 18, 30 by 30 and 66 by 54 for the outer, middle and innermost domains. The grid spacings of these domains were 9 km, 3 km, and 1 km respectively, and their time increments were 20, 10 and 5 s. Further details of the model setup as applied to the Plateau are given by Heimbach and Hall (1994).

Figure 7 depicts the terrain modeled for the innermost domain and shows the locations of AHS, RRS

and TAR. The terrain has been twice run through a two dimensional nine-point smoother to insure computational stability. The gross features of the terrain have been captured; however, smaller canyons have been smoothed out.

"Warm cloud" microphysics are simulated using a modified form of the Kessler (1969) bulk parameterization. In this context warm cloud means unfrozen condensate which may be supercooled. The bulk parameterization assumes a Marshall-Palmer raindrop distribution. Condensation and evaporation are included. The ice microphysics are parameterized using the techniques of Koenig-Murray (Clark and Hall 1994, Bruintjes et al. 1994). There are two types of ice particles in this approach; those which are initially small and are produced by heterogeneous nucleation (type A), and those produced by freezing rain which are initially larger (type B). In the model, both types are allowed to be nucleated, grown by diffusion and accretion, and lost by sublimation and melting. The aggregation process is not included in the current version of the Clark model. Solar heating was not available in the version used.

The model was initialized using a sounding composited from Mount Pleasant (RAW) and Ely, NV, rawinsonde data, and aircraft observations. The 0900 RAW sounding had a saturated, nearly pseudoadiabatic layer between 803 and 695 mb. This layer became unsaturated by the 1100 RAW sounding. The 0500 Ely sounding likewise had a moist pseudoadiabatic layer. All the soundings had a surface inversion. The 0900 RAW sounding was used as a template for the initialization because this sounding was taken near the start of the experiment. The surface layer was changed from an inversion to a slightly stable lapse rate. The surface boundary layer winds were increased to 2 m s^{-1} and given a more westerly direction to reduce the sheltering influence of the Sanpete Valley. To incur computational stability, the last level of the composite sounding was repeated to 5 mb. The composite sounding is shown in Fig. 8.

The model was run on the NCAR CRAY-YMP computer. Job submission and graphics processing were done using workstations accessing the CRAY via the Internet. The model was run for one hour of simulated time with the warm cloud and ice options turned on for stabilization before tracer material was released. After one hour, the AHS AgI release was turned on at 22.5 gm hr^{-1} and the

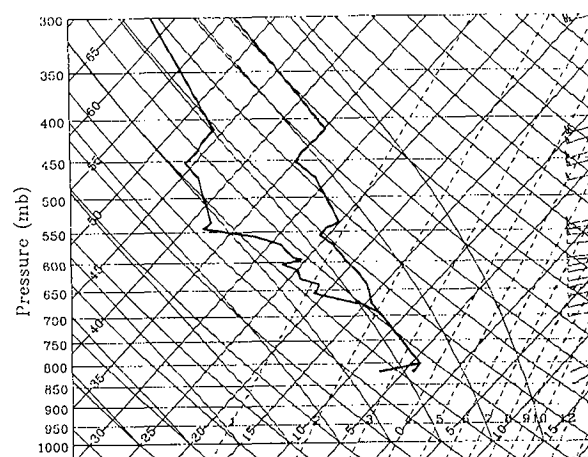


Fig. 8. Sounding used to initialize the model. This was composited from Ely, NV, and Mount Pleasant rawinsonde data, and aircraft data.

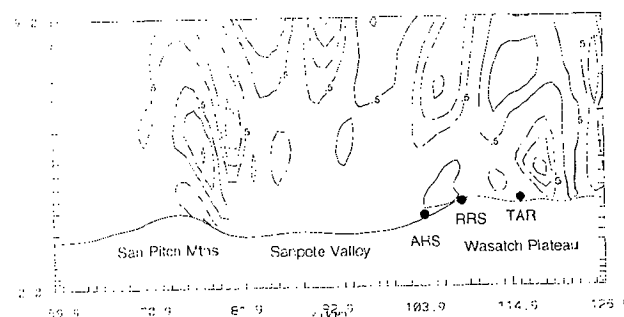


Fig. 9. West-to-east vertical cross section of vertical velocity after 3 h of simulated time. The north-south position of the cross section is approximately through AHS. The solid lines contour positive velocities and the broken lines are negative contours. The contour interval is 0.5 m s^{-1} .

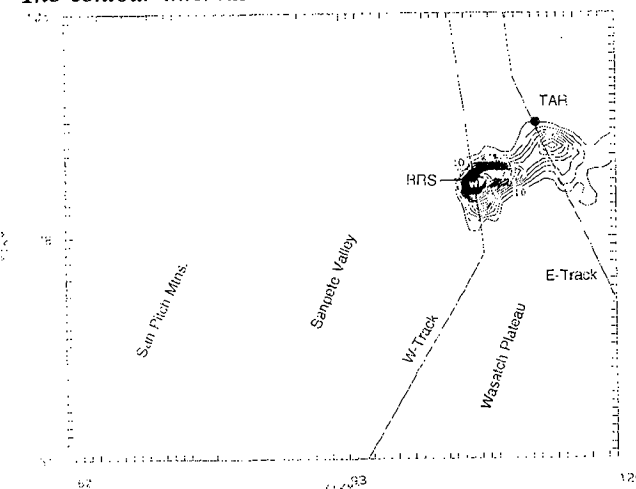


Fig. 10. Model estimates of AgI concentration at the 2.9 km altitude after a 2 h release from AHS. The minimum contour and contour interval are 10 pg m^{-3} .

model was run for an additional two hours. Approximately three hours of CPU time are needed for each hour of simulated time with this configuration.

7.2 Model Results

The model predicted little positive buoyancy at low levels over the Plateau (figure not included). Throughout the run there was negative buoyancy over the Plateau's western edge; that is, a generally stable atmosphere. The overall stable conditions suggest that vertical transport of the plumes was by mechanical means or perhaps by the gravity waves forcing weak convection at some locations. To the south and east outside the experimental area, some limited positive buoyancy was simulated. The initializing sounding was saturated-pseudoadiabatic throughout a deep layer which limited the opportunity for convection to develop within the model. As the upper levels dried out during the experiment, convection was more probable though only observed as weak shallow elements. Aircraft scientist voice notes reported intermittent in-cloud conditions at 3.7 km altitude.

The low level flow was weak and generally westerly throughout the simulation. Figure 9 is a west-to-east vertical cross section of vertical velocity, w , after 3 h of simulation. The cross section is at the 80 km mark in the model which runs approximately through AHS. Gravity waves are present but are weak and poorly organized over the Sanpete Valley due to the limited boundary layer wind speeds. The Rossby number, defined by,

$$R_o = \frac{U}{fL},$$

can be applied to confirm the type of wave motion excited by terrain (Steenburg and Mass 1994). U is the base state wind speed which for this case is on the order of 10 m s^{-1} . The half width of the terrain barrier, L , is approximately 10 km and f is the Coriolis parameter which is approximately 10^{-4} s^{-1} . This gives R_o a value larger than unity, making the Coriolis effect relatively small and giving gravity waves precedence over inertial waves assuming a stable domain is present. If R_o was less than unity, then Rossby waves would be generated.

Above approximately 5 km altitude, the vertical velocity becomes complicated with w having cores of alternating signs in a checker-board pattern. In

this region the model predicted positive buoyancy, which would eliminate the gravity wave process. A secondary core of positive w is simulated over the vicinity of the eastern flight track and this is joined aloft with that over the western Plateau. Between these is a zone of $w < 0$ over the central portions of the Plateau.

The model-simulated AgI transport over the Plateau was weak until the plume reached sufficient altitude to become entrained in organized flow. This took approximately an hour after the start of release one hour into the simulation. Figure 10 is a horizontal depiction of the AgI plume at the 2.9 km level. The contours are in pico grams per cubic meter ($10^{-12} \text{ g m}^{-3}$, hereafter pg m^{-3}). There are two centers of concentration. The western center is over the RRS while the eastern center is southeast of TAR with TAR just on the north edge of the simulated plume. Aircraft measurements indicated the AgI and SF_6 plumes were generally south of a line from RRS to TAR, in good agreement of the model's estimates. At the release point, weak surface winds and numerical diffusion combined to simulate an unrealistically wide lateral plume spread near the surface (figure not shown). Figure 11 is a south-north vertical cross section of the AgI plume which transects a point between AHS and RRS. It shows that in spite of negative buoyancy, an element of the AgI plume did ascend nearly 1 km above ground level. Some IN were detected above cloud tops implying that vertical IN transport did not rely entirely upon saturated processes.

The aircraft detected a strong IN plume at 3.9 km, but found none at 4.1 km. In Fig. 11, the smallest IN concentration contour (10 pg m^{-3}) reaches an elevation of 3.8 km. At 3.9 km, the model's estimated peak IN concentration was 10 pg m^{-3} (figure not shown). We assume the output of the DRI AgI generator was about $10^{16} \text{ IN gm}^{-1}$ at -20°C . This is an order of magnitude more than at the coldest temperature sampled (-12°C) in a recent calibration of the DRI generator. This extrapolation is justified by comparing the DRI generator's calibration curve to that of other generators burning the same solution. This generator output combined with the model results implies 100 IN L^{-1} (at -20°C) are possible at 3.9 km. Using co-released SF_6 as an indicator of plume width, the aircraft required 28 s to cross the plume. The NCAR IN counter sample rate was 12.2 L min^{-1} and the total number of IN detected during that penetration was 272. Assuming a 10:1 cloud chamber loss results in 477 IN L^{-1}

effective at -20°C , the cloud chamber temperature. The model's estimate is approximately 20 percent of this calculated value. At the surface, the model predicted concentrations of AgI in excess of 100 pg m^{-3} . Converting this value as above gives surface concentrations in excess of 1000 L^{-1} . Values this high generally were not measured on the surface. The van data in the plume averaged 270 L^{-1} . However, large IN values were seen at TAR during the wind shift interval (average 948 L^{-1}) and for a 71-second part (average 1475 L^{-1}) of van pass 2 after the windshift started (both near Fig. 2 abscissa -37). While the plume was usually more dense at the surface on other dates, it appears to have been lifted during this study.

Figure 10 shows an AgI plume width of about 9 km at the Plateau top. This is in disagreement with the 2 to 5.5 km width actually measured at the lower aircraft and van levels and the 7 km width of the sheared tops along the eastern track (Fig. 2). The low wind speeds, long transport times and plume initialization procedures in the model are likely responsible for this difference. The actual plume (Fig. 4c) appears to have risen more rapidly and farther upwind from RRS than shown in Figs. 10 and 11. The secondary peak near TAR, however, is confirmed with the actual data in Fig. 4c. Actually, the case study measurements are the more unusual. The normal plumes over the Plateau on other dates appeared to hug the ground, be of higher concentration there, and were generally wider at Plateau top than at aircraft levels. As seen in Fig. 2, the aircraft level plume widths were the same as or wider than those measured by the van during this particular experiment.

The model predicted weak warm cloud processes over the Plateau which were forced by orography and gravity waves, while not being supported by buoyancy. Figure 12 depicts modeled cloud liquid water concentrations at 2.9 km after 3 h of simulated time. The occurrences are intermittent but are concentrated along the western edges of both the Plateau and the San Pitch Mountains. The major concentration southwest of RRS is in close agreement with the actual measurements shown in Fig. 2a. Both show a cloud of roughly 10 km size near the west track. Most aircraft passes did not explore the extent of the cloud upwind of RRS. Pass 14, flying along the plume from NE to SW, exited the cloud near the "approx. plume edge" position of Fig. 4. The LWC of 0.05 g m^{-3} in the 2 km zone upwind of the SF_6 plume was about twice that in

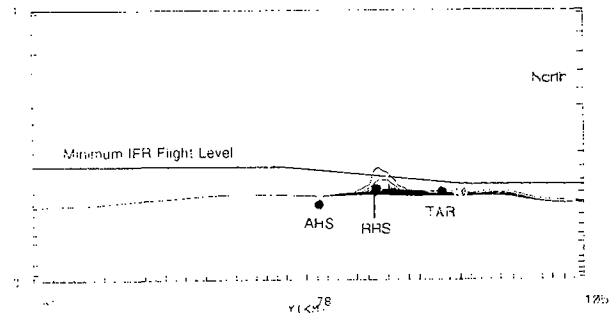


Fig. 11. AgI concentrations on a south-north vertical cross section through a point between AHS and RRS after 2 hr release time. The minimum contour and contour interval are 10 pg m^{-3} .

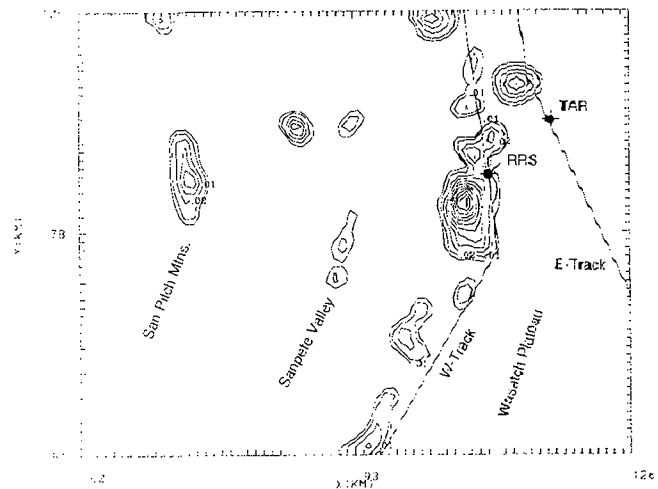


Fig. 12. Cloud liquid water concentrations at 2.9 km altitude after 3 hr simulated time. The minimum contour level and contour interval are 0.01 g m^{-3} .

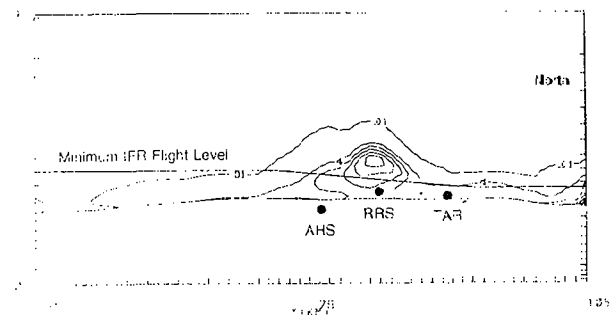


Fig. 13. Concentrations of small homogeneously-nucleated ice particles (Type A) on a south-north vertical cross section through a point between RRS and AHS. The contour interval is 4.0 L^{-1} and the 0.01 contour has also been drawn.

the adjacent plume. Perhaps the cloud was indeed more extensive upwind and wetter at earlier times in the day. The model-predicted intermittent occurrence of cloud elements is supported by aircraft scientist observations of, "in and out of clouds at 12.3 kft" (3.7 km). There are also several elements over the Sanpete Valley which are in response to weak gravity waves. A convective element was observed over the Sanpete Valley by the air crew.

In an analogous application of the Clark model to the Mogollon Rim in Arizona, Bruintjes et al. (1994) found complex flow and condensation patterns forced by orography and gravity waves. Likewise, Heimbach and Hall (1994) found complicated tracer and condensation patterns predicted by the model for a 1991 case on the Plateau. Both cited cases had stronger low-level winds and the gravity wave patterns were better organized than for the present case study. Although the present case had weak surface winds, gravity waves still appeared to be important for the vertical transport of seeding material and formation of condensation.

The model simulated ice formation within the warm cloud process. Figure 13 shows concentrations of ice type A (small heterogeneously nucleated crystals) on a south-north vertical cross section between AHS and RRS. The top of the ice is variable, as was the case for the warm cloud top, and the greatest ice elevation corresponds to that of the warm cloud top and peak vertical velocity. Type A ice was simulated in the vicinity of TAR, but higher concentrations were found to the south. Areas of type B ice occurrence were found by the model to be limited to zones in the vicinity of RRS and HAS (figure not shown).

8. SUMMARY AND CONCLUSIONS

The 21 February 1994 case was analyzed for plume characteristics including seeding responses for a single AgI plume co-released with SF₆ tracer gas well up the windward side of the Wasatch Plateau. The day was characterized by weak winds primarily from the southwest with weak convection enabling vertical transport of AgI to flight levels. The exposure of sites and mobile sampling platforms to the plume was estimated using a frame of reference which moved with the average wind. This enabled spatial and temporal coordination of multiple plume encounters, and allowed a uniform objective definition of nonseeded periods and locations. For the

sampling aircraft, nonseeded portions of a flight path were 24 s flight intervals 12 s on either side of the co-released SF₆ plume. The nonseeded zones for the instrumented van were 2 km distances 1 km outside the SF₆ plume.

The plume was estimated to have been over particular ground sites for 4.25 h and to have generally moved from 235 degrees with a short period having a more southerly component. The angular plume width over the west flight track was estimated to have been 15 degrees with a brief wider period associated with a wind shift. Vertical plume transport to the Plateau top and to flight levels was rapid in the presence of limited horizontal wind speeds.

High concentrations of ice particles were associated with measured and predicted plumes at locations sampled by the van and aircraft. Ice particle concentrations and precipitation rates were enhanced, compared to nonseeded zones, by factors of about 10 for upwind highway van measurements, 40 for west track aircraft measurements, and variable amounts for east track aircraft passes. Ice water contents were always greater in the plume than in the nonseeded zones. Particle trajectories and concentration patterns indicated that most growth and precipitation occurred near the west track, where there was the most SLW available. Aggregation of high concentrations of ice particles appeared to be the mechanism for greater precipitation rates in the plume. Little snow was left to fall over the eastern ridge of the Plateau. Winds were atypically light during this experiment so that seeded snowfall for windier cases might be expected to settle further eastward.

Comparisons of precipitation totals between seeded and nonseeded gauges were suggestive that seeding may have produced a limited snowfall increase over period of the experiment of perhaps 0.5 mm at some gauges. However, one eastern seeded gauge received less snowfall than two nonseeded gauges also on top of the Plateau. Analyses of observations and physical reasoning suggest that most seeded snowfall settled to the Plateau top before crossing to its east edge, and perhaps before reaching the middle of the Plateau top at gauge TARSW. In retrospect, one or more gauges would have been useful along the upwind highway a few km north of RRS.

Updrafts predicted by the Clark model were associated with the windward edge of the Plateau and

were generally limited to 0.5 m s^{-1} near the surface. There were areas of stronger down drafts over the Plateau, reaching speeds of -1.5 m s^{-1} . The complex gravity wave pattern forced a secondary maximum of tracer material several km south of TAR and some additional condensation over the northern portions of the eastern flight track.

The model suggests the case had weaker transport and diffusion of tracer material over the Plateau than indicated by field measurements. The plume transport time over the Plateau was slower than reality; however, the model ultimately simulated transport of AgI into liquid water cloud over the Plateau. The heights to which the simulated plumes were transported were in reasonable agreement with aircraft observations, but the simulated lateral spread was excessive at the surface. The model's smoothed terrain likely contributed to the less organized transport because the simulated canyons were shallow enough to limit the funneling of the poorly organized surface winds. The actual terrain consisted of a pronounced canyon downwind of AHS which likely limited crosswind horizontal dispersion within the canyon. The simulated clouds and ice were weak and shallow because buoyancy was not part of their formation. It is believed that buoyancy from solar heating did contribute to the observed clouds, and for that reason also contributed to a more vigorous vertical plume transport than was simulated. Overall, the model simulation produced a reasonable first-approximation of reality.

In summary, AgI seeding during this experiment produced strong microphysical evidence of markedly enhanced ice particle concentrations on the Plateau top and at aircraft levels. Plumes released on the windward slope were readily transported over the Plateau in spite of limited horizontal winds. Plume widths were limited, suggesting seeding generators at similar high altitude sites should be spaced no more than 5 km crosswind. Horizontal dispersion from other high altitude sites could be more or less than from AHS depending upon local topography.

Seeding apparently increased the snowfall, especially on the western portion of the Plateau top, but accumulations were limited. Seeding appeared to significantly increase the aggregation of snowflakes along the upwind highway. Best estimates of snowfall rates caused by seeding are 0.4 mm h^{-1} based on 2D-C estimates along the upwind highway

(Table 2), and less than half that rate from gauges on the central and eastern portions of the Plateau top (Sec. 6). Of course, SLW amounts were quite limited during this weak and diminishing final portion of the storm, so seeding potential would be expected to be quite limited as well.

Overall, the results of this experiment are in general agreement with current physical understanding of how winter orographic seeding should work.

Acknowledgments

Many individuals contributed to the success of the 1994 Wasatch Plateau field program. Notable among them are Clark Ogden, Erick Faatz, Dennis Faatz and Barry Saunders of the Utah Division of Water Resources; Dennis Wellman and Stan Wilkison of NOAA; Arlen Huggins and Melanie Wetzel of the Desert Research Institute; Glenn Cascino, Jack McPartland, Arlen Hilton and Roger Hansen of the Bureau of Reclamation; and Bill Hauze of North American Weather Consultants. Gerhard Langer checked the field operation of the NCAR IN counter. Terry Clark and Bill Hall of NCAR provided generous help in adapting their numerical model to the Utah program and in interpreting the results. This applied research was primarily funded by the Utah/NOAA AMP in cooperation with the Utah Division of Water Resources. Various equipment resources were supplied by the Bureau of Reclamation, and CRAY-YMP computer time was provided by NCAR which is partly funded by the National Science Foundation. The reviewers are thanked for their many helpful comments which improved this paper.

9. REFERENCES

- Benner, R.L. and R. Lamb, 1985: A fast response continuous analyzer for halogenated atmospheric tracers. *J. Atmos. Oceanic Tech.*, **2**, 582-589.
- Bruintjes, R.T., T.L. Clark and W.D. Hall, 1994: Interactions between topographic air flow and cloud precipitation developing during the passage of a winter storm in Arizona. *J. Appl. Meteor.*, **51**, 48-67.
- Clark, T.L., 1977: A small scale dynamic model using terrain following coordinate transformation. *J. Comp. Physics*, **24**, 186-215.

- _____ and R.D. Farley, 1984: Severe down-slope windstorm calculations in two and three spatial dimensions using anelastic interactive grid nesting: a possible mechanism for gustiness. *J. Atmos. Sci.*, **41**, 329-350.
- _____, W.D. Hall and R.M. Banta, 1994: Two- and three-dimensional simulations of the 9 January 1989 severe Boulder windstorm: comparison with observations. *J. Atmos. Sci.*, **51**, 2317-2343.
- DeMott, P.J., A.B. Super, G. Langer, D.C. Rogers, and J.T. McPartland, 1995: Comparative characterizations of the ice nucleus ability of AgI aerosols by three methods. *J. Wea. Mod.*, **27**, in press.
- Deshler, T.D. and D.W. Reynolds, 1990: The persistence of seeding effects in a winter orographic cloud seeded with silver iodide burned in acetone. *J. Appl. Meteor.*, **29**, 477-488.
- _____, _____, and A.W. Huggins, 1990: Physical response of winter orographic clouds over the Sierra Nevada to airborne seeding using dry ice or silver iodide. *J. Appl. Meteor.*, **29**, 288-330.
- Finnegan, W.G. and R.L. Pitter, 1988: Rapid ice nucleation by acetone-silver iodide generator aerosols. *J. Wea. Mod.*, **20**, 51-53.
- Griffith, D.A., J.R. Thompson and D.A. Risch, 1991: A winter cloud seeding program in Utah. *J. Wea. Mod.*, **23**, 27-34.
- Goodison, B.E., 1978: Accuracy of Canadian snow gage measurements. *J. Appl. Meteor.*, **17**, 1542-1548.
- Heimbach, J.A. and A.B. Super, 1988: The Bridger Range, Montana, 1986-1987 snow pack augmentation program. *J. Wea. Mod.*, **20**, 19-26.
- _____, and W.D. Hall, 1994: Applications of the Clark Model to winter storms over the Wasatch Plateau. *J. Wea. Mod.*, **26**, 1-11.
- Heymsfield, A.J., 1986: Aggregates as embryos in seeded clouds. *Precipitation Enhancement-A Scientific Challenge, Meteor. Monogr.*, No. 43, Amer. Meteor. Soc, 33-41.
- Hogg, D.C., F.O. Guiraud, J.B. Snider, M.T. Decker and E.R. Westwater, 1983: A steerable dual-channel microwave radiometer for measurements of water vapor and liquid in the troposphere. *J. Climate Appl. Meteor.*, **22**, 789-806.
- Holroyd, E.W., 1987: Some techniques and uses of 2D-C habit classification software for snow particles. *J. Atmos. Ocean. Tech.*, **4**, 498-511.
- _____, and J.E. Jiusto, 1971: Snowfall from a heavily seeded cloud. *J. Appl. Meteor.*, **10**, 266-269.
- _____, J.T. McPartland and A.B. Super, 1988: Observations of silver iodide plumes over the Grand Mesa of Colorado. *J. Appl. Meteor.*, **27**, 1125-1144.
- Huggins, A.W., 1994: *Final report; Desert Research Institute Field Operations 1994 NOAA/UTAH Field Program*. Reno, NV. 77pp.
- _____, 1995: Mobile microwave radiometer observations: Spatial characteristics of supercooled cloud water and cloud seeding implications. *J. Appl. Meteor.*, **34**, 432-446.
- Kessler, E., 1969: On the distribution and continuity of water substance in atmospheric circulations. *Meteor. Monogr.*, No. 32, Amer. Meteor. Soc., 94pp
- Langer, G., 1973: Evaluation of NCAR ice nuclei counter. Part I: Basic operations. *J. Appl. Meteor.*, **10**, 1000-1011.
- Steenburg, W.J. and M.J. Mass, 1994: The structure and evolution of a simulated Rocky Mountain lee trough. *Mon. Wea. Rev.*, **122**, 2740-2761.
- Super, A.B., 1994: Implications of early 1991 observations of supercooled liquid water, precipitation and silver iodide on Utah's Wasatch Plateau. *J. Wea. Mod.*, **26**, 19-32.
- _____, 1995: Case studies of microphysical responses to valley-released operational AgI seeding of the Wasatch Plateau, Utah. *J. Wea. Mod.*, **27**, in press.

Super, A.B. and B.A. Boe, 1988: Microphysical effects of wintertime cloud seeding with silver iodide over the Rocky Mountains. Part III: Observations over the Grand Mesa, Colorado. *J. Appl. Meteor.*, **27**, 1166-1182.

_____, _____, E.W. Holroyd and J.A. Heimbach, 1988: Microphysical effects of wintertime cloud seeding with silver iodide over the Rocky Mountains. Part I: Experimental design and instrumentation. *J. Appl. Meteor.*, **27**, 1145-1151.

_____ and J.A. Heimbach, 1983: Evaluation of the Bridger Range winter cloud seeding experiment using control gages. *J. Climate Appl. Meteor.*, **22**, 1989-2011.

_____ and _____, 1988: Microphysical effects of wintertime cloud seeding with silver iodide over the Rocky Mountains. Part II: Observations over the Bridger Range, Montana. *J. Appl. Meteor.*, **27**, 1152-1165.

_____ and E.W. Holroyd, 1994: Estimation of effective AgI ice nuclei by two methods compared with measured ice particle concentrations in seeded orographic cloud. *J. Wea. Mod.*, **26**, 33-40.

**CASE STUDIES OF MICROPHYSICAL RESPONSES TO VALLEY-RELEASED
OPERATIONAL AgI SEEDING OF THE WASATCH PLATEAU, UTAH**

Arlin B. Super

Bureau of Reclamation
Denver, CO 80225

ABSTRACT

An experimental field program was conducted on the Wasatch Plateau of central Utah in early 1991. Objectives included monitoring of the transport and dispersion of valley-released silver iodide and associated microphysical effects within the seeded clouds. Silver iodide ice nuclei were monitored by acoustical ice nucleus counters in a truck, an aircraft and at a Plateau-top observatory. An aircraft-mounted ice particle imaging probe was used to search for ice particle concentration differences between the seeded cloud and crosswind, nonseeded cloud. Other instruments monitored wind, cloud liquid water content, temperature and other parameters of interest.

Six experiments are described in detail, representing all aircraft sampling periods during which valley-released AgI (silver iodide) was transported to both Plateau-top and aircraft altitudes. Embedded convection was present during five of the experiments which probably enhanced vertical AgI transport. Clouds bases were generally a few hundred meters below the Plateau top with one exception which had bases above the Plateau. The valley-released AgI consistently had a pronounced vertical gradient above the Plateau. Concentrations of AgI ice nuclei, effective at -20°C , were typically at least an order of magnitude less at lowest aircraft altitudes than found on top of the Plateau. Silver iodide was seldom detected as high as 1 km above the Plateau top.

No evidence was found for enhanced ice particle concentrations at aircraft altitudes during the three experiments with sampling zone temperatures of -9°C and above. However, suggestions of increased ice particle concentrations were found when sampling zone temperatures were colder. Silver iodide ice nuclei estimates, effective at prevailing supercooled liquid cloud temperatures, were lower than believed desirable for effective seeding during the three experiments with warmer cloud at aircraft sampling altitudes.

The results presented are believed to indicate that current operational cloud seeding in Utah produces insignificant increases in ice particle concentrations and snowfall rates during warmer storm episodes. The main problem appears to be that concentrations of effective ice nuclei are too low for the typical mildly supercooled liquid water clouds reached by the AgI. Seeding appeared to markedly increase the ice particle concentration in colder supercooled clouds, and precipitation observations suggested associated limited snowfall increases during some cases. A number of recommendations are made for increasing ice particles concentrations in the warmer supercooled liquid clouds.

1. INTRODUCTION

The Utah/NOAA (National Oceanic and Atmospheric Administration) Atmospheric Modification Program conducted a series of experiments over the Plateau (Wasatch Plateau) of central Utah between mid-January and mid-March 1991. The main experimental goals were to monitor the transport and dispersion of ground-released AgI (silver iodide) IN (ice nuclei), and possible associated changes in cloud microphysics. The most obvious cloud microphysical change was expected to be increased IPC (ice particle concentration) when AgI IN created additional ice crystals in SLW (supercooled liquid water) cloud.

The main purpose of this paper is to attempt to document seeding effects, in particular IPC changes, at aircraft sampling altitudes during storm periods seeded by valley generators (ground-based AgI generators located in mountain valleys). It is important to document any microphysical changes associated with valley seeding because the Utah operational seeding program relies almost completely on valley AgI releases. In order for the valley seeding to be effective in snowfall enhancement, the seeding must increase IPC within SLW cloud, at least part of the time with orographic (mountain-induced) clouds present.

Experimental periods were selected which had significant valley AgI IN transport into SLW cloud over the Plateau. The AgI was monitored along a 6.7 km north-south portion of the Plateau top's windward edge and at aircraft levels.

Some past physical studies have questioned the effectiveness of valley seeding in Utah. For example, Super and Huggins (1992a) showed a low frequency of above-background silver-in-snow from valley AgI seeding. Limited silver-in-snow was found even above a canyon that had consistent AgI transport from its lower portions to a sampling site well up the canyon. Super and Huggins (1992a) presented calculations that suggested the Utah valley AgI generator network was unlikely to produce snowfall enhancements approaching 10 percent unless

either: (a) AgI IN effectiveness in winter orographic clouds was substantially greater than indicated in cloud simulation laboratory generator calibrations or (b) ice multiplication was often effective in Utah winter clouds.

Super and Huggins (1992a) made a number of optimistic assumptions in their calculations including that, on average, 5×10^{13} ice nuclei per gram of AgI effective at SLW cloud temperatures would be produced by the NAWC (North American Weather Consultants) manual AgI generators operationally used in Utah. That assumption was based on the most recent Colorado State University Cloud Simulation Laboratory calibration of the NAWC generator then available, done in 1981 (reported April 1982). Their assumption has been reconsidered because a more recent calibration, reported by DeMott et al. (1995), showed greatly enhanced ice formation activity at temperatures warmer than -10°C , apparently due to improvements in the combustion design of the NAWC generator. The latest calibration indicates that 5×10^{13} ice nuclei per gram of AgI might be achieved at cloud temperatures colder than -7.5°C . Consequently, the generator effectiveness value used in the calculations by Super and Huggins (1992a) now appears more realistic than optimistic. Nevertheless, review of the several other optimistic assumptions they made suggests there remains a need to be concerned about possible low seeding rates in the Utah operational program.

Super and Huggins (1992b) presented the results of five aircraft missions under near-storm prefrontal conditions during early 1990. Four of the missions showed real or simulated (tracer gas) valley-released AgI was transported parallel to the mountain barrier rather than over it, or the material was trapped by low-level stability. The single mission with plume transport over the barrier suggested low AgI IN concentrations. However, the five missions did not have embedded convection present, as did all but one of the early 1991 missions to be presented.

Sassen and Zhao (1993) discussed the

cloud seeding implications of remote-sensing data obtained in the Tushar Mountains of southern Utah. They concluded that, "there appears to be only a limited 'window' for success involving mainly the upper portions of the relatively warm (greater than -7°C cloud-base temperature) SLW clouds containing significant (>0.15 mm) LW depths. In other words, cloud layers with inferred cloud-top temperatures of colder than about -12°C in this region appear to be efficient users of orographically generated SLW." Therefore, according to Sassen and Zhao (1993), clouds with the top of their SLW layer warmer than -12°C and their base warmer than -7°C appear to be the primary "target" for southern Utah cloud seeding. (Visual cloud tops may be much higher and colder than the inferred SLW cloud tops if the former consist of ice particles.) As will be discussed, it may be difficult to achieve significant IPCs in such warm clouds with AgI seeding as currently practiced in Utah.

Super (1994) summarized AgI IN observations on the Plateau top during 12 days of the early 1991 field program that had valley seeding and observations during at least part of the day. The 6 experiments described herein are from 4 of those 12 days. Figure 4 of Super (1994) suggests that less than half of the 144 h with AgI IN observations and detectable SLW would have exceeded 2 IN L^{-1} on the Plateau top, effective at -10°C . The AgI would have to be transported well above the Plateau top to reach the -10°C level during most winter storms, and, as will be shown, AgI IN concentrations decrease rapidly with altitude above the Plateau top. However, Super (1994) based his estimates on a 1981 calibration of the NAWC AgI generator which indicated AgI IN effectiveness at -10°C was 1 percent of that measured at -20°C (the cloud chamber temperature for the acoustical IN counter used to monitor AgI concentrations). A recent calibration of that generator reported by DeMott (1995) indicates that the -10°C effectiveness is about 33 percent of the -20°C value. Hence, the abscissa values of Fig. 4 of Super (1994) should be multiplied by 33 to correspond with the latest calibration, resulting in a more optimistic assessment of valley seeding potential. However, a major

uncertainty in that assessment remains; namely, how representative are Plateau top observations of AgI IN concentrations at higher, colder altitudes where AgI nucleation is more likely. The present study addresses that uncertainty.

2. EXPERIMENTAL APPROACH

Some past investigations have documented physical seeding effects from high altitude, ground-based AgI generators (e.g., Super and Heimbach 1988; Super and Boe 1988; Super and Holroyd 1994) or aircraft seeding (e.g., Deshler et al. 1990; Deshler and Reynolds 1990). A recent paper documents physical responses to a high-altitude ground release of AgI over the Plateau (Holroyd et al. 1995). The most obvious microphysical effect in these studies was a distinct increase in the IPC associated with seeding plumes. Accordingly, the early 1991 Utah experiments were designed to monitor the IPC within seeded orographic clouds and neighboring (crosswind) unseeded clouds. An aircraft-mounted Particle Measuring Systems 2D-C laser imaging probe was used for IPC measurements in the 1991 Utah field program. The software of Holroyd (1987), used in most of the studies referenced in this paragraph, was also used with the Utah data in this investigation. As in the past studies, particles smaller than $100 \mu\text{m}$ (4 pixels length) were ignored by the processing software.

No surface IPC measurements were made on top the Plateau during the experiments to be discussed. An attempt to monitor IPCs with a truck-mounted 2D-C probe was thwarted by a road accident earlier in the field program. A network of five shielded precipitation gauges, sited in locations protected from the wind, provided snowfall rates with a resolution of 0.25 mm h^{-1} . Some visual observations were made of snowfall rates and ice crystal types and sizes. These surface observations will be referred to where appropriate.

Silver iodide was released from a network of AgI generators of the type discussed by Griffith et al. (1991). Each generator released $8 \text{ g AgI IN h}^{-1}$ according to Griffith

et al. (1992). The north-south extent of the network, shown on Fig. 1, was 40 km. The number of generators was increased for the 1991 experiments to reduce the probability of nonseeded gaps between plumes over the Plateau. Eight generators were used during the 1991 field program in the portion of the Sanpete Valley shown on Fig. 1 rather than the five generators used before and after that field program. Generator elevations ranged from 1735 to 1835 m with the exception of the northernmost generator which was at 2050 m (all elevations and altitudes are given above mean sea level).

Silver iodide IN was monitored by three NCAR (National Center for Atmospheric Research) acoustical IN counters (hereafter NCAR counter), described by Langer (1973). One NCAR counter was located in the NOAA KingAir C-90 instrumented aircraft, one was located in a 4-wheel drive vehicle (hereafter Suburban), and one was located at the DOT (Department of Transportation snowplow shed) weather observatory located at 2700 m near the head of Fairview Canyon which is

east-northeast of the town of Fairview (Fig. 1). This pronounced canyon was expected to provide a preferred path for transport of valley-released AgI IN to the Plateau top.

Rawinsondes were released and tracked from the MPA (Mt. Pleasant Airport) at 1780 m during experimental periods. Surface winds, temperatures, and relative humidities were monitored by automated weather stations at the airport, at two sites within Fairview Canyon (2025 and 2205 m) and at the 2500 m HAS (High Altitude seeding Site), all shown on Fig. 1. Wind, temperature and dewpoint temperature observations were made at the DOT. A microwave radiometer (Hogg et al. 1983) measured vertically-integrated SLW above the DOT which was rarely warmer than 0°C during storms.

Six aircraft missions (also called experiments) were selected for detailed analysis from 4 days: 28 February, 1 March, 2 March, and 6 March, 1991. These missions provided the most comprehensive 1991 aircraft observations during valley-seeded storm periods which had AgI transported over the Plateau. A few other aircraft missions were conducted during storm periods with valley seeding, but possible problems exist with aircraft data (e.g., suspected ice blockage of sample air intake), or little evidence of valley-released AgI was found at aircraft altitudes (e.g., the experiment of 17 February discussed by Super and Holroyd 1994). Transport to aircraft levels on the dates noted is believed to have been aided by embedded convection with the possible exception of 6 March which, however, experienced an upper level trough passage.

Instrumentation characteristics and analysis procedures are described in detail for 28 February, the first experiment discussed, except for the surface precipitation network. Since no snowfall was measured during the 28 February experiment the surface precipitation network is instead described with the first experiment of 1 March. The same types of measurements and procedures were used with the other experiments.

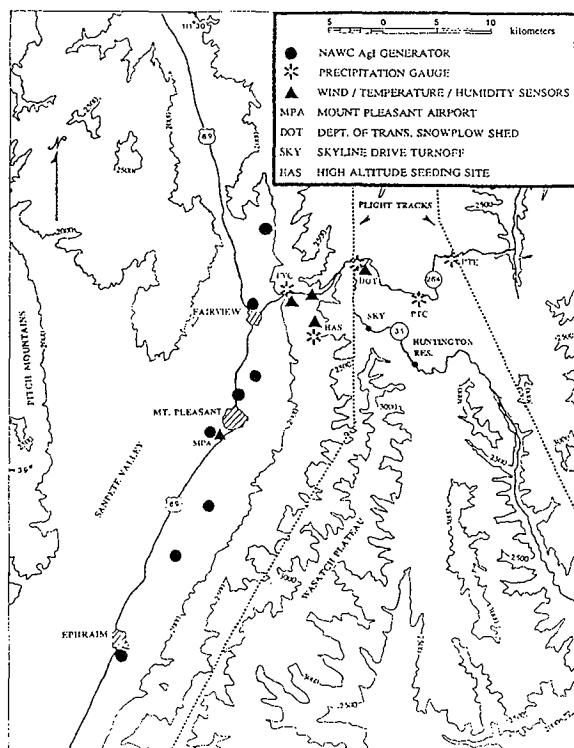


Fig. 1. Map of the Wasatch Plateau Experimental Area. Contours are in meters above mean sea level.

3. SINGLE EXPERIMENT OF 28 FEBRUARY

3.1 Overview

All eight valley AgI generators were ignited between 0800 and 0900 (all times MST [mountain standard time]) and continued to operate throughout the day. Aircraft sampling over the Plateau was done between 1330 and 1620 in marginal VFR (visual flight rules) and IFR (instrument flight rules) conditions.

Although a mid-morning frontal passage had occurred, conditions during the experiment were more typical of a prefrontal environment because southwesterly flow continued with significant SLW over the Plateau (Huggins et al. 1992).

The MPA rawinsonde launched at 1500 showed a neutral atmosphere below cloud base and convective instability within the cloud layer. The liquid cloud base was above the Plateau near 3500 m. Visible cloud bases were variable in altitude above the Plateau. Weak embedded convection was visible and occasional snow showers reached the ground. Clouds tops, as measured by K_a -band radar and visual observations, were between 4200 and 5500 m during the aircraft mission. Corresponding radar top temperatures, estimated from rawinsonde observations, were between -12 and -21°C .

Surface winds measured about 3 km east of the entrance to Fairview Canyon, at 2205 m elevation, were westerly (up-canyon) during the experiment at between 3 and 4 m s^{-1} . (All references to canyon flow are from this site's measurements.) Winds on top of the Plateau at the DOT were southwesterly between 5 and 9 m s^{-1} . The DOT site is a relatively protected location and its winds were consistently less than occasionally measured at canyon heads along the upwind highway. Aircraft-measured winds were southwesterly between 10 and 18 m s^{-1} in the 3000 to 4000 m layer.

The lower panel of Fig. 2 shows the time history of vertically-integrated SLW observed by microwave radiometer above the DOT site.

Figure 2 indicates that SLW was present throughout the experiment with amounts sometimes exceeding 1 mm, a relatively high value for Utah winter storms (Super 1994). The rapid SLW fluctuations over time are characteristic of embedded convection.

The DOT air temperature and dewpoint temperature were nearly constant during this experiment, at 0 and -5°C , respectively.

3.2 NCAR Counter Observations

Each ice crystal nucleated in the NCAR counter's cloud chamber that grows larger than about 20 μm produces an audible "click" when exiting the chamber through a specially-shaped glass sensor. This sound is electronically monitored, producing a "count." About 10 L of air are drawn through the cloud chamber each minute. The raw counts were multiplied by a factor of ten to correct for known crystal losses to glycol-covered cloud chamber walls and bottom cone (Langer 1973). All NCAR counter IN concentrations will be reported as effective at -20°C , the cloud chamber

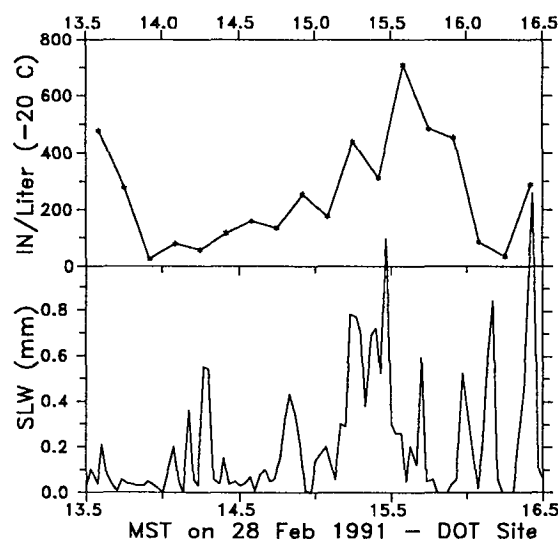


Fig. 2. Temporal distributions of vertically-integrated SLW (microwave radiometer) and AgI IN (NCAR counter) at the Wasatch Plateau DOT site during the aircraft mission of 28 February 1991. Averaging times are 2 min for SLW and 10 min for AgI IN.

temperature, unless otherwise noted, and all IN concentrations will include the times ten correction for crystal losses. A recent series of comparisons between NCAR counters (using the times ten correction) and the Colorado State University isothermal cloud chamber showed reasonable agreement with AgI aerosol (DeMott et al. 1995).

The 1991 field observations showed that IN concentrations as measured by the NCAR counter did not exceed 1 IN L^{-1} in the absence of AgI release, and were usually well below that value. This is in agreement with past and more recent NCAR counter observations in the intermountain West. It is unknown how well such observations represent actual concentrations of natural and anthropogenic IN in the absence of AgI. However, with the low background under 1 IN L^{-1} , the NCAR counter is very sensitive to AgI IN concentrations exceeding even a few per liter.

The upper panel of Fig. 2 shows the presence of AgI IN from the valley generators as measured by the DOT NCAR counter. Ice nuclei concentrations were mostly between 100 and 500 IN L^{-1} . Similar IN concentrations were measured with the Suburban-mounted NCAR counter during this experiment along the portion of Highway 31 which follows the Plateau top's west edge, hereafter called the "upwind highway." Referring to Fig. 1, the upwind highway extends from the junction of Highways 31 and 264, just north of the DOT, to SKY (Skyline Drive turnoff), a north-south distance of 6.7 km. Elevations along the upwind highway increase from 2695 m on its north end to 2985 m on its south end.

3.3 Aircraft Observations

Figure 3 summarizes averaged aircraft observations for the seven terrain-following passes made over the west track (Fig. 1), above the Plateau top's windward edge. All measurements are referenced to horizontal distance north or south of SKY.

The lower panel shows the aircraft altitude and the terrain altitude beneath the aircraft as monitored by the aircraft's radar altimeter. The dashed line is the aircraft-

measured air temperature. The eight "G" symbols along the bottom of the figure represent the north-south positions of the AgI generators in the valley west of the Plateau, also shown on Fig. 1.

North and south edges of the valley-released AgI plume, or more likely intermingled plumes (hereafter referred to simply as a plume), were estimated from NCAR counter data for individual passes. These edge positions are noted by "N" and "S" for north and south entry edges, respectively. Only the entry location can be estimated on each pass because of the slow decay of the NCAR counter's response to IN. A 60-s lag was used between the initial response of the NCAR counter, defined as the first second of

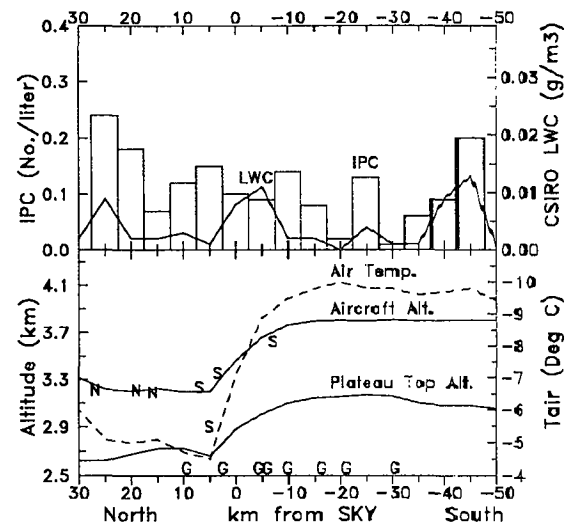


Fig. 3. A north-south oriented vertical cross section referenced to SKY on the Wasatch Plateau top. Data are averaged for 7 terrain-following passes on 28 February 1991. The upper panel shows the distributions of IPC (bar graph) and cloud LWC (solid line). The lower panel shows aircraft altitude (upper solid line), Plateau top altitude (lower solid line), and air temperature (dashed line). North and south AgI plume edges are noted by "N" and "S" for individual passes. The north-south position of each valley AgI generator is noted by a "G" along the bottom of the plot (all 8 generators were west of the cross section).

the first 10-s block with 2 or more counts. Comparisons between co-released tracer gas plumes and AgI plumes on 17 February and 14 March, 1991, showed lag times ranged from 40 to 75 s for the limited AgI IN per pass found at aircraft altitudes. At aircraft sampling speeds, NCAR counter plume edge positions should be accurate to within 1.5 km or better.

Figure 3 shows that the lowest-level aircraft sampling was done in a terrain-following mode rather than at constant altitude. Aircraft sampling was done under a special waiver from the Federal Aviation Administration that permitted in-cloud flight to within 300 m of the *highest* terrain within 8 km of the flight path (standard rules require a 600-m vertical separation). Aircraft navigation used LORAN (long range navigation) with GPS (global positioning system) as a backup. The GPS was not then certified for in-cloud navigation. Flight operations under the special waiver resulted in typical vertical separations of 600 m between the *average* Plateau top and the lowest aircraft sampling tracks. The observations will show that AgI plumes would rarely have been sampled by the aircraft on any mission if flight operations had been done under standard terrain clearance rules, with lowest sampling 300 m higher than actually occurred. Constant altitude sampling would also have resulted in fewer detections of the AgI plume. The results to be presented illustrate the need for careful selection of terrain and aircraft sampling procedures in order to sample ground-released plumes during IFR conditions.

As seen on Fig. 3, AgI plume edges were detected from 7 km south to 27 km north of SKY, although most edges were found between 3 and 20 km north of SKY. Most plume encounters during this mission were below liquid cloud base which was near 3500 m (virga showers sometimes lowered visible bases). The plume location was in the vicinity of the head of Fairview Canyon, suggesting that the canyon provided a preferred transport path over the Plateau. Silver iodide may have been transported over the Plateau farther south, but at lower

altitudes than could be safely sampled by aircraft.

3.4 NCAR Counter Estimates of Effective IN

Super and Holroyd (1994) discussed use of NCAR counter measurements in estimating effective IN concentrations. They showed first approximation agreement between such estimates and measured IPCs for the single experiment considered, using a Montana State University AgI generator rather than the NAWC type used for Utah valley seeding. Super and Holroyd's (1994) IN concentrations based on NCAR counter observations were usually lower than the IPCs observed with the 2D-C probe, on average by about a factor of two, but with considerable scatter. Two major factors contribute to the uncertainty of the estimates: (a) uncertainties in how well NCAR counter AgI IN concentrations represent AgI IN effective in orographic cloud, and (b) how well cloud simulation laboratory calibrations of AgI generator effectiveness represent the temperature dependence of AgI nucleation effectiveness in orographic cloud. While Super and Holroyd (1994) used a dated 1972 AgI generator calibration, recent results reported by DeMott (1995) were very consistent with the earlier Montana State University generator tests.

Any secondary production of ice particles would also exacerbate differences between AgI IN estimates and observed IPCs, as would unobserved very recently nucleated ice particles (less than 100 μm size) and errors in aircraft IPC sampling. Gayet et al. (1993) showed IPC measurement differences up to 1.5 depending upon individual 2D-C probes. Different external mounting points on various aircraft resulted in smaller variations.

Although the Super and Holroyd (1994) study suggested NCAR counter observations could be used to estimate effective AgI IN concentrations with some accuracy, it is not known how well similar estimates would simulate reality with the NAWC AgI generators and different cloud conditions. However, such estimates will be made, assuming they are within an order of

magnitude or so of seeded IPCs. Even such approximate values can be useful because AgI's ability to nucleate ice crystals varies over several orders of magnitude with changes in SLW cloud temperature. Another reason for estimating AgI IN concentrations from NCAR counter data is that aircraft observations can be compared with surface observations made at the DOT and with the Suburban NCAR counter.

The average AgI IN concentration will now be estimated for several aircraft passes. It is recognized that *instantaneous* AgI IN concentrations vary markedly from average values depending upon how much AgI is being transported up to aircraft altitudes, plume width and meandering and other factors. However, it can be argued that for seeding to be effective in augmenting seasonal snowfall, average conditions are important over long time intervals (hours). A high AgI IN concentration over a brief period may significantly increase the snowfall rate during that period. However, sustained snowfall enhancement will be required over many hours to produce economically important amounts. Consequently, it is believed appropriate to examine average AgI IN concentrations from several aircraft passes.

Total NCAR counts per pass for the seven aircraft passes of Fig. 3 were between 9 and 93 with an average of 30. This average value will be used to estimate the average concentration of effective IN at -20°C . Similarly, because the average distance between north and south plume edges on Fig. 3 is about 20 km, that value will be used in the calculations. The NCAR counter sampled about 10 L min^{-1} outside air while the aircraft speed was near 85 m s^{-1} . Consequently, the average volume of air sampled by the NCAR counter while passing through the AgI was:

$$(20,000\text{ m}/85\text{ m s}^{-1}) \times (10\text{ L}/60\text{ s}) = 39\text{ L}$$

Using the usual times 10 correction factor for known ice crystal losses, the average IN concentration, effective at -20°C , is:

$$(30\text{ counts} \times 10\text{ IN/count})/39\text{ L} = 8\text{ IN L}^{-1}$$

Several early 1991 field comparisons between the DOT NCAR counter and the Suburban-mounted NCAR counter parked nearby resulted in similar concentrations measured by the two counters. These counters rarely differed by a factor of two, and usually were in much closer agreement. A single comparison was made between the Suburban unit parked near the aircraft while both were in the plume of a NAWC AgI generator. The aircraft unit consistently counted a factor of three less than the Suburban unit. Therefore, for the purpose of comparing aircraft AgI IN observations with surface observations from the other two NCAR counters, all aircraft NCAR counter data reported in this paper have been adjusted upward by a factor of three.

In this example, a mean concentration of 24 IN L^{-1} (3×8) resulted from the aircraft measurements. This result is about an order of magnitude less than the 100 to 500 L^{-1} observed at the DOT and along the upwind highway during this experiment, and suggests the aircraft was near the AgI plume top. Observations on several other missions indicated the aircraft was near plume top, because AgI IN concentrations were much lower than found on the Plateau top, and/or because no AgI was detected on some (sometimes none) of the lowest-level, terrain-following aircraft passes. Part of the difference between Plateau-top and aircraft-level AgI IN measurements might be attributed to greater AgI removal by nucleation of ice particles at the colder aircraft levels. Conversely, scavenging of AgI by falling ice particles might remove more AgI at Plateau top levels where snowfall rates are greater. The net effect of losses of AgI by nucleation and scavenging is not known, but is assumed to be a secondary factor in the observed order of magnitude decreases from Plateau-top to aircraft-level AgI IN concentrations. That is, the typical large decrease in AgI IN with altitude observed above the Plateau is believed to be primarily caused by transport and dispersion processes.

Thus far, AgI IN concentrations have been reported effective at -20°C , the NCAR counter cloud chamber temperature.

However, the concentration of interest is that effective at the cloud temperature outside the aircraft. This concentration will be estimated using the recent cloud simulation laboratory calibration of the NAWC AgI generator by DeMott et al. (1995). That calibration showed that under natural tunnel draft conditions typical of light valley winds during most storms, 0.2, 8 and 75 percent of the IN effective at -20°C (1.8×10^{15} IN g^{-1} of AgI) were effective at temperatures of -6 , -8 and -12°C , respectively. The effectiveness at -16°C was essentially the same as at -20°C . These measured values were plotted and values were estimated for intermediate temperatures where necessary to correspond to aircraft sampling temperatures. Using these values assumes the cloud simulation laboratory calibration provides a good approximation of AgI's temperature dependence as an effective IN in natural orographic clouds over the Plateau. That assumption is admittedly open to question, but some indication of its validity will be provided by later examination of aircraft-measured IPC's within seeded cloud.

Because most aircraft sampling within the AgI plume was near the -5°C level during the experiment under discussion (Fig. 3), the concentration of effective AgI IN would be expected to be less than 0.2 percent of the -20°C value; that is, 0.002×24 IN L^{-1} , or about 0.05 IN L^{-1} . As discussed by Super (1994), ice crystal concentrations less than 10 IN L^{-1} do not appear likely to produce economically beneficial snowfall rates under most cloud conditions. Moreover, most aircraft sampling within the AgI plume was below cloud base during this experiment.

Some AgI may have ascended to higher, colder altitudes above cloud base, resulting in nucleation and settling of ice particles down to terrain-following aircraft sampling altitudes. It appears unlikely that significant IPCs were formed in this manner in view of the low IN concentrations sampled by the aircraft's NCAR counter. Moreover, no valley-released AgI was detected by a pair of passes (not shown) flown at a constant altitude of 3950 m (-10.5°C over the west flight track).

3.5 Ice Particle Concentrations

The best evidence for any seeding effects is believed to be the IPC calculated from 2D-C observations. Of course, even if the IPC is enhanced by seeding at aircraft levels, that does not prove that seeding affected the surface snowfall because the crystals may be small and may not settle to the surface before being transported beyond the Plateau. However, if no IPC increase can be demonstrated within the AgI plume at relatively cold aircraft levels, it might be expected that seeding was ineffective in modifying surface snowfall on the Plateau.

Cloud conditions did not appear particularly suitable for seeding at aircraft altitudes during the mission of 28 February in spite of the relative high SLW amounts observed by the microwave radiometer (Sec. 3.1). Cloud at aircraft levels had very limited LWC (liquid water content) as measured by the aircraft CSIRO probe (King et al. 1985). The solid line on the upper panel of Fig. 3 shows the LWC averaged for 5-km intervals and multiple passes. The low average LWC would be expected on the northern portion of the flight track because the aircraft was frequently below cloud base. However, the LWC was also quite low even on the southern portion of the flight track where the aircraft was usually in cloud. Liquid water contents were somewhat higher, between 0.02 and 0.15 g m^{-3} , on the pair of passes flown at 3950 m, about 500 m above cloud base.

The bar graph on the upper panel of Fig. 3 shows the IPC averaged for 5-km intervals. The argument previously given for examining average AgI IN concentrations for several aircraft passes is believed equally valid for examination of average IPCs between seeded and nonseeded zones.

Average IPCs were calculated for individual 5-km intervals without regard for whether the aircraft was in or out of visual cloud. The large majority of time the aircraft was in cloud during the experiments to be discussed. However, visual breaks sometimes occurred in the cloud decks and some sampling was done below visual cloud base on 28 February. Of course, ice crystals can

exist between visual cloud elements, or below visual cloud base, in concentrations too low to appear as cloud.

Ice particle concentration averages for multiple aircraft passes were weighted in the following way. The total count of particles over all passes within each 5-km interval was divided by the sum of the sample volumes actually observed by the 2D-C probe, which normally recorded two buffers of data per second. When the IPC was high (not observed on this day), the 2D-C probe sampled a limited volume of air each second. A simple average of IPC values from multiple passes could therefore be biased by one or more high concentration values from potentially unrepresentative samples. In other words, the calculated simple average might be higher than the real average because of equal weight being given to a one or more very high values that represented only very small cloud volumes. Conversely, the weighted averages to be presented may err in the opposite direction, letting low concentrations from large volumes dominate the average.

The weighted average IPCs tended to be a factor of two or three to sometimes a factor of several lower than the simple averages. However, the weighted IPC average is believed to provide the more conservative and correct means of assessing possible changes resulting from cloud seeding.

Figure 3 shows low average IPCs over the 75-km north-south distance portrayed, with maximum values near 0.2 ice particles L^{-1} . No convincing evidence exists to show that valley seeding increased the IPC. The IPC in the region of AgI plume is similar to that found farther crosswind. Of course, aircraft sampling was often about 300 m below visual cloud base in the zone where the AgI IN were found, and no AgI was detected on the pair of passes 500 m above cloud base. Consequently, one might not expect any seeding effects during this experiment. Cloud bases were below the Plateau top on the other experiments to be examined.

3.6 Precipitation Observations

No precipitation was detected by any of the five Plateau gauges during this experiment at the minimum gauge resolution of 0.25 mm h^{-1} . A trace was suggested by the gauge chart on the center of the Plateau top (all charts were carefully reduced with the aid of magnification). With the southwesterly flow, the AgI plume detected by aircraft may have been transported north of the two easternmost gauges. However, AgI probably existed below practical aircraft sampling altitudes farther south than shown on Fig. 3. Silver iodide in that region could have the potential to affect gauge snowfall east of the aircraft track if enough ice crystals were nucleated. Therefore, the absence of measurable precipitation on top the Plateau can be considered further evidence that seeding was ineffective during the experiment of 28 February.

More detailed discussion of the implications of precipitation gauge network measurements is given for the following experiment which had measurable snowfall at all gauges.

3.7 Summary of 28 February Experiment

Although the microwave radiometer detected relatively high SLW amounts above the Plateau, the liquid water presumably was concentrated above the highest aircraft sampling altitude of 3950 m because cloud LWC was low at aircraft levels. Consequently, seeding potential might have been anticipated to be limited or nonexistent. The lack of observed snowfall certainly indicates that valley seeding was unsuccessful in converting cloud SLW into precipitation during this experiment.

4. FIRST EXPERIMENT OF 1 MARCH

4.1 Overview

The eight valley AgI generators were operated continuously from the morning of 28 February until the afternoon of 2 March. Two experiments were conducted on 1 March. Aircraft sampling over the Plateau took place between 1125 and 1410 during the first

experiment. The aircraft was in cloud during all 12 sampling passes.

Prefrontal southwesterly flow persisted during the first mission. The 1200 rawinsonde showed relative humidities near 100 percent from the Plateau top to 5700 m. K_a -band radar tops were near 6300 m (-27°C) from 1200 till the end of the experiment, and higher earlier. The rawinsonde data showed a stable layer between 3500 and 4000 m (equivalent potential temperature increased with altitude) with neutral stability in the rest of the cloud layer. A stable layer existed in the first few hundred meters above the valley floor.

The wind in Fairview Canyon was up-canyon (westerly) during the experiment, but averaged only about 1 m s^{-1} . Winds were unusually light at the DOT, averaging 190° in direction and decreasing from 3 to 1 m s^{-1} in speed during the experiment. Aircraft-measured winds at 3200 and 3800 m were both near 215° and 11 m s^{-1} .

4.2 Plateau Top Observations

Observations along the upwind highway indicated the Plateau top was generally in cloud with light snowfall rates. Visibility was quite limited near the heads of canyons because of local liquid cloud production.

The DOT air temperature was -2°C during the period of aircraft sampling and the dewpoint depression was about 1°C .

The vertically-integrated SLW above the DOT (Fig. 4) was limited prior to 1200 and thereafter increased with time until about 1345. Ice nuclei concentrations at the DOT were quite low until almost 1300. After 1300, both IN and SLW increased, and both peaked just after 1330. The aircraft crew noted increased turbulence about 1300, suggesting enhancement of embedded convection as the first deep cloud band left the Plateau. The 1500 sounding, between aircraft missions, showed a moist, unstable atmosphere from the valley floor to 4300 m (equivalent potential temperature decreased with altitude).

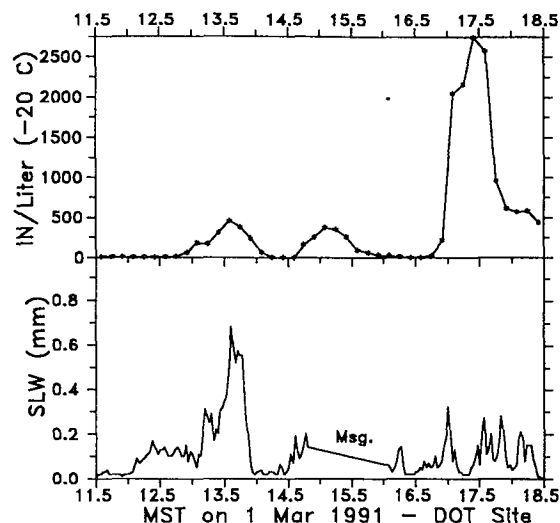


Fig. 4. Similar to Fig. 2 except for the aircraft missions of 1 March 1991.

DOT IN measurements shown on Fig. 4 were 5 to 25 IN L^{-1} until 1245, and thereafter 200 to 500 IN L^{-1} . Similar low values were found along the upwind highway prior to 1245, with values between 200 and 800 IN L^{-1} during the remainder of the aircraft mission.

The highest portion of the upwind highway (SKY) is about 300 m higher and 2°C colder than the DOT, so the SKY temperature was about -4°C during this experiment. Consequently, AgI IN concentrations effective at temperatures along the upwind highway would be expected to be very low.

4.3 Aircraft Observations

All 12 aircraft passes were made in the terrain-following mode over the west flight track. Entry positions into the AgI plume were estimated for 10 of the passes; amounts were too low on the others. Figure 5 shows the estimated positions of the north and south edges of the AgI plume, and average values of other parameters, for 10 passes. It is seen that the AgI was concentrated on the lower portion of the flight track, generally above the head of Fairview Canyon. Cloud temperatures were near -6.5°C in that region. Two AgI encounters occurred about 25 km

south of SKY where the temperature was below -9°C . Silver iodide may have been transported over the Plateau south of SKY during the other passes, but below the aircraft.

Liquid water measured by the CSIRO probe was not continuous and amounts varied rapidly when liquid was detected. Peak LWC values were 0.2 to 0.3 g m^{-3} , but mean values shown on Fig. 5 were an order of magnitude less.

Average IPCs were in the 0.2 to 0.4 L^{-1} range all along the flight track. No suggestion of higher IPCs occurred in the region from 5 to 25 km north of SKY, where AgI was most commonly found. It is not known how long the AgI was in cloud before being sampled by the aircraft, but only a few minutes after nucleation would usually be required for growth to the $100\text{ }\mu\text{m}$ minimum size used with the processing software.

The lack of obvious seeding-enhanced IPCs at aircraft altitudes is probably because of two factors. The cloud temperature was relatively warm and the concentrations of seeding material were low at aircraft levels. The average NCAR counter counts per pass ranged between 8 and 46 with an average value of 21. Figure 5 indicates most of the AgI was found along a 20-km portion of the flight track. Using the approach previously shown, the mean estimated IN concentration over the 20-km width is 15 IN L^{-1} at -20°C , similar to Plateau top values prior to 1245, but much lower than later Plateau top concentrations. The corresponding concentration of effective IN for the cloud temperatures sampled by the aircraft is estimated as about 0.3 IN L^{-1} .

Figure 4 showed that Plateau-top AgI IN concentrations increased markedly after 1245. Total NCAR counter counts per aircraft pass averaged 11 for the 6 passes prior to 1245 and 32 for the 6 passes after 1245. Although the increase at aircraft altitudes was much less dramatic than on the Plateau top, a decision was made to calculate IPCs for the 6 passes after 1245 which may have had a larger seeding signal. A plot similar to Fig. 5 was prepared (not shown).

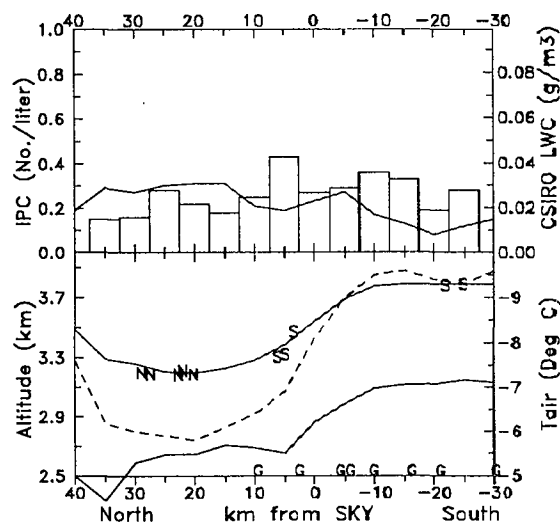


Fig. 5. Similar to Fig. 3 except for 10 terrain-following passes on the first mission of 1 March 1991.

The 6 plume entry edges were between 3 and 30 km north of SKY. The average IPC in that region ranged between 0.2 and 0.6 L^{-1} , with an average of 0.4 L^{-1} . The IPC in the 35 km south of the seeded region ranged from 0.1 to 0.4 L^{-1} , with an average of 0.2 L^{-1} , half that of the seeded region. Samples were not available north of the seeded region. The observed differences might suggest some increase in IPC associated with seeding. However, the seeded zone IPC was still quite low.

4.4 Precipitation Observations

The surface precipitation will now be considered. Typical ice crystals with a fall speed of 75 cm s^{-1} would require between 10 and 23 min to settle from terrain-following aircraft pass locations over the west track to the two eastern precipitation gauges. These gauges, shown on Fig. 1 as PTC (Plateau top center) and PTE (Plateau top east), were located at 2720 and 2850 m, respectively. (The gauge on the Plateau top's west edge, near the DOT, was directly under the west track.) This calculation ignores any net vertical motion in the atmosphere over the Plateau because no vertical wind observations were available. With a southwest flow and wind speed of 10 m s^{-1} , 17

min would be required for horizontal transport from SKY to the PTE gauge. Less time would be required to reach the PTC gauge. Based on these calculations, it is reasonable to assume that some of the ice particles measured along the west track's lowest passes could impact the two downwind gauges about 15 min after aircraft detection. The PTC and PTE gauges will hereafter be referred to as the "target gauges" with the realization that this refers to their potential targeting by ice particles observed by the aircraft over the west track.

The DOT gauge on the Plateau top's west edge could also be affected by valley seeding nucleating ice particles upwind of, and at lower altitude than, the west aircraft sampling track. Under some conditions (sufficiently cold and moist), valley-released AgI might nucleate ice crystals near the windward slope which could settle to the surface along the upper portion of the windward slope and western portion of the Plateau top including the DOT gauge. In support of this hypothesis, yet to be reported observations during the 1994-95 winter have sometimes shown modest snowfall increases at a site on the upwind highway associated with AgI seeding from a site 1 km south of HAS on Fig. 1. The horizontal distance between the generator used during the 1994-95 winter and the upwind highway ice particle and snowfall observing site is 4.4 km. Typical wind speeds near the windward slope between these two sites translate into about 15 min growth time provided that ice crystals nucleate near the AgI generator. This is sufficient time for crystals to grow to a few hundred micrometers or larger under some conditions.

Valley seeding would not be expected to affect the westernmost gauge, FVC on Fig. 1, located at the mouth of Fairview Canyon at 2010 m. Moreover, it is unlikely that valley seeding would significantly modify snowfall at the HAS gauge. To affect snowfall, valley-released AgI must be transported vertically to relatively cold SLW cloud where nucleation can take place. Contact nucleation, known to be a slow process, would be expected with the type of AgI used (DeMott et al. 1995). After nucleation, ice particles must grow large

enough to achieve significant fall velocities and then must settle to the surface. All these processes must take place in air forced to ascend over the Plateau's windward slope for seeding to affect the HAS gauge. For all but rare conditions, it can be assumed that the Fairview Canyon mouth and HAS gauges will not be affected by seeding. Those gauge observations can be used to make a crude estimate of natural snowfall rates on top of the Plateau.

Total precipitation was examined for the entire early 1991 field season to provide some basis for comparing individual gauge observations during experiments. Of course, natural short-term variations among gauges can be significantly greater than seasonal variations, so the field season comparisons provide only a very general idea of what the natural (nonseeded) snowfall pattern might be during an individual experiment.

All gauge measurements will be referenced to the HAS gauge in this and following discussions of precipitation patterns over the Plateau. Hours with missing data from one or more gauges were excluded from the seasonal comparisons. The HAS gauge collected a total of 119 mm snowfall during 115 hours with detectable snowfall (all references to precipitation or snowfall will use melted snow water equivalent, not snow depth). The median snowfall rate was 0.64 mm h^{-1} . Using the HAS seasonal total as 100 percent, the west-to-east profile from the 5 gauges over the Plateau was 62, 100, 122, 116 and 87 percent for gauges FVC, HAS, DOT, PTC and PTE, respectively. The greatest snowfall (122 percent of HAS or 145 mm) fell at the DOT gauge near the Plateau top's west edge which detected snowfall on 169 h with a median rate of 0.51 mm h^{-1} .

For the prevailing south-southwesterly flow from the Plateau top to aircraft levels during the first experiment of 1 March, most of the AgI shown on Fig. 5 would have been transported north of the target gauges. However, two of the five southerly plume edges shown on Fig. 5 were more than 20 km south of SKY. Silver iodide may have been transported that far south on other aircraft passes, while below the aircraft. If so, any

seeded ice crystals should have been transported toward the target gauges.

Aircraft sampling was conducted between 1125 and 1410, so the corresponding target gauge period of interest is about 1140 to 1425, using the 15 min fall and transport time lag previously discussed. The total snowfall at the HAS gauge during this period was 0.51 mm corresponding to 0.18 mm h^{-1} , a low rate. The west-to-east profile, using 0.51 mm as 100 percent, was 100, 100, 200, 250 and 375 percent. The 3 Plateau top gauges received more snowfall than would be expected from the comparison of seasonal amounts. However, snowfall rates were limited during the 2.75 h experiment and the observed snowfall profile over the Plateau may simply represent natural variability. Even the PTE gauge which received the most snowfall had an average hourly rate of only 0.69 mm h^{-1} . Hourly rates during all experiments are summarized in Table 2 of Sec. 9.

4.5 Summary of First Experiment of 1 March

Precipitation gauge observations suggest that seeding may have provided limited enhancement of the Plateau top snowfall during this experiment. However, the microphysical and AgI IN observations do not support the hypothesis of significant snowfall enhancement caused by seeding. The most defensible conclusion is that seeding did not significantly increase the Plateau top snowfall during this experiment.

5. SECOND EXPERIMENT OF 1 MARCH

5.1 Overview

The second aircraft mission of the day encountered well-developed convection in a line of showers associated with a cold front passage. The cold front passed the area at about 1700 (Huggins et al. 1992). A total of ten aircraft passes were made over the west track between 1645 and 1830. Five passes followed the terrain contour and five were flown at a constant altitude near 3750 m.

Radar tops descended rapidly from 9000

m ($<-40^{\circ}\text{C}$) at 1610 to 4000 m (-11°C) at 1710. After 1730, the aircraft was in and out of cloud at 3750 m. By the final pass, the cloud deck was breaking up and visual ground contact was frequent. The 1800 sounding showed an unstable atmosphere throughout the cloud layer and considerable drying above 3800 m.

Fairview Canyon winds were light and variable during the experiment. Winds at the DOT averaged 250° and increased in speed from 2 to 7 m s^{-1} . Average aircraft wind speeds were 12 m s^{-1} at both 3200 and 3750 m. Aircraft-level wind directions had become more westerly since this day's first experiment, veering from 225 to 240° in the 3200 to 3750-m layer.

5.2 Plateau Top Observations

The DOT air temperature was -2.5°C during this experiment and the dewpoint depression averaged less than 1°C .

Figure 4 shows vertically-integrated SLW amounts measured by the DOT microwave radiometer varied rapidly during the second mission, characteristic of embedded convection. The average value exceeded 0.1 mm and peak amounts were near 0.3 mm. For reference, the median value was 0.06 mm for all 333 h that the DOT microwave radiometer detected SLW during the 1991 field program and only 10 percent of all hours had an average value exceeding 0.3 mm (Super 1994).

The upper panel of Fig. 4 shows that little AgI reached the DOT until after 1645. Then, an unusually high maximum of 2750 IN L^{-1} occurred between 1700 and 1745, followed by a rapid decrease in IN. This rapid change in IN coincided with an abrupt veering of wind direction and increase in wind speed on top the Plateau, believed to be caused by the frontal passage. High AgI IN values also were detected along the upwind highway with the Suburban NCAR counter. Four Suburban passes were made from 1654 to 1814 during the aircraft mission. The IN concentrations were averaged by 0.5-km intervals north of SKY, and resulting values ranged between 600 and 1500 IN L^{-1} . In

higher than the observed IPCs.

Five constant altitude passes were flown over the west track near 3750 m (not shown). Entry edges into the AgI plume could be estimated on only two of the passes because of the low NCAR counter response. The 5-km IPC averages did not exceed 0.5 L^{-1} , and no indication existed to show that seeding increased the IPC above background levels.

5.4 Precipitation Observations

With the southwesterly flow, the AgI plume shown on Fig. 6 should have been transported over the two target gauges. Recalling that aircraft sampling took place between 1645 and 1830, the corresponding precipitation gauge period of interest is 1700 to 1845. Using the 1.52 mm received by the HAS gauge as 100 percent, the west-to-east profile was 33, 100, 183, 83 and 83 percent. This profile does not suggest that seeding increased the Plateau-top snowfall with the possible exception of the DOT gauge.

5.5 Summary of Second Mission of 1 March

The observations that were presented do not lend strong support to the hypothesis that valley seeding had a significant impact on cloud microphysics or precipitation during this experiment.

6. FIRST EXPERIMENT OF 2 MARCH

6.1 Overview

All eight valley AgI generators had been on continuously since the morning of 28 February. They were operated until near 1600 on this day, which was characterized by moist, post-frontal flow. Mt. Pleasant Airport soundings showed a shift to northwesterly flow with drying in the upper levels after 1000 (Higgins et al. 1992). The morning had thick orographic clouds with embedded convection. The cloud deck became broken during the afternoon.

Both aircraft missions on 2 March were terminated early because of icing-related problems. The first mission sampled over the

Plateau only from 1015 to 1110. The mission was ended when the outside air sampling manifold froze over. The second mission was terminated because heavy airframe and antenna icing affected aircraft performance and receipt of radio navigation signals, respectively.

Rawinsondes were released from MPA at 1000 and 1200. The 1000 sounding indicated a stable atmosphere below the Plateau top, instability in the lowest kilometer above the Plateau top and a neutral-to-stable atmosphere above that layer. The 1200 sounding indicated an unstable atmosphere from the valley floor to about 1 km above the Plateau top and stability at higher altitudes. Rawinsonde winds in the lowest kilometer above the Plateau top were west-northwesterly near 14 m s^{-1} . Steady up-canyon winds prevailed during the first aircraft mission, between 3 to 4 m s^{-1} . Winds at the DOT were 255° between 5 to 7 m s^{-1} . Aircraft winds in the 3300- to 3800-m sampled layer were west-northwesterly near 20 m s^{-1} .

The K_a -band radar monitored cloud tops near 4700 m (-19°C) throughout the first mission. The aircraft was in cloud the entire mission except for a brief breakout above cloud top at 1101, which occurred 25 km north of SKY at 3800 m.

6.2 Plateau Top Observations

The DOT air temperature and dewpoint temperature were both -4°C during this experiment.

Figure 7 shows the temporal distribution of vertically-integrated SLW above the DOT radiometer. Peak amounts over 0.3 mm were common during both missions. The rapid fluctuations are further evidence of convective activity. Graupel was sometimes observed at the surface along the upwind highway during this experiment, indicating relatively high cloud LWC. All indications are that substantial moisture existed over the Plateau on this day.

The upper panel of Fig. 7 shows that valley-released AgI was transported to the

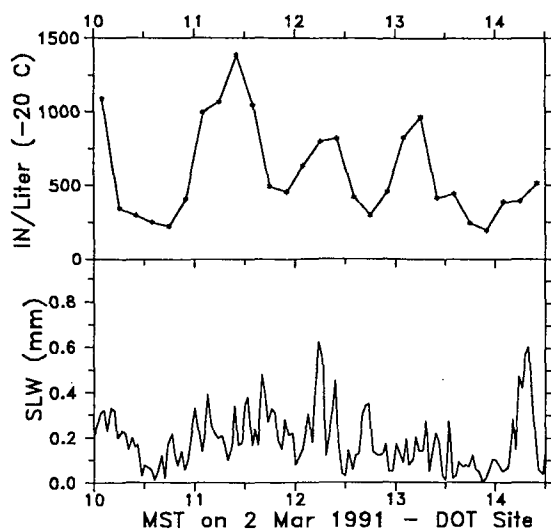


Fig. 7. Similar to Fig. 2 except for 2 aircraft missions of 2 March 1991.

Plateau top during and between the two 2 March missions (the second mission was between 1300-1430). Concentrations of AgI IN observed at the DOT during the first mission ranged between 250 and 1250 IN L⁻¹. Similar values were found along the upwind highway with the Suburban's NCAR counter between 0954 and 1049. Suburban sampling was thereafter interrupted because the vehicle became stuck in a snowdrift until after the aircraft mission.

Since upwind highway temperatures were between -4 and -6°C, AgI IN concentrations effective along the upwind highway are estimated as usually less than 1 IN L⁻¹.

6.3 Aircraft Observations

Four passes were made prior to freeze-up of the air sampling manifold, all over the west track. The first three were terrain-following passes, and the fourth pass was level at 3750 m. Cloud LWC was high, with considerable spatial variation indicating convection. Pass average values according to the CSIRO probe were near 0.1 g m⁻³ at 3300 m and near 0.2 g m⁻³ at 3750 m, with peak contents about 3 times the mean values.

Total NCAR counter counts per pass ranged from 59 to 105 on the first 3 aircraft

passes, and these encounters occurred in the 3300- to 3500-m layer. Only background level IN concentrations were found on the higher fourth pass.

Figure 8 portrays the three estimated AgI plume edges from the first mission. Both north edges were 17 km north of SKY and the single south edge was 19 km south of SKY. The average IPC for that zone was 20 ice particles L⁻¹, twice that found in the 10 km immediately south of the seeded zone. However, the concentration was 16 L⁻¹ in the 10 km just north of the seeded zone, and only two of the seven 5-km seeded zone intervals had markedly higher concentrations. Therefore, while seeding may have enhanced the IPC, the evidence is not conclusive. The difference in the seeded zone's IPC and the average IPC for the two 10-km zones just north and south of the seeded zone was 7 L⁻¹ which supports the hypothesis that seeding did increase the IPC. Seeded zone cloud temperatures on individual passes ranged from -9 to -12.5°C, certainly cold enough for AgI nucleation. Some IPC enhancement could have been expected within the seeded zone.

Further support for the hypothesis of seeding-caused IPC enhancement is provided by the NCAR counter observations. The

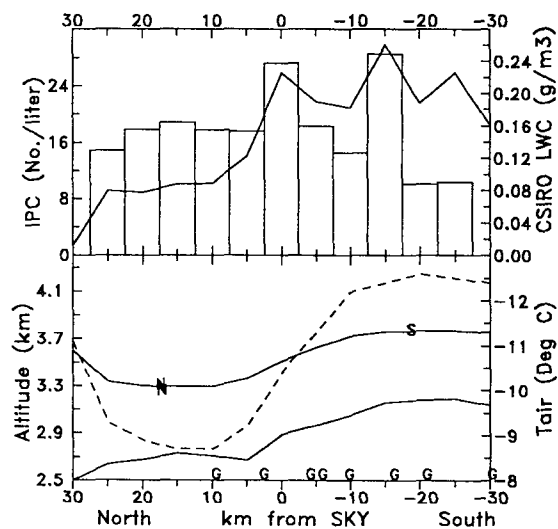


Fig. 8. Similar to Fig. 3 except for 3 terrain-following passes on the first mission of 2 March 1991.

average NCAR counter values for the 3 passes shown on Fig. 8 was 84 counts per pass. Assuming that average affected a 36-km north-south distance as suggested by Fig. 8's estimated plume edges, and applying the approach discussed earlier, yields a mean IN concentration of 35 IN L⁻¹. When adjusted from the cloud chamber temperature to the sampled cloud temperatures, resulting concentrations of effective IN would be near 15 IN L⁻¹.

It is possible that seeding produced IPCs sufficient to affect snowfall rates for some distance below lowest aircraft sampling levels. The temperature increased by about 6°C from the terrain-following aircraft passes (near -11 °C) to the upwind highway (near -5 °C). Silver iodide IN effectiveness varies by about three orders of magnitude over that temperature range, but in a non-linear manner. The vertical distribution of total AgI IN (at -20°C) is not known between the upwind highway, where observed concentrations were high, and the lowest aircraft sampling altitudes where concentrations were usually more than an order of magnitude lower. Therefore, the net effect of more total AgI IN at warmer cloud levels below the aircraft is not known. But if AgI IN concentrations were relatively high up to altitudes not far below the aircraft, IPCs of a few to several per liter could have resulted.

6.4 Precipitation Observations

With the prevailing winds, the AgI plume shown on Fig. 8 should have been transported over the two target gauges, PTC and PTE. Allowing 15 min for ice crystal settling and transport, the precipitation period corresponding to aircraft sampling was 1030 to 1125. The HAS gauge received 0.51 mm during this period and the corresponding west-to-east profile over the Plateau was 50, 100, 325, 200 and 125 percent. The Plateau-top percentages are markedly higher than the seasonal values, but are based on a limited snowfall total at the HAS and may reflect nothing but natural variability. With that caveat in mind, it is nevertheless a real possibility that seeding increased snowfall on the Plateau top during this experiment. It

will be recalled that cloud liquid water content was abundant and AgI reached relatively cold cloud levels.

6.5 Summary of First Mission of 2 March

In summary, the various observations obtained during this experiment suggest that seeding increased the IPC above the Plateau top and snowfall on the Plateau top.

7. SECOND EXPERIMENT OF 2 MARCH

7.1 Overview

Aircraft sampling over the Plateau resumed at 1300 and continued until 1430, by which time airframe and antenna icing forced termination of the second mission. The aircraft scientist noted that several turrets rose above the general cloud deck, indicating embedded convection was present. Radar tops ranged between 3400 m (-9°C) and 4700 m (-18°C) during aircraft sampling.

The MPA rawinsonde launched at 1500 showed a slightly stable atmosphere below 3500 m, then a 1 km unstable layer overlain by stability aloft. Rawinsonde winds in the first 1.5 km above the Plateau top were near 275° at 12 m s⁻¹.

Up-canyon flow continued during the second experiment with speeds between 1 and 4 m s⁻¹. The DOT winds were steady near 255° and 5 m s⁻¹, and aircraft-measured winds near 3750 m averaged 285° at 14 m s⁻¹.

7.2 Plateau Top Observations

As during the earlier mission on this day, the DOT air temperature and dewpoint temperature were both -4°C during aircraft sampling.

Figure 7 shows a peak vertically-integrated SLW amount of 0.6 mm observed by the DOT radiometer near the end of the second aircraft mission, and earlier peaks between 0.1 and 0.2 mm. Continued transport of valley-released AgI to the DOT in concentrations between 200 to 1000 IN L⁻¹ is also shown on Fig. 7.

Suburban sampling along the upwind highway showed 0.5 km means of 200 to 700 IN L^{-1} during this aircraft mission, in good agreement with the DOT observations. Again because of the slightly supercooled temperatures along the upwind highway, AgI IN concentrations effective at those temperatures are estimated at less than 1 IN L^{-1} .

7.3 Aircraft Observations

Five aircraft passes were made over the west track, all at a constant altitude. Because of the high average LWC (Fig. 9) and associated heavy airframe icing, no lower-level, terrain-following passes were attempted.

All five passes encountered AgI in spite of the relatively high altitude, near 3750 m. The estimated entry edge positions are shown on Fig. 9, between 6 km north to 3 km south of SKY. The narrowness of the AgI plume suggests it may have come from only one or two generators and/or been funneled up the two major canyons upwind of the DOT and SKY. Silver iodide from other generators may have been below the aircraft both north and south of the detected AgI plume. Cloud temperatures at aircraft altitudes were near -12.5°C , certainly cold enough for substantial nucleation by AgI.

The upper panel of Fig. 9 indicates a pronounced IPC enhancement associated with the AgI plume position. The maximum IPC was 24 L^{-1} in the 5-km interval centered on SKY, which appears to be the plume core according to the entry edges. The background IPC was about 2 to 4 L^{-1} , except in the 10 km south of the IPC maximum where concentrations were 10 L^{-1} . It is speculated that this 10-km region may have been affected by seeding, if the AgI was transported above the aircraft and the wind direction veered with height. But even if the 10 L^{-1} region was a natural phenomena associated with the high LWC region, the data strongly suggest that seeding caused an IPC enhancement of at least 14 L^{-1} directly over SKY.

Total NCAR counter counts per pass

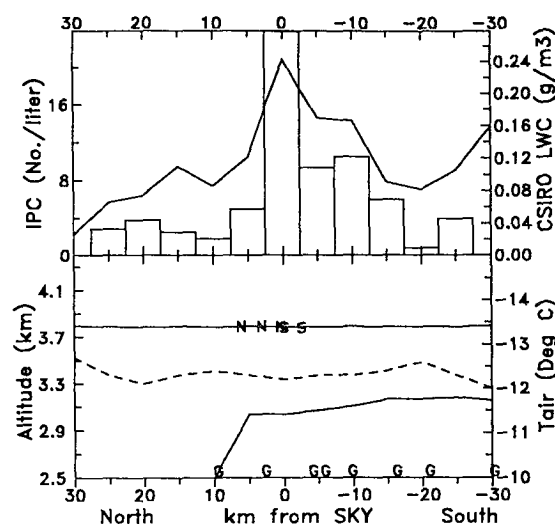


Fig. 9. Similar to Fig. 3 except for 5 constant altitude passes on the second mission of 2 March 1991.

ranged between 10 and 64 with an average of 30. Assuming the plume width averaged only 5 km at the relatively high sampling altitude, as suggested by Fig. 9, and applying the previous approach yields an estimated IN concentration of 90 L^{-1} . This concentration is about half of the lowest values sampled on the Plateau top. This relatively high aircraft average value at 3750 m indicates good vertical transport, presumably aided by embedded convection.

The cloud simulation chamber calibration reported by DeMott et al. (1995) indicates AgI IN effectiveness at -12°C , near the sampled cloud temperature, to be 75 percent of that at the NCAR cloud chamber temperature. Using that adjustment results in an estimated effective IN concentration of about 70 L^{-1} , well above the enhanced IPC of 14 to 20 L^{-1} suggested by Fig. 9. Of course, not all available AgI IN necessarily nucleated ice crystals, especially if relatively slow contact nucleation occurred as expected with the AgI solution used.

This aircraft mission was the first of the series of missions reported in this paper that demonstrated an obvious IPC enhancement associated with valley AgI seeding. The IPC appears to have been increased by 14 to 20

L^{-1} by the seeding, a high enough enhancement to potentially have affected the snowfall rate.

The AgI plume was centered just north of SKY at an altitude of 3750 m. Passes were not made at lower levels where the plume was likely much wider than shown on Fig. 9. With the observed westerly flow, the seeding plume was probably transported over target gauges PTC and PTE.

7.4 Precipitation Observations

Precipitation rates had decreased from the morning mission though vertically-integrated SLW values above the DOT were similar during both missions. The second mission's period of interest for precipitation gauge observations is 1315 to 1445. The only gauges to detect snowfall during this period were the DOT gauge and the PTE gauge, each of which recorded the minimum detectable amount of 0.25 mm h^{-1} .

7.5 Summary of Second Experiment of 2 March

Even though seeding apparently increased the IPC at the aircraft sampling level, available precipitation gauge observations do not indicate any significant increase during this experiment as snowfall rates were very low. Seeding potential might have been expected to be high during this experiment since cloud liquid water amounts were relatively abundant and snowfall rates were minor. However, the valley seeding did not result in significant snowfall on the Plateau.

8. SINGLE EXPERIMENT OF 6 MARCH

8.1 Overview

The 6 March case was the coldest storm sampled during the 1991 field program. The eight valley AgI generators were ignited between 1215 and 1335 and thereafter operated until after the experiment. Aircraft sampling over the Plateau took place between 1620 and 1915.

Northwesterly flow was affecting Utah at

700 and 500 mb because the State was west of the mean long wave trough axis (Huggins et al. 1992). A small region of moisture and cold air advection reached Utah on this day, associated with movement of a short wave. A distinct band of cold-topped clouds accompanied an upper level trough passage during the experiment. The cloud band passed over the Plateau from 1300 to 2000.

The only K_a -band radar echo to reach the Plateau top did so between 1700 and 2000, during and after the aircraft mission. The upper level cloud produced very weak echo to a maximum altitude of 5100 m (-27°C). However, the vertically-pointed radar was unable to detect cloud higher than 4000 m (-20°C) most of the time during the mission.

The 1500 MPA rawinsonde showed a slightly stable atmosphere from the Sanpete Valley floor to near 3500 m, and increased stability at higher altitudes. The only layer with relative humidity above 90 percent was between 3300 to 3500 m. Rawinsonde winds were westerly near 6 m s^{-1} at Plateau top levels. The 1800 sounding showed neutral stability from the valley floor to about 3300 m and increased stability above that altitude. The single thin layer of high relative humidity persisted, with values exceeding 90 percent between 2800 to 3500 m. Rawinsonde winds at Plateau-top levels remained westerly near 7 m s^{-1} . Higher level winds were west-northwest and the speed increased to 13 m s^{-1} near 3750 m.

Light up-canyon flow persisted during the experiment, near 1 m s^{-1} . The DOT winds were westerly, usually between $3\text{-}4 \text{ m s}^{-1}$. Aircraft winds were not available for this mission.

This experiment was simulated with a numerical model by Heimbach and Hall (1994). Their results showed pooling of valley-released AgI but some transport over the Plateau in a shallow layer. The vertical transport was apparently enhanced by gravity waves in the stable atmosphere.

8.2 Plateau Top Observations

The DOT air temperature and dewpoint temperature both averaged -11°C during this experiment.

A mesoscale feature moved over the Plateau from about 1630 to 1700, characterized by aggregation of ice crystals and reduced visibility on top the Plateau. Aircraft and ground scientists speculated at the time that a convective band was passing by. That view is not supported by the available rawinsonde data which indicate a stable atmosphere, or the model simulation by Heimbach and Hall (1994) based on sounding data. But the small mesoscale feature moved through the area between the 1500 and 1800 rawinsondes and likely escaped detection. At any rate, both the SLW and AgI IN monitored at the DOT peaked between 1700 and 1730, a period of increasing visibility with limited ice particles settling along the upwind highway. A mobile radiometer detected the greatest SLW amount of the experiment, with a maximum value of 0.25 mm, while being driven midway up Fairview Canyon between 1710 and 1725 (Huggins et al. 1992). (Further discussion of 1991 mobile radiometer sampling is given by Huggins 1995.) Clearly, some mesoscale phenomena affected the Plateau from about 1630 to 1730, resulting in increased SLW and AgI transport over the Plateau.

Figure 10 shows that valley-released AgI was transported to the Plateau top during aircraft sampling in concentrations between 200 and 1500 IN L^{-1} . Six Suburban passes were made during the aircraft mission. The Suburban data, when averaged for 0.5 km-intervals north of SKY, ranged between 400 and 1000 IN L^{-1} . As temperatures along the upwind highway were -11 to -13°C , effective AgI IN concentrations in that region are estimated as about 75 percent of the values just cited. Presuming that liquid condensate was being produced along the Plateau's west slope, high concentrations of seeded ice crystals would be anticipated along the upwind highway.

Several visual observations of ice crystals were made while driving along the upwind

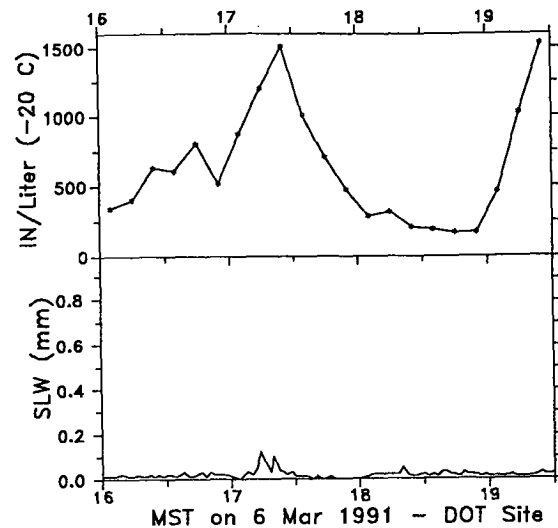


Fig. 10. Similar to Fig. 2 except for the aircraft mission of 6 March 1991.

highway during this experiment. Crystals were typically very small, but aggregates were sometimes observed. However, no evidence of riming existed, which indicates SLW was limited. The impression along the upwind highway was of being within an essentially all-ice cloud. The largely ice particle cloud may have been primarily a natural phenomena because of the cold prevailing temperatures. But if any excess SLW did exist, it seems probable that the AgI seeding converted much of it to ice crystals.

The bottom panel of Fig. 10 shows this day had little vertically-integrated SLW observed by the DOT radiometer. The highest peak was 0.1 mm, but most of the period was in the range 0.0 to 0.03 mm. These observations suggest that natural and/or seeded ice crystals were rapidly converting any liquid condensate, produced by uplift over the Plateau, into ice crystals. The result was an orographic cloud composed predominantly of ice over the Plateau top, with minor amounts of SLW occasionally observed.

8.3 Aircraft Observations

Figure 11 shows averages for the seven terrain-following passes made over the west flight track. The NCAR counter entry edges

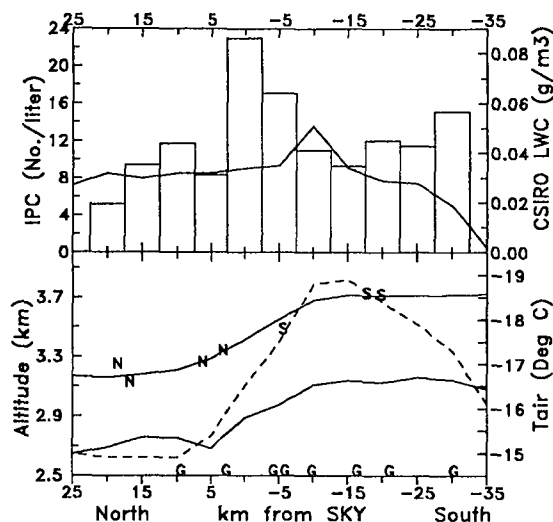


Fig. 11. Similar to Fig. 3 except for 7 terrain-following passes on 6 March 1991.

into the AgI plume shown on Fig. 11 vary considerably with extremes between 18 km north to 20 km south of SKY. On average, the plume was between 11.2 km north to 14.4 km south of SKY, a width of 26 km.

Average CSIRO LWC values were low, generally in the 0.02 to 0.04 g m⁻³ range, both for terrain-following passes (Fig. 11) and for constant altitude passes flown near 3750 m (Fig. 12).

A strong indication exists in Fig. 11 that seeding increased the IPC in the 5-km intervals from 2.5 km north to 7.5 km south of SKY. The average IPC for this 10-km zone is 20 L⁻¹, compared with 10 L⁻¹ for the remaining intervals, and 11 L⁻¹ for the four 5-km zones that rarely had AgI present (1 northernmost and 3 southernmost). The 10-km zone of apparently enhanced IPC corresponds to the AgI core according to the entry edge positions; that is, AgI appeared to be present in that zone on every pass. Silver iodide was detected north and south of that zone on some of the passes.

Temperatures were cold in the seeded zone along the lowest aircraft sampling profile, between -15 and -19°C on individual passes.

Figure 12 is similar to Fig. 11 except for the five passes made at a constant altitude of 3750 m where the temperature was near -19°C. The two 5-km intervals from 2.5 to 12.5 km south of SKY had the highest IPC with an average of 37 L⁻¹. For comparison, the average for the remaining intervals is 10 L⁻¹. The 10-km zone with increased IPC is again in good spatial agreement with the north and south AgI plume entry edges which, on average, were located between 3 and 13 km south of SKY. The southward shift of the IPC maximum from Fig. 11 to Fig. 12 is consistent with rawinsonde observations that showed the wind direction veering with altitude.

The total NCAR counter counts per pass for the 7 passes of Fig. 11 ranged between 30 and 355 with an average of 115. Assuming this average affected a 26-km width, the resulting AgI concentration was about 70 IN L⁻¹. No adjustment is needed for the cold prevailing cloud temperatures because AgI IN effectiveness is essentially constant at temperatures below -15°C for the NAWC generator (DeMott et al. 1995). Once again the NCAR counter-based estimate of AgI IN was above the 10 IN L⁻¹ IPC enhancement indicated by the 2D-C probe observations. The AgI was consistently found at the higher, colder 3750-m level, so seeded crystals from

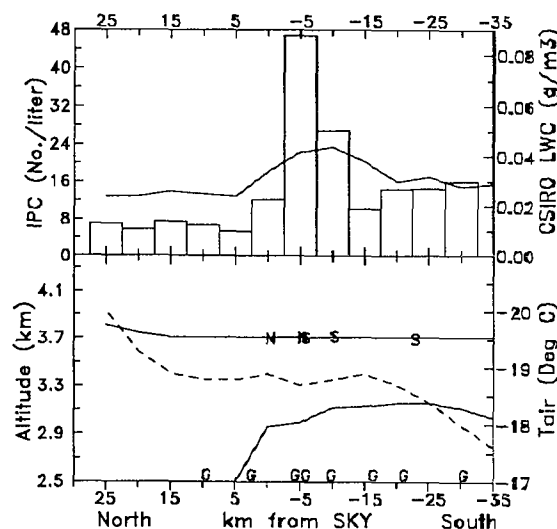


Fig. 12. Similar to Fig. 3 except for 5 constant altitude passes on 6 March 1991.

above may have settled to the altitude of the terrain-following passes. Any such enhancement of the observed IPC would result in less agreement with the AgI IN estimation, as would any adjustment for expected slow nucleation by the AgI in the cold, dry cloud. It is speculated that only a fraction of the available AgI IN nucleated ice crystals because cloud liquid water was very limited. Conversely, better agreement was found for the 5 passes of Fig. 12 for which total NCAR counter counts per pass ranged between 17 and 78 with an average of 40. Assuming a 10-km plume width results in an estimated AgI concentration of 60 IN L^{-1} for the cold air temperature. This AgI IN estimate is in reasonable agreement with the IPC enhancement of 27 L^{-1} suggested by Fig. 12.

8.4 Precipitation Observations

The AgI plume position shown on Fig. 11 should have been transported over the target gauges with observed winds between westerly and west-northwesterly. The aircraft sampling period, increased by 15 min for ice crystal settling to gauge altitudes, was 1635 to 1930. The total precipitation recorded during this period was none in the two west slope gauges, 0.76 mm at the DOT, 0.38 mm on the Plateau-top center, and 0.25 mm at the easternmost gauge. The fact that no snowfall was observed on the west slope while some fell on the Plateau top suggests that seeding may have enhanced Plateau-top snowfall. Of course, there is no way to be certain that the observed snowfall distribution represents anything but natural processes. However, it can be stated that if seeding was effective, the *maximum* possible rate averaged 0.25 mm h^{-1} at the DOT gauge and less further downwind.

8.5 Summary of Experiment of 6 March

Valley seeding appears to have markedly increased the IPC during this experiment. The increased IPC zone was spatially consistent with the AgI plume position. The NCAR counter-based estimates of effective AgI IN concentrations also support the view of IPC enhancement within the seeded zone. Apparently, the limited amount of LWC was

sufficient for nucleation of additional ice particles at the unusually cold cloud temperatures reached by the AgI. The seeding may have increased snowfall on the Plateau top, but at limited rates, presumably because of the limited SLW available in the cold cloud system.

9. SUMMARY AND CONCLUSIONS

Six early 1991 seeding experiments were examined in which AgI, released from a network of eight valley generators, was observed over the Wasatch Plateau of central Utah. These experiments, corresponding to aircraft sampling periods over the Plateau, were selected as all available cases with valley-released AgI detected at aircraft altitudes over the Plateau. Therefore, these cases are not representative of valley seeding in general. Valley-released AgI was not transported to Plateau top and aircraft altitudes during some other early 1991 sampling periods (e.g., Super and Holroyd 1994, Super 1994).

All the storm periods reported herein had SLW cloud over the Plateau as measured by microwave radiometer and aircraft, although amounts were very limited in the coldest experiment and the SLW was well above the Plateau top during another experiment. Five of the experimental periods had embedded convection present. The sixth period, the coldest storm sampled during 1991, experienced passage of a mesoscale feature which may have aided transport over the Plateau.

Silver iodide IN were measured by NCAR acoustical IN counters in an aircraft, in a 4-wheel drive vehicle and at a fixed site near the head of a major canyon. Concentrations of AgI IN, effective at -20°C in each NCAR counter's cloud chamber, were often hundreds per liter at the fixed site and along the upwind highway following the Plateau top's windward edge for a 6.7 km north-south distance. Concentrations at lowest aircraft sampling altitudes were typically over an order of magnitude less than along the Plateau top. These measurements indicate a consistent, rapid decrease in valley-released AgI IN concentrations with height above the

Plateau. Little AgI IN were found as high as 1 km above the Plateau top, and the aircraft sometimes overflowed the plume while within 600 m of the Plateau top.

The evidence available suggests it is reasonable to assume that ground-released AgI is seldom transported as high as 1 km above the Plateau. This is in agreement with earlier observations over other mountain barriers. Because cloud temperatures are usually only slightly supercooled in this shallow seeded layer, the challenge is to produce enough AgI IN, *effective* at slightly supercooled temperatures. An abundance of observations exists in the intermountain West to demonstrate that the lowest kilometer over mountain barriers is often too warm for significant nucleation with conventional types of AgI and generators, and typical release rates. The problem is even more serious in the Sierra Nevada, which led the State of California to investigate propane seeding (Reynolds 1991).

Aircraft 2D-C probe measurements of IPC were examined for possible microphysical changes associated with the AgI seeding. NCAR counter observations were used to estimate the average positions of the AgI plume (or, more likely, intermingled plumes), and in-plume IPCs were compared with natural IPCs crosswind from the AgI.

The main findings of the six previously described experiments are summarized in Tables 1 and 2. NCAR counter measurements and a recent cloud simulation

laboratory generator calibration were used to estimate AgI IN concentrations effective at in-plume aircraft sampling temperatures in Table 1. The most important and reliable values in Table 1 are the IPC increases based on *observed* differences in 2D-C particle imaging probe measurements within and crosswind from seeded zones.

Table 1 shows increases for both the estimated AgI IN concentrations and the observed IPC enhancements as the seeded zone temperature decreases. No discernable increase occurred in seeded zone IPC in the first three experiments where temperatures were no colder than -9°C. Valley seeding during the first experiment of 2 March may have increased the IPC. The second experiment of 2 March and the single experiment of 6 March both strongly suggest IPC enhancements within the seeded zone. The 6 March case showed IPC increases from both terrain-following and constant altitude passes. The two experiments with apparent IPC increases had the coldest clouds, below -12°C at aircraft sampling altitudes.

The AgI IN estimates in Table 1 and the estimates of seeding-caused IPC are in reasonable agreement when it is recognized that not all available AgI IN will nucleate ice crystals, especially when cloud LWC is limited. The type of AgI used is expected to result in contact nucleation, a slow process. The degree of agreement between AgI IN and IPC in Table 1 may be fortuitous. Instrumentation limitations and the uncertainties in the representativeness of

Table 1. - Summary of results for six valley seeding experiments. All values are averages for the seeded zone. The IPC calculations ignored particles smaller than 100 μm size.

MMDD/Exp.	Temp. range (°C)	Ave. Plume width (km)	Est. AgI IN conc. (L ⁻¹)	2D-C IPC increase (L ⁻¹)
0228/1*	-5 to -9	20.6	0.05	0
0301/1	-6 to -9	30.8	0.3	<0.2
0301/2	-6 to -9	25.2	3	<0.5
0302/1	-9 to -12.5	36.2	15	<7
0302/2	-12.5	4.7	70	>14
0306/1	-15 to -18.5	25.6	70	10
0306/1	-19	10.2	60	27

* Most aircraft AgI IN observations were made below cloud base.

Table 2. - Summary of precipitation network measurements during six early 1991 experiments from west to east over the Plateau. Values are average *hourly* precipitation rates in mm h⁻¹ for the indicated time periods. The times correspond to the aircraft sampling periods lagged by 15 min.

MMDD/Exp.	MST	FVC	HAS	DOT	PTC	PTE
0228/1	1345-1635	0.0	0.0	0.0	0.0	0.0
0301/1	1140-1425	0.18	0.18	0.37	0.46	0.69
0301/2	1700-1845	0.29	0.87	1.60	0.73	0.73
0302/2	1030-1125	0.28	0.55	1.79	1.10	0.69
0306/1	1315-1445	0.0	0.0	0.17	0.0	0.17
0306/1	1635-1930	0.0	0.0	0.26	0.13	0.09

cloud chamber generator calibrations result in lack of precision for the AgI IN estimates. Estimates of seeding-caused IPC are also approximations, but should be significantly more accurate than the AgI IN estimates.

None of the estimated average AgI plume widths of Table 1 are as wide as the 40-km north-south extent of the AgI generator network. The median plume width from Table 1 is 25 km, suggesting that either some of the individual generator plumes were not transported over the Plateau or that the aircraft was simply overflying some plumes. The latter case is suspected to be most common because the generators were all located in similar valley floor locations. Moreover, observations along the upwind highway indicated that when AgI was transported over the Plateau, it usually was found all along the 6.7 km north-south extent of the highway. These highway observations suggest that AgI from multiple generators was usually transported over the Plateau when any Plateau-top transport was occurring.

Observations from the network of 5 precipitation gauges could not be expected to be conclusive regarding the effectiveness of seeding since only a limited number of non-randomized experiments was conducted. However, the gauge observations may be suggestive and they do set upper limits on possible snowfall enhancement. No seeding effects would be expected at gauges FVC and HAS on the Plateau's western slope.

The gauge observations given in Table 2 do not provide evidence of significant seeding-related snowfall increases on top of the Plateau during two of the six experiments

because hardly any snow fell. Little AgI IN reached the high-based SLW cloud of 28 February so no significant response to seeding would be anticipated. Limited snowfall rates may have been caused by seeding during some of the other experiments, each of which had cloud base located below the Plateau top. Seeding may have increased snowfall particularly during the first experiment of 2 March and the single experiment of 6 March. But any enhancement of snowfall rates was limited, especially on 6 March, as shown by the average hourly rates in Table 2.

The minor snowfall amounts of the second experiment of 2 March raise special cause for concern. Supercooled liquid water amounts were relatively abundant as measured by microwave radiometer and an aircraft probe. Further, the mission was terminated early because of aircraft icing. Relatively high AgI IN concentrations were transported up to aircraft altitudes where cloud was certainly cold enough for nucleation of much of the AgI. A noticeable increase in IPC resulted in the seeded zone. However, in spite of the apparently quite seedable conditions and transport of AgI to aircraft altitudes, the valley seeding did not result in significant snowfall on the Plateau top.

10. RECOMMENDATIONS

The overall results summarized in Sec. 9 provide cause for concern about valley AgI seeding as practiced in the Utah operational program. While not the topic of this paper, targeting of valley-released AgI to cloud levels is known to be a problem under some storm conditions (e.g. pooling during valley-

based inversions). Although SLW cloud frequently is present during winter storms, the temperature of the region reached by ground-released AgI is often only mildly supercooled. The measurements presented strongly suggest that concentrations of AgI, effective at SLW temperatures in the lowest several hundred meters above mountain barriers, should be higher than are being obtained with the current operational combination of AgI generator locations, generator type, seeding rates, type of AgI solution, and generator spacing.

It is recommended that effective AgI IN concentrations at supercooled cloud levels be increased in the Utah operational program. This increase could be achieved by some combination of a denser AgI generator network, higher AgI release rates, use of AgI solutions that promote nucleation at warmer temperatures, and improved generator siting. It also may be possible to increase generator yield although a recent cloud simulation laboratory calibration indicates the present operational generators are already quite effective at slightly supercooled cloud temperatures.

Where practical, siting of generators on windward slopes can markedly improve targeting frequency as compared with valley generators. Observations downwind of the HAS site in early 1991 and two similar high altitude sites in early 1994 showed that released AgI and tracer gas routinely reached Plateau-top altitudes and often aircraft altitudes. Similar experience was gained over the Bridger Range of Montana (e.g., Super and Heimbach 1988) and Grand Mesa of Colorado (e.g., Holroyd et al. 1988). High altitude, windward slope siting usually requires use of remote-control generators, admittedly a more expensive option than using manual generators along valley floors. However, high altitude generators avoid the problem of pooling of AgI within a shallow layer on the valley floor. Such pooling can result in failure to treat potentially seedable clouds during some storm conditions. A further advantage of high altitude generators may be rapid nucleation at relatively warm temperatures because of forced condensation-freezing (e.g., Finnegan and Pitter 1988, Chai

et al. 1993).

While delivery of relatively high concentrations of AgI to cloud levels can and should be improved, a significant fraction of winter storm periods probably will be too warm for effective ice nucleation with ground-released AgI. It is recommended that means be investigated of effectively seeding storm periods with only slightly supercooled temperatures (0 to -4°C) in the lowest several hundred meters above mountain barriers, where ground-released seeding material is transported. Such storm episodes often have very abundant SLW flux. Liquid propane seeding may provide a possible augmentation to AgI seeding in such conditions. The technology exists to automatically release liquid propane when SLW is present (Super et al. 1995). However, further physical evidence of the effectiveness of liquid propane seeding is needed. Development of a technology to effectively seed warmer storms should substantially increase the frequency of storms that can be seeded.

The recommendations given above could significantly improve the effectiveness of the Utah operational seeding program. Moreover, many of the recommendations should be pertinent for other operational programs designed for winter orographic cloud seeding.

Acknowledgements

Many individuals contributed to the 1991 Wasatch Plateau field program. These include Clark Ogden and Barry Saunders of the Utah Division of Water Resources; James Heimbach of the University of North Carolina at Asheville; Arlen Huggins of the Desert Research Institute; Dennis Wellman and Stan Wilkison of NOAA; Glenn Cascino, Roger Hansen, Ed Holroyd and Jack McPartland of the Bureau of Reclamation; and Don Griffith, Bill Hauze and George Wilkerson of North American Weather Consultants. Gerhard Langer reconditioned the NCAR counters and checked their field operation.

Journal of Weather Modification
reviewers and Curt Hartzell of the Bureau of

Reclamation are thanked for their many helpful comments which improved this paper.

This applied research was primarily funded by the NOAA Atmospheric Modification Program in cooperation with the Utah Division of Water Resources. The Bureau of Reclamation provided various instrumentation and equipment resources.

REFERENCES

- Chai, S.K., W.G. Finnegan and R.L. Pitter, 1993: An interpretation of the mechanisms of ice-crystal formation operative in the Lake Almanor cloud-seeding program. *J. Appl. Meteor.*, **32**, 1726-1732.
- DeMott, P.J., A.B. Super, G. Langer, D.C. Rogers and J.T. McPartland, 1995: Comparative characterizations of the ice nucleus ability of AgI aerosols by three methods. *J. Wea. Mod.*, **27**, in press.
- Deshler, T.D. and D.W. Reynolds, 1990: The persistence of seeding effects in a winter orographic cloud seeded with silver iodide burned in acetone. *J. Appl. Meteor.*, **29**, 477-488.
- , D.W. Reynolds, and A.W. Huggins, 1990: Physical response of winter orographic clouds over the Sierra Nevada to airborne seeding using dry ice or silver iodide. *J. Appl. Meteor.*, **29**, 288-330.
- Finnegan, W.G. and R.L. Pitter, 1988: Rapid ice nucleation by acetone-silver iodide generator aerosols. *J. Wea. Mod.*, **20**, 51-53.
- Gayet, J.F., P.R.A. Brown and F. Albers, 1993: A comparison of in-cloud measurements obtained with six PMS 2D-C probes. *J. Atmos. Ocean. Technol.*, **10**, 180-194.
- Griffith, D.A., J.R. Thompson, and D.A. Risch, 1991: A winter cloud seeding program in Utah. *J. Wea. Mod.*, **23**, 27-34.
- , G.W. Wilkerson, W.J. Hauze, and D.A. Risch, 1992: Observations of ground released sulfur hexafluoride tracer gas plumes in two Utah winter storms. *J. Wea. Mod.*, **24**, 49-65.
- Heimbach, J.A. and W.D. Hall, 1994: Applications of the Clark Model to winter storms over the Wasatch Plateau. *J. Wea. Mod.*, **26**, 1-11.
- Hogg, D.C., F.O. Guiraud, J.B. Snider, M.T. Decker, and E.R. Westwater, 1983: A steerable dual-channel microwave radiometer for measurements of water vapor and liquid in the troposphere. *J. Climate Appl. Meteor.*, **22**, 789-806.
- Holroyd, E.W., 1987: Some techniques and uses of 2D-C habit classification software for snow particles. *J. Atmos. Ocean. Technol.*, **4**, 498-511.
- , J.T. McPartland, and A.B. Super, 1988: Observations of silver iodide plumes over the Grand Mesa of Colorado. *J. Appl. Meteor.*, **27**, 1125-1144.
- , J.A. Heimbach and A.B. Super, 1995: Observations and model simulation of AgI seeding within a winter storm over Utah's Wasatch Plateau. *J. Wea. Mod.*, **27**, in press.
- Huggins, A.W., 1995: Mobile microwave radiometer observations: Spatial characteristics of supercooled cloud water and cloud seeding implications. *J. Appl. Meteor.*, **34**, 432-446.
- , M.A. Wetzel, and P.A. Walsh, 1992: Investigations of Winter Storms over the Wasatch Plateau during the 1991 Utah/NOAA Field Program, Final Report to the Utah Division of Water Resources from the Desert Research Institute, Reno, NV, 198 pp. plus appendices.
- King, W.D., J.E. Dye, J.W. Strapp, D. Baumgardner, and D. Huffman, 1985: Icing wind tunnel tests on the CSIRO liquid water probe. *J. Atmos. Ocean. Technol.*, **2**, 340-352.
- Langer, G., 1973: Evaluation of NCAR ice nucleus counter. Part I: Basic Operation. *J. Appl. Meteor.*, **12**, 1000-1011.
- Reynolds, D.W., 1991: Design and field testing of a remote ground-based liquid propane dispenser. *J. Wea. Mod.*, **23**, 49-53.
- Sassen, K. and H. Zhao, 1993: Supercooled liquid water clouds in Utah winter mountain storms: Cloud-seeding implications of a remote-sensing dataset. *J. Appl. Meteor.*, **32**, 1548-1558.
- Super, A.B. 1994: Implications of early 1991 observations of supercooled liquid water, precipitation and silver iodide on Utah's Wasatch Plateau. *J. Wea. Mod.*, **26**, 19-32.
- , and B.A. Boe, 1988: Microphysical effects of wintertime cloud seeding with silver iodide over the Rocky Mountains. Part III: Observations over the Grand Mesa, Colorado. *J. Appl. Meteor.*, **27**, 1166-1182.
- , and J.A. Heimbach, 1988: Microphysical effects of wintertime cloud seeding with silver iodide over the Rocky Mountains. Part II: Observations over the Bridger Range, Montana. *J. Appl. Meteor.*, **27**, 1152-1165.
- , and A.W. Huggins, 1992a: Investigations of the targeting of ground-released silver iodide in Utah. Part I: Ground observations of silver-in-snow and ice nuclei. *J. Wea. Mod.*, **24**, 19-34.
- , and -----, 1992b: Investigations of the targeting of ground-released silver iodide in Utah. Part II: Aircraft Observations. *J. Wea. Mod.*, **24**, 35-48.
- , and E.W. Holroyd, 1994: Estimation of effective AgI ice nuclei by two methods compared with measured ice particle concentrations in seeded orographic cloud. *J. Wea. Mod.*, **26**, 33-40.
- , E. Faatz, A.J. Hilton, V.C. Ogden and R.D. Hansen, 1995: A status report on liquid propane dispenser testing in Utah with emphasis on a fully-automated seeding system. *J. Wea. Mod.*, **27**, in press.

A STATUS REPORT ON LIQUID PROPANE DISPENSER TESTING IN UTAH
WITH EMPHASIS ON A FULLY-AUTOMATED SEEDING SYSTEM

Arlin B. Super*, Erick Faatz**, Arlen J. Hilton*,
V. Clark Ogden** and Roger D. Hansen*

* Bureau of Reclamation

** Utah Division of Water Resources

Abstract. Liquid propane dispensers were tested on the Wasatch Plateau of central Utah during the winters of 1992-93 and 1993-94. Remote operation of the radio-controlled dispensers proved to be highly reliable, in large part because of the mechanical simplicity of the devices. A prototype *fully-automated* liquid propane seeding system was tested during early 1994 on the west (windward) slopes of the Plateau. An icing rate device was used to detect supercooled liquid water at the center station of three exposed propane dispenser stations. Wind speed and direction and air temperature were also monitored at the center station. When certain predetermined weather criteria were met, the three propane dispensers were automatically turned on. Propane continued to be dispersed until one or more of the weather criteria were out-of-bounds for 2 h.

Post-season analysis of recorded data showed that the fully-automated seeding system operated as designed for the most part. Some minor problems were encountered, but can easily be corrected. Recommendations are made for simplifying the automated decision process.

A means of detecting supercooled liquid water in the absence of commercial electrical power was also tested during early 1994. It proved to be practical and reliable. Accordingly, the technology exists to operate fully-automated networks of liquid propane dispensers in remote mountain locations. Costs of such networks would not be excessive, and reliability can be expected to be high. However, further physical experimentation is recommended to document the effectiveness of liquid propane seeding for snowfall enhancement because such evidence is quite limited.

1. INTRODUCTION

Operational seeding of winter orographic (mountain-induced) clouds for snowfall enhancement has been conducted in the western United States and elsewhere since the 1950's. The basic concept is to convert excess SLW (supercooled liquid water) into additional snowfall. This is done by creating more ice crystals in SLW clouds expected to have low concentrations of natural ice crystals. Such clouds may be naturally inefficient in snowfall production.

By far the most common seeding agent for winter orographic clouds has been AgI (silver iodide). The AgI may be produced in relatively pure form, or complexed with other chemicals to alter ice nucleating characteristics. Silver iodide is released

as very tiny particles from generators or pyrotechnic flares. Releases may be from ground locations or from aircraft. The Utah operational seeding program uses ground-based AgI generators primary at valley locations, with a few generators in canyon mouths (Griffith et al. 1991). The following discussion will not include aircraft seeding or use of flares, techniques not used in Utah because of associated expense and operational difficulties.

The effectiveness of AgI in nucleating ice crystals is determined by several factors including the particular chemical composition of the solution, generator characteristics, ambient winds, time available for nucleation and others. But the most important factor is the SLW cloud temperature. For commonly used AgI generators, solutions, and release rates, and typical AgI plume dispersion,

ice crystal nucleation is believed negligible for temperatures above about -5°C . Ice crystal nucleation may be very limited even at -8 to -10°C for some operational seeding programs. The number of ice crystals produced per gram of AgI (yield) can increase by three orders of magnitude or more as the temperature decreases from -6 to -20°C (e.g., DeMott et al. 1995). There is usually no interest in seeding SLW clouds below -20°C because abundant natural ice crystal concentrations and limited SLW can be expected at such cold temperatures.

2. PROPANE SEEDING NEED AND FEASIBILITY

Research conducted in several western States during the past decade has revealed that most orographically-produced SLW cloud exists in the lowest 1 km above mountain barriers. This SLW zone is often too warm for effective seeding with typical AgI solutions and release rates. For example, the statistical analysis presented by Super and Heimbach (1983) strongly suggested that AgI seeding was effective over Montana's Bridger Range only when crest temperatures were below -9°C . About half the Montana winter storm periods had crest temperatures above -9°C , and these tended to be the wetter periods.

Several winters of observations over the Sierra Nevada of California led Reynolds (1989) to conclude that a seeding agent was needed to convert SLW into ice at temperatures between 0 and -5°C . Most of the SLW over the Sierra Nevada was observed in this warm temperature range where AgI is believed generally ineffective.

Observations in Utah's Tushar Mountains (e.g., Sassen and Zhao 1993) and Wasatch Plateau (e.g., Super 1994, Huggins 1995) have indicated most SLW cloud is warmer than about -10°C . While Utah orographic clouds are generally colder than those found in California, a significant portion of Utah's orographically-produced SLW appears to be too warm for effective AgI seeding by current operational methods (Super 1995). This problem is common throughout the intermountain West.

Vardiman et al. (1971) demonstrated that the release of liquid propane was successful in clearing fogs with temperatures only slightly below 0°C .

The release of liquid propane as a fine mist results in rapid vaporization of the propane and subsequent chilling of the cloudy air immediately downwind of the spray nozzle. Some of the air is chilled cold enough for homogeneous nucleation of ice crystals. Hicks and Vali (1973) presented laboratory and field observations indicating that about 10^{11} to 10^{12} ice crystals resulted per gram of propane.

Assuming that liquid propane release produces 5×10^{11} ice crystals g^{-1} , the typical release rate of 3 gal h^{-1} discussed in this paper is equivalent to $6,000 \text{ g h}^{-1}$ of propane, or 3×10^{15} ice crystals h^{-1} . For comparison, a recent calibration of the manual North American Weather Consultants (NAWC) AgI generator by DeMott et al. (1995) for natural draft conditions shows a liquid cloud temperature below -9.5°C is needed for the same ice crystal source strength with the generator's AgI release rate of 8 g h^{-1} .

The ice particle concentration to be expected downwind of a point source strength of 3×10^{15} ice crystals h^{-1} can be estimated by assuming reasonable average values for plume dimensions of 15 deg width and 600 m depth (e.g., Holroyd et al. 1988), and a typical wind speed of 5 m s^{-1} near the windward slope of a mountain barrier. It can be shown that the resulting average ice particle concentration 10 km downwind of the source is about 100 L^{-1} , an order of magnitude higher than the minimum concentration estimated by Super (1994) for production of observable snowfall. These calculations suggest that the liquid propane seeding rates used in the tests to be discussed are sufficient to potentially enhance snowfall under suitable conditions.

Reynolds (1989) expanded upon earlier fog suppression work by developing propane dispensing systems for mountain locations. The units were transported by helicopter to high altitude sites in the Sierra Nevada where electrical power was provided by solar panels. Radio telemetry was used to interrogate and control the propane dispensers from a valley base station. These dispensers have been tested and refined the past few years as documented by Reynolds (1991) and Reynolds (1994). The liquid propane dispensing system developed by Reynolds is considered fully operational. The system is relatively simple, with few moving parts (e.g., solenoid valves), and has proven to have high reliability.

Propane release is confirmed in real-time by monitoring both the flow rate and the temperature near the propane nozzle.

Past work with propane seeding for snowfall enhancement has been limited and further research is needed to demonstrate how effective it might be with winter orographic clouds. However, prior observations have shown that liquid propane release can significantly enhance the ice particle concentration within SLW cloud that is only slightly below 0°C (e.g., Vardiman et al. 1971, Hicks and Vali 1973, Reynolds 1994).

3. PROPANE DISPENSER TESTS DURING THE WINTER OF 1992-93

The ability of liquid propane seeding to create abundant ice crystals at even slightly supercooled temperatures, and the successful operation of the State of California propane dispensing system, led the Utah Division of Water Resources (hereafter Division) to test a similar system in Utah. Such a system might eventually augment AgI seeding during warmer storm periods to increase overall seeding effectiveness. But the first step was to develop local experience and competence with a liquid propane dispenser.

A propane dispenser system was fabricated in Utah, based on the California design. The Utah prototype dispenser was somewhat simplified, having only one nozzle. A different type of data logger/controller (hereafter data logger) was used in Utah (a Campbell CR-10) because of local familiarity with that product. The data logger was programmed to control and monitor the propane dispenser and various other equipment, and a radio communication system was developed that could be accessed by telephone.

A testing program for various equipment was conducted from December 1992 through March 1993 on the west slope of the Wasatch Plateau. The test site was at the HAS (High Altitude Site) east of Fairview, Utah, shown on Fig. 1 of Super (1995). The site's elevation was 2500 m (all elevations above mean sea level). Technicians frequently traveled to the test site by over-snow vehicle throughout this period, especially during and after storms. The only equipment to be discussed in this paper is the

propane dispenser and associated weather sensors. An internal report, which documented the results of the 1992-93 tests, was prepared by Hansen et al. (1993). The report concluded, with respect to the propane system:

a. The modified propane dispenser was very reliable and should prove to be a useful addition to Utah's operational cloud seeding program.

b. One possible improvement to the modified (propane) dispenser would be to provide enhancements so the units could be automated (turned on and off without human intervention).

c. The real-time radio/telephone communication system was very reliable.

4. PROPANE DISPENSER TESTS DURING THE WINTER OF 1993-94

Based on the success of the 1992-93 testing of a single propane dispenser, it was decided to continue and expand propane dispenser testing during the winter of 1993-94. The single propane dispenser used in 1992-93, and all five tested in 1993-94, had the same type of nozzle. Propane release rates, as monitored by a flowmeter with each dispenser, were usually in the range 2.5 to 3.5 gal h⁻¹. Different rates could be achieved with different nozzle designs, if desired. It would be desirable to compare calculated propane consumption based on flowmeter measurements with actual consumption based on before and after weighing of the propane tanks. Such a comparison has not yet been accomplished.

4.1 Testing of Two Radio-controlled Propane Dispensers

The 1993-94 tests were conducted in two areas on the Wasatch Plateau. Two high altitude propane dispensers were operated as part of the Utah/NOAA AMP (Atmospheric Modification Program) field program between mid-January and mid-March 1994. One site was the "new" HAS at 2540 m elevation, located 1 km south of the previous winter's HAS in order to be more exposed to south and southwest winds. The second site was AHS (Aspen Hills Site), located 4 km south of the new HAS at 2340 m

elevation. These sites are shown on Fig. 1 of Holroyd et al. (1995). Both sites were southeast of Fairview, and were controlled by radio as during the prior winter. That is, someone decided when to turn the dispensers on and off and manually did so via computer, modems and radio telemetry. One or both of these dispensers were operated during a limited number of short-term experiments when instrumented aircraft sampling was conducted and ground observations were made during orographic storms.

The purpose of the HAS/AHS propane seeding experiments was to physically evaluate the effectiveness of such seeding in enhancing the ice particle concentration in SLW clouds. The effectiveness of propane seeding in enhancing snowfall will also be examined, but this is a far more difficult problem to physically evaluate. Analyses of the propane seeding experiments have yet to be accomplished, so little can be stated about the results. The propane dispensers proved to be reliable, similar to the prior winter's tests. Tracer gas co-released with the propane was routinely detected on and above the Wasatch Plateau. Consequently, it can be assumed that ice crystals created by releasing propane in SLW cloud were also transported over the Plateau. Ice particle characteristics were monitored with three 2D-C imaging probes as discussed by Holroyd et al. (1995). Results of analyzing data from these ice particle imaging probes will be presented in future papers.

4.2 Testing of an Automated Propane Seeding System

The main topic of this paper is the preliminary testing of a prototype automated propane seeding system. Such a system, if successful, would have a number of advantages. As far as the authors are aware, the propane seeding system tested during early 1994 was the first fully-automated system ever used for winter orographic cloud seeding. Once the system was installed, it required no human intervention or decision-making.

The system was intended to respond to observed weather conditions. This would eliminate the need for weather forecasting which is costly and of limited accuracy in mountainous terrain where observations are scarce. Seeding material (propane) would be released only when conditions were suitable for the formation of ice crystals. This would enable

potentially seedable conditions to be seeded which does not happen when weather forecasts are "blown."

The test area for the automated propane seeding system was on the west slopes of the Wasatch Plateau east of Ephraim, Utah, approximately 30 km south of the two propane dispensers east of Fairview (see Fig. 1 of Holroyd et al. 1995). This area was judged to be sufficiently crosswind to prevent possible seeding effects from influencing the Utah/NOAA (Fairview) experimental area. Yet all five dispensers were in close enough proximity to be interrogated by radio from a single base station located at the Utah/NOAA headquarters near Fairview. The data logger at each dispenser stored observations for about one week before the earliest observations were overwritten by new observations. The data logger's memories were periodically downloaded via radio telemetry and modems to a personal computer at the base station.

Three high altitude propane dispensers were configured into a network in the Ephraim test area. The center dispenser was located on an exposed windy ridge known as Freds Flat at an elevation of 2755 m. This site was near an existing electrical power line which permitted operation of various weather instruments. The most important instrument for deciding when to seed was a tower-type Rosemount icing rate device which detected the presence of SLW. Supercooled liquid water is crucial to effective cloud seeding since it is the "raw material" that is intended to be converted to snowfall. Unfortunately, SLW is difficult to automatically monitor at remote locations without electrical power. Power availability at Freds Flat also permitted use of a heated Hydrotech wind vane and anemometer for wind direction and speed measurements. (Rosemounts and Hydrotechs consume too much power for practical operation with solar panels). Air temperature and relative humidity were also measured at Freds Flat, but these sensors required little power.

It would, of course, be preferable to monitor the weather at each propane dispenser and to operate individual dispensers only when they were in SLW cloud with appropriate wind speed and direction. The approach used in the 1994 testing assumed that the Freds Flat observations represented all three dispenser sites. This assumption is simplistic but is probably valid for many storm periods since the

sites were not far apart and had similar altitudes and local exposures. Moreover, it is more realistic to base a seeding decision for a particular site on measurements made even several kilometers distant than on a weather forecast for mountainous terrain based on synoptic-scale observations.

The Freds Flat data logger was programmed to monitor SLW presence, wind speed and direction and air temperature. When certain criteria were met, noted in Table 1, the Freds Flat propane dispenser was automatically turned on. Similar dispensers were also turned on via radio link between Freds Flat and the data loggers at two satellite locations near the same altitude. These sites were on the south end of Hell Hole Ridge, located 3 km north of Freds Flat at 2785 m, and near the top of Bald Mountain, located 6 km southwest of Freds Flat at 2575 m. All three sites were expected to frequently be in SLW cloud during storms.

Propane continued to be released by all three dispensers until the specified weather criteria were not met for a pre-selected time. The data logger's "decisions" could be manually overridden at any time; for example, if it were desired to suspend seeding because of a well-above-normal snowpack. Manual override of individual data loggers was possible either from the base station or from any computer connected to the base station by modem and commercial telephone. Moreover, each satellite dispenser had its data logger programmed to stop releasing propane if either:

- (a) no communication was received from the weather observing site for an extended period, or
- (b) the sensor in the propane stream did not detect a substantial temperature decrease which was expected with proper propane release.

Table 1 shows that 1 h averaging periods were used for all measurements with the exception of the Rosemount icing meter. It was decided to require 2 cycles of the Rosemount icing meter before initiating seeding to insure that a "significant" SLW episode was occurring. For example, it was thought that the slow accumulation of "feather rime" might sometimes cause a single icing meter cycle when seeding potential was negligible. A 2 h period was used with the icing rate device because of concerns

TABLE 1. Criteria for automated propane seeding based on Freds Flat meteorological observations.*

I. Initiate liquid propane release from all dispensers when:

A minimum of two Rosemount cycles occurred during the past 2 h, and the average values for the past 1 h for air temperature was at or below 0.0°C; wind direction was greater than 180 but less than 330 degrees true; and wind speed** was greater than 1.0 m s⁻¹.

II. Terminate liquid propane release from all dispensers when:

No Rosemount cycles have occurred during the past 2 h and/or one or more of the average values of air temperature, wind direction and wind speed was outside the criteria stated above for the past 1 h.

III. Terminate liquid propane release from either or both of the two satellite dispensers when:

They have lost radio communication with the Freds Flat station for over 12 h, or the temperature sensor just downstream of the propane nozzle did not detect a significant temperature drop after the dispenser was turned on.

* All averages for the past 1 h, and the total Rosemount cycles for the past 2 h, were recalculated every 12 min.

** Because of the high starting threshold of the Hydrotech anemometer, a zero voltage output was considered to represent 0.7 m s⁻¹ in all calculations.

that 2 cycles might not occur within 1 h with light winds and/or low SLW contents. Low frequencies of icing meter cycles have been experienced at some mountain locations with the low cloud water contents characteristic of orographic clouds.

Seeding was continued for 2 h after the last Rosemount cycle, if other weather criteria were

still being met. It is known that ice crystals can be created by expansion of liquid propane in the absence of SLW as long as the atmosphere is saturated with respect to ice. Such crystals will even grow if the atmosphere is subsaturated with respect to water but supersaturated with respect to ice. Ice saturation is very difficult to measure in the field. Therefore, seeding was continued for 2 h after the end of SLW detection in anticipation that the atmosphere might still permit ice crystal formation and growth by release of propane.

The propane tanks, dispenser systems and weather instruments were installed during the fall of 1993 when truck travel to the sites was still practical. The propane dispensers were not visited during the January to March 1994 test period, partially because of higher priority work (the Utah/NOAA physical seeding experiments east of Fairview; e.g. Holroyd et al. (1995). Measurements from the network were periodically reviewed and a problem was recognized with one site as will be discussed. The problem's cause was suspected and verified by on-site inspection after the winter season.

The California experience, described in the previously cited articles by Reynolds, was that dispensers rarely required visitation after installation each fall.

5. SUMMARY OF AUTOMATED PROPANE DISPENSER SYSTEM OPERATION

5.1 Freds Flat Dispenser Operation

The Freds Flat propane dispenser system automatically turned itself on and off 17 times between January 5 and mid-March 1994. This was a period with a low storm frequency. For example, the Utah/NOAA program did not have any weather suitable for experimentation from mid-January until 26 January, or after February 27 till the program end on March 15. No SLW was monitored at Freds Flat during the latter period.

Every time 2 or more Rosemount cycles occurred within a 2 h block, the Freds Flat system began to dispense propane, as the wind speed and direction were always within the limits specified in Table 1. The air temperature criteria was, of course, redundant. The Rosemount will not cycle (i.e.,

time ice will not form on the probe) unless the temperature is below 0°C. In most instances the 2 Rosemount cycles occurred within 0.5 h or less, often in adjoining 12 min sampling periods and sometimes in the same sampling period.

Propane was released from the Freds Flat dispenser for a total of 83 h so the average release duration was 4.9 h. Individual release periods ranged from a single 1.0 h period to maximum 10.4 h. The median period was 4.0 h. It is apparent that SLW episodes were relatively brief at Freds Flat.

Examination of the data revealed that had a single Rosemount cycle been used to initiate seeding, only 8 cases existed without a second cycle within 2 h. Four of these 8 cases would have been rejected because either the wind speed or wind direction was out of limits.

Termination of seeding at Freds Flat was always based on the absence of SLW for about 2 h, although in 2 cases the last hour's wind direction became greater than 330 degrees which would also terminate seeding. The period between the last Rosemount cycle and termination of propane release was not always 2 h as had been intended. With the 12 min sampling interval, 2 h corresponds to 10 intervals. In fact, the intervals between the last Rosemount cycle and propane shutoff ranged between 8 and 13 intervals (1.6 to 2.6 h) in 15 of the 17 seeding episodes. Shutoff occurred after only 3 and 5 cycles in the remaining 2 episodes. In none of the early shutoff cases were the wind or temperature criteria out of bounds. It is believed that a programming "bug" was responsible for the variation in shutoff time, although this was not verified. At any rate, the dispenser system always turned itself off after icing ceased, and usually about 2 h after the last Rosemount cycle as intended.

The lack of SLW was always the determining factor in propane shutoff. Few "false alarms" would have occurred if seeding had been initiated by a single Rosemount cycle. Consequently, future automated propane seeding could be simplified, at least if based on Freds Flat observations. It is recommended that seeding be initiated whenever the first Rosemount cycle occurs, and seeding should thereafter continue until 2 h pass without any Rosemount cycles. This would insure that all

potentially seedable episodes are seeded in their entirety. Some limited seeding would occur during periods with unsuitable meteorological conditions with this simplified scheme. However, the only negative consequence should be the loss of relatively small amounts of propane.

5.2 Hell Hole Ridge Dispenser Operation

Hell Hole Ridge data were inadvertently not downloaded for a week period in early February which had 4 Freds Flat seeding episodes. However, data are complete for the remaining 13 seeding episodes. With a single exception, Hell Hole Ridge propane releases were an exact match in time with the Freds Flat releases. That is, both initiation and termination of propane release were always within the same 12 min sampling periods as had been intended.

On February 19 the Hell Hole Ridge dispenser was turned on at the same time as Freds Flat. However, the Hell Hole Ridge dispenser continued to release propane for 5.6 h after Freds Flat shut down. The reason for the shutdown delay is not known, but may have been caused by radio communication problems. With this single exception, the available data indicate that Hell Hole Ridge propane dispensing system worked just as intended.

5.3 Bald Mountain Dispenser Operation

The Bald Mountain dispenser did not operate as well as the other 2 dispensers in the automated network. The main problem was verified after the field season when the site was visited for the first time since early winter. The temperature sensor for the propane spray did not have a secure mechanical holder. As a consequence, the sensor did not hold the same position, but could be moved by the propane spray and the local airflow.

All 3 data loggers were programmed to shut down their dispenser if the temperature sensor did not indicate at least -40°C when the propane valve was turned on. The Bald Mountain sensor was seldom this cold. With a single exception, the Bald Mountain dispenser was turned on at the same time (within 12 min) as the Freds Flat master unit. However, in the large majority of the 17 seeding episodes, the Bald Mountain dispenser would turn

itself off after 24 min. It would later respond to the continued signal from Freds Flat that seeding should be conducted and would turn on again about 0.4 or 0.6 h after shut down. The Bald Mountain dispenser would continue to cycle on and off in this manner throughout the seeding episode.

During a few storms the propane spray temperature sensor was cold enough that the Bald Mountain dispenser operated properly throughout the seeded period.

The solution to the Bald Mountain dispenser problem is simple. A more rigid holder for the temperature sensor needs to be fabricated.

6. FURTHER PRACTICAL CONSIDERATIONS AND TESTING

Electrical power lines are uncommon in mountains. Consequently, it would be desirable to use meteorological sensors that did not require much electrical power in future applications of automated propane seeding. Unfortunately, the authors are not aware of any icing rate sensor that requires significantly less power than a Rosemount icing rate device. Testing of relative humidity sensors from three manufacturers (Handar, Rotronics, Vaisala) at the HAS in 1992-93 did not encourage their use for estimation of SLW cloud presence. The sensors would sometimes indicate relative humidities below 90 percent when in cloud, and sometimes higher relative humidities when no cloud was present. It appeared that use of conventional relative humidity sensors would result in a high frequency of false alarms. That is, seeding often would be initiated when conditions were not suitable, and often would not be initiated when conditions were suitable.

Propane-heated wind sensors have been developed, and thermal wind sensors exist which consume much less power than a Hydrotech system. Consequently, it is believed practical to measure wind (and air temperature) at remote sites that do not have power lines or electrical generators. The chief problem is the measurement of SLW presence. To further address this problem, a test was conducted in early 1994 at the HAS. A propane-powered Telan thermoelectric generator (60 watt output) was used to continually charge batteries which powered a Rosemount icing meter through a dc-to-ac inverter

(tower-type Rosemounts require 115 vac power). This approach proved to be practical and very reliable, and icing rate observations were obtained at the HAS throughout the field season.

It is desirable to further simplify and economize remote observations of SLW and wind within orographic cloud on windward mountain slopes. However, the existing technology is adequate to obtain such observations and to use them to control the release of cloud seeding agents. Remote-controlled AgI generators are available, but existing units are expensive and complex. The simplicity of propane dispensers results in their much lower per-unit price and significantly higher reliability compared with remote-controlled AgI generators.

Of course, AgI seeding has advantages over propane seeding that may favor the former in particular circumstances. For example, unlike propane, AgI can be released well upwind of supercooled cloud and well below cloud base and still be effective in causing ice particles. Such AgI releases would be expected to disperse through a much larger volume of atmosphere than would ice particles caused by propane release within the cloud. These factors favor AgI seeding provided that AgI released upwind of orographic cloud is transported into sufficiently cold cloud regions in adequate concentrations to be effective in snowfall enhancement.

7. SUMMARY AND RECOMMENDATIONS

A propane dispenser was tested during the 1992-93 winter, well up the west slope of the Wasatch Plateau east of Fairview, Utah. The dispenser was based on the design of Reynolds (1989, 1991), with some modifications. The dispenser was turned on and off by a data logger/controller upon receipt of appropriate radio signals from a valley base station. Human intervention and a computer were used to initiate the radio signals. Various data were logged at the site and periodically downloaded to the base station.

A technician was often at the dispenser site, monitoring its operation, while a second technician turned the system on and off. These visual observations helped to confirm the very reliable operation of the propane dispenser.

Further testing was done during early 1994, in two different modes. In the first mode, two dispensers were used during physical seeding experiments with system start-up and shutdown done as in the prior winter (human intervention, radio telemetry and computers). The physical seeding experiments have yet to be analyzed and reported, but dispenser operation was again very reliable.

The second testing mode involved a prototype seeding system which was automatically turned on and off according to weather observations. The weather (SLW, wind and temperature) was monitored at a central dispenser. That dispenser, and two satellite dispensers, were controlled by the presence/absence of SLW, wind measurements, and (redundant) air temperature observations.

The automated seeding system had some problems, but they are considered minor and easily correctable. The system generally functioned very well, especially considering that no visits were made to the dispensers once testing started. Some improvements should be made in the data logger program. A more rigid holder for the propane stream temperature sensor would eliminate the cycling problem experienced by the Bald Mountain dispenser.

It is recommended that future use of an automated propane dispenser system use simplified criteria. The presence of SLW would continue to be measured by a Rosemount icing rate device well up the windward slope. Seeding would commence as soon as the first Rosemount cycle occurred. Seeding would continue for some time (about 2 h) after the last Rosemount cycle in an episode. Wind speed and direction could be monitored but are not believed essential because SLW rarely occurred unless wind speed and direction were appropriate for targeting the Wasatch Plateau. (It is anticipated that most north-south oriented mountain ranges would experience similar conditions.) Some propane would be released during essentially unseedable conditions if only SLW presence/absence was used to control seeding. However, the amount of wasted propane is expected to be minor.

A thermoelectric generator-battery-inverter combination, as used at the HAS in early 1994, is a practical means of powering a Rosemount icing rate

device, a data logger/controller, a propane dispenser and radio gear at an exposed remote location in all weather conditions. This system could be the master station controlling a number of satellite dispensers located at similar high altitude sites crosswind of the master station. All sites should be chosen where local SLW production is expected. If one wanted to be sure that SLW existed at each dispenser, each site could monitor SLW with a Rosemount device. This would be a superior but more costly approach.

Propane dispenser testing in California and Utah in recent years has demonstrated the feasibility of a completely automated system that is both reliable and economical. Analysis of the early 1994 physical seeding experiments should improve understanding of the snowfall-enhancing capability of propane seeding. Prior research leaves no doubt that propane seeding can markedly enhance ice crystal concentrations with liquid cloud at or below 0°C. However, it is recommended that the ice crystal yield of the currently-used (in Utah) propane nozzle and release rate be documented. The previously-cited yield values of 10^{11} to 10^{12} ice crystals per gram of propane are based on investigations done over two decades ago. These studies used different release rates and nozzles than recently used in California and Utah. It is of obvious interest to test the current design to determine whether yield values are as high as expected.

Additional key questions to be answered concern ice crystal growth and fallout times downwind of propane dispenser sites. To be effective, propane dispensers need to be within SLW cloud, or at least not far below SLW cloud base where saturation with respect to ice exists. This requires that dispensers be located well up the windward slopes of mountain barriers. Such siting limits the time (distance) available for ice crystal growth to snowflake sizes and fallout to the mountain surface. There is concern that this time (distance) may frequently be too limited for significant snowfall to occur before the seeded ice crystals are carried into the lee subsidence zone where sublimation and evaporation occur.

Another concern with high altitude releases of propane (or AgI) is that crosswind dispersion may be limited, requiring that the crosswind spacing of generators also be limited to avoid unseeded "gaps" between seeding plumes. It may be possible to have

greater spacing between AgI generators located further downslope or in upwind valleys thereby requiring fewer seeding sites. Of course, use of lower altitude sites assumes adequate routine transport from them into SLW cloud zones as well as adequate source strengths.

It is recommended that analysis of the early 1994 microphysical observations, and additional future observations, be combined with numerical modeling to address the above concerns. A sophisticated microphysical model, combined with a two or three dimensional airflow model, should be adequate to address ice particle growth and fallout trajectories.

It may be that only relatively wide mountain barriers offer sufficient time and distance for propane seeding to routinely affect snowfall on that barrier. In that case, the best use of high altitude propane seeding may be in seeding a secondary downwind barrier similar to the Bridger Range Experiment target (Super and Heimbach 1983). In any event, the frequency of orographic SLW cloud at temperatures too warm for AgI nucleation is significant over mountains of the western U.S. That fact alone argues for continued experimentation with alternative seeding methods such as release of liquid propane which might augment AgI seeding when slightly supercooled clouds are present.

Acknowledgements. The authors gratefully acknowledge the considerable efforts of Joe Hanks who served as a field technician for the Fairview area tests, and the overall guidance from Barry Saunders of the Utah Division of Water Resources. This work was supported by the NOAA Atmospheric Modification Program and the Bureau of Reclamation, both in cooperation with the Utah Division of Water Resources.

8. REFERENCES

- DeMott, P.J., A.B. Super, G. Langer, D.C. Rogers and J.T. McPartland, 1995: Comparative characterizations of the ice nucleus ability of AgI aerosols by three methods. *J. Wea. Mod.*, 27, in press.
- Griffith, D.A., J.R. Thompson and D.A. Risch, 1991: A winter cloud seeding program in Utah. *J. Wea. Mod.*, 23, 27-34.

- Hansen, R., A. Super, C. Ogden and A. Hilton, 1993: Evaluation of remote-controlled cloud seeding technologies, Bureau of Reclamation Technical Assistance to States Report for the Utah Division of Water Resources: Fiscal Years 1992 and 1993.
- Hicks, J.R., and G. Vali, 1973: Ice nucleation in clouds by liquified propane spray. *J. Appl. Meteor.*, **12**, 1025-1034.
- Holroyd, E.W., J.T. McPartland and A.B. Super, 1988: Observations of silver iodide plumes over the Grand Mesa of Colorado. *J. Appl. Meteor.*, **27**, 1125-1144.
- _____, J.A. Heimbach and A.B. Super, 1995: Observations and model simulation of AgI seeding within a winter storm over Utah's Wasatch Plateau. *J. Wea. Mod.*, **27**, in press.
- Huggins, A.W., 1995: Mobile microwave radiometer observations: Spatial characteristics of supercooled cloud water and cloud seeding implications. *J. Appl. Meteor.*, **34**, 432-446.
- Reynolds, D.W., 1989: Design of a ground based snowpack enhancement program using liquid propane. *J. Wea. Mod.*, **21**, 29-34.
- _____, 1991: Design and field testing of a remote ground-based liquid propane dispenser. *J. Wea. Mod.*, **23**, 49-53.
- _____, 1994: Further analysis of a snowpack augmentation program using liquid propane. *J. Wea. Mod.*, **26**, 12-18.
- Sassen, K., and H. Zhao, 1993: Supercooled liquid water clouds in Utah winter mountain storms: Cloud-seeding implications of a remote-sensing dataset. *J. Appl. Meteor.*, **32**, 1548-1558.
- Super, A.B., 1994: Implications of early 1991 observations of supercooled liquid water, precipitation and silver iodide on Utah's Wasatch Plateau. *J. Wea. Mod.*, **26**, 19-32.
- _____, 1995: Case studies of microphysical responses to valley-released operational AgI seeding of the Wasatch Plateau, Utah. *J. Wea. Mod.*, **27**, in press.
- _____, and J.A. Heimbach, 1983: Evaluation of the Bridger Range winter cloud seeding experiment using control gages. *J. Appl. Meteor.*, **22**, 1989-2011.
- Vardiman, L, E.D. Figgins and H.S.Appleman, 1971: Operational dissipation of supercooled fog using liquid propane. *J. Appl. Meteor.*, **10**, 515-525.

CLOUD SEEDING AND ATMOSPHERIC TRACER PROGRAM CONDUCTED IN THE TSENGWEN RESERVOIR AREA OF TAIWAN DURING THE 1992 MEI-YU SEASON

By

Jack Ming-Sen Lin and Paul Tai-Kuang Chiou
Taiwan Central Weather Bureau, Taiwan, R.O.C.
Don A. Griffith, George W. Wilkerson and Mark E. Solak
North American Weather Consultants,
Salt Lake City, Utah, U.S.A.

ABSTRACT

North American Weather Consultants (NAWC) of Salt Lake City, Utah, U.S.A. was contracted by the Taiwan Central Weather Bureau (CWB) to assist in the design, operation and analysis of a cloud seeding and atmospheric tracer program. This program was conducted from April 22 to June 23, 1992. The area of interest was the Tsengwen River drainage located in south central Taiwan. The program was conducted during a portion of the Mei-Yu season which is the transition period between the northeast and southwest monsoon seasons.

A network of 15 ground based silver iodide (AgI) generators was utilized to conduct the cloud seeding program. A tracer gas, sulfur hexafluoride (SF_6), was also released at one of the silver iodide generator sites on some of the operational days. The SF_6 was tracked by an instrumented van on some of these tests. The SF_6 was tracked on one test with instrumentation carried on-board a C-130 cargo aircraft. The goal of this tracer work was to attempt to document the vertical transport of SF_6 and by inference AgI. The question being considered was whether the use of AgI ground generators in Taiwan offers an effective means of seeding clouds in Taiwan.

1.0 INTRODUCTION

Drier than normal conditions occurred in portions of Taiwan during the normally wet typhoon season in the summer of 1991. Representatives of the Central Weather Bureau (CWB) of Taiwan, Republic of China contacted North American Weather Consultants (NAWC) in December 1991 to discuss the potential application of cloud seeding to alleviate some of the negative impacts of the drought conditions. NAWC personnel performed an assessment of the potential application of cloud seeding in Taiwan. The main recommendation of this assessment was that the application of cloud seeding technology appeared to be suitable for application in Taiwan.

A two month operational cloud seeding program with an associated transport and dispersion research component was conducted. This program was conducted during the Mei-Yu season in Taiwan which marks the transition from the winter (northeast) monsoon to the summer (southwest) monsoon. It is during this season (April to June) that southern Taiwan receives approximately three-fourths of its annual precipitation (Chen and Kuo, 1991). The target area for the two month program was the Tsengwen River drainage located in south-central Taiwan.

2.0 PROGRAM DESIGN

An operations center was established at the Tsengwen Dam complex. NAWC and CWB

personnel operated from this facility. A network of 15 ground based silver iodide generators was established to be operated during the two month period (April 22 to June 23, 1992). This ground seeding mode was selected on the basis of a long-term cloud seeding program which had been conducted in central Taiwan in the years of 1951 to 1978. An evaluation of this program had indicated precipitation increases in the target area (Chin-Fei Hsu, 1981). NAWC recommended that a tracer gas capability be added to this ground based design in an attempt to verify the vertical transport of the silver iodide nuclei. To be effective, the silver iodide nuclei would need to reach at least the -5°C level, approximately 5.5 to 6.0 km in Taiwan. A real-time gas analyzer (Benner and Lamb, 1985) was installed in a van and later in an aircraft to track sulfur hexafluoride (SF_6) released from one of the silver iodide generator sites. The CWB arranged for special rawinsonde observations in support of the program. Figure 1 provides the location of the target area and associated features.

3.0 OPERATIONS

Only three different seeding events were attempted due to a number of program suspensions related to concerns about heavy rainfall and/or impacts on orchard areas in the foothill regions adjacent to the target area.

A total of seven SF_6 tracer studies were conducted. Five of these studies involved surface sampling and two involved airborne sampling. The airborne sampling was accomplished in a rather unique manner which involved driving the van equipped with the SF_6 real-time analyzer into a Taiwanese Air Force C-130 cargo aircraft.

4.0 RESULTS

Visual observations classified days into potentially seedable and non-seedable primarily based upon the presence of convective clouds observed over the target area. Of the 52 days, 22 were considered to present some seeding potential. Of these 22 days 13 were classified as associated with frontal systems and 9 as airmass events. Table 1 summarizes some statistics from the project rawinsonde data for these 22 days.

The tracer van was able to detect the SF_6 plume released from a single location at the surface on three different experimental days. In essence the detection of SF_6 at the surface implies that at least

a portion of the ground released silver iodide was not being transported above the surface of the earth. There is therefore some question about the effectiveness of ground based seeding during these experiments.

Two aircraft tracer missions were flown near the end of the operational period. The first mission was aborted early due to mechanical problems. The SF_6 plume released from a single surface location was, however, encountered three times before the mission was terminated. These plumes were detected at approximately 900 m above ground level.

The second aircraft mission was more successful. SF_6 was released from a surface location (near sea level) at a rate of 75 kg/hr. A special project rawinsonde, taken from Tainan near the SF_6 release point, is provided in Figure 2. The SF_6 plume was encountered 17 different times on this flight with observed concentrations varying from 20 to 800 parts-per-trillion (ppt). The SF_6 plume was observed quite close to the release site at altitudes from .9 km to 2.4 km. The highest level at which the SF_6 plume was observed corresponded well with a slight inversion as observed on the special rawinsonde observation (Figure 2). Of interest was the fact that the SF_6 plume was encountered in several small cumulus clouds which developed during the experiment. Of note is the fact that the top of the plume only rose to a minimum temperature of $+12^{\circ}\text{C}$, far above the temperature activation threshold of approximately -6°C for silver iodide to serve as an ice nucleant.

The data collected from this experiment can be utilized to calculate the potential maximum number of ice crystals that could be produced from a ground release of silver iodide. The following factors are important in such a calculation: 1) the SF_6 release rate was 75 kg/hr or 20.81 g/s, 2) a silver iodide release rate from one of NAWC's manual generators would have been 13 g/hr or .0036 g/s, 3) $1\text{ }\mu\text{g}/\text{m}^3$ of $\text{SF}_6 = 167$ ppt at standard temperature and pressure, 4) the average observed concentration of SF_6 at the highest detected plume height (2.4 km) was 31 ppt, 5) the C-130 aircraft was pressurized to sea level, 6) the NAWC silver iodide generator in a recent cloud chamber test at Colorado State University yielded an average 9×10^{14} ice crystals per gram of silver iodide consumed with a supercooled water content of $0.5\text{ g}/\text{m}^3$ (DeMott, 1994).

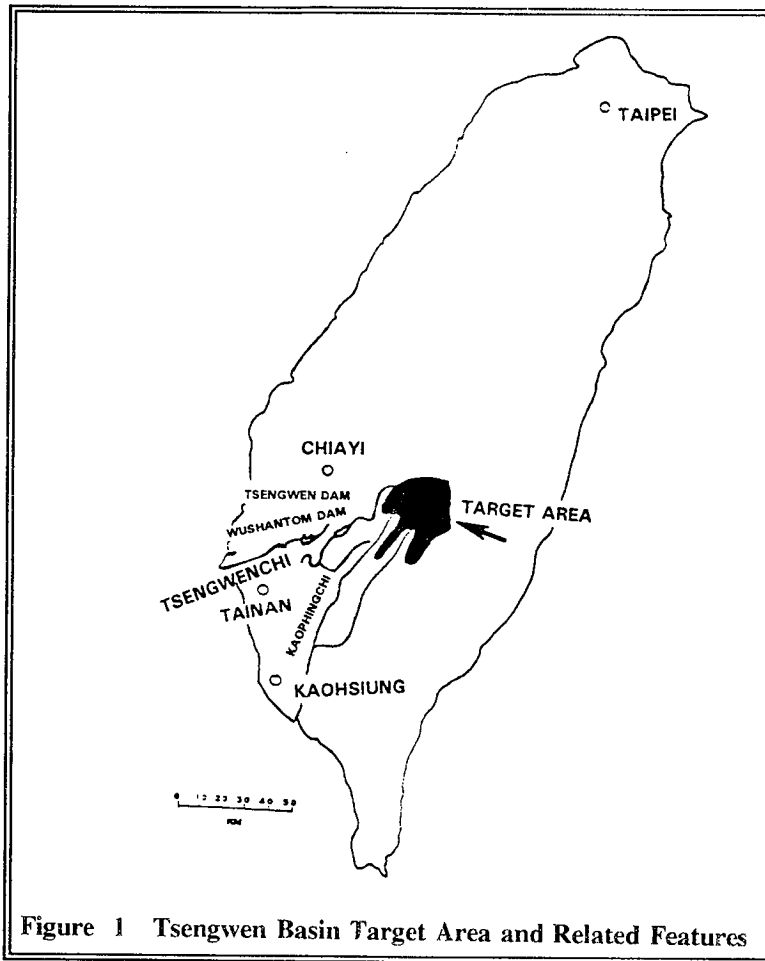


Table 1 Sounding Climatology for Seedable Cases

	0°C Level MB	-5°C Level MB	-10°C Level MB	K Index	TT Index	850 MB Temp °C	850 MB DP °C	700 MB Temp °C	700 MB DP °C	500 MB Temp °C
SEEDABLE CASES (BOTH FRONTAL AND AIR MASS - 44 SOUNDINGS)										
MEAN	577	508	457	34	43	16.9	14.5	8.3	5.2	-5.8
MINIMUM	536	475	420	22	36	11.8	8.2	2.4	-3.6	-8.9
MAXIMUM	638	560	491	41	49	21.6	18.7	11.2	10.2	-1.3
SEEDABLE CASES (FRONTAL ONLY - 26 SOUNDINGS)										
MEAN	575	506	454	34	42	16.8	14.5	8.5	5.5	-5.5
MINIMUM	547	475	420	22	36	13.8	8.8	6.0	-2.6	-8.7
MAXIMUM	609	534	491	39	47	19.0	17.2	11.2	10.2	-1.3
SEEDABLE CASES (AIR MASS ONLY - 18 SOUNDINGS)										
MEAN	580	512	461	34	44	17.1	14.4	8.0	4.7	-6.1
MINIMUM	536	488	440	23	38	11.8	8.2	2.4	-3.6	-8.9
MAXIMUM	638	560	488	41	49	21.6	18.7	11.0	9.0	-3.7

Using this information, the expected concentration of silver iodide at 2.4 km can be calculated from the following equation:

$$\chi \text{ AgI} = \frac{\chi \text{ SF}_6 \bullet Q \text{ AgI}}{Q \text{ SF}_6}$$

Where:

$\chi \text{ AgI}$ = silver iodide concentration

$\chi \text{ SF}_6$ = sulfur hexafluoride concentration

$Q \text{ AgI}$ = release rate of silver iodide

$Q \text{ SF}_6$ = release rate of sulfur hexafluoride

$$\chi \text{ AgI} = \frac{(2.3 \times 10^{-4} \text{ } \mu\text{g/l})(.0036 \text{ g/s})}{20.81 \text{ g/s}}$$

$$\chi \text{ AgI} = 3.98 \times 10^{-14} \text{ g/l}$$

If this concentration had been observed at -10°C in a cloud with 0.5 g/m^3 supercooled liquid water content and all of the silver iodide nuclei reacted in a short period of time (i.e., ≤ 1 minute), the calculated AgI concentration would yield $(3.98 \times 10^{-14} \text{ g/l} \times 9.0 \times 10^{14} \text{ crystals/g})$ 36 ice crystals/l in the cloud at -10°C . Since the average SF_6 concentration was, however, observed at 2.4 km ($+12^\circ\text{C}$) an adjustment in the SF_6 concentration was necessary. If it is assumed that the SF_6 would disperse at the same rate in going from sea level to 2.4 km as it would from 2.4 km to 6.1 km (-10°C) then this calculation would yield approximately 14 crystals/l at -10°C . This concentration is slightly above the 1 to 10 crystals/l range often cited as the desired number of crystals in a cloud to be produced from a cloud seeding program.

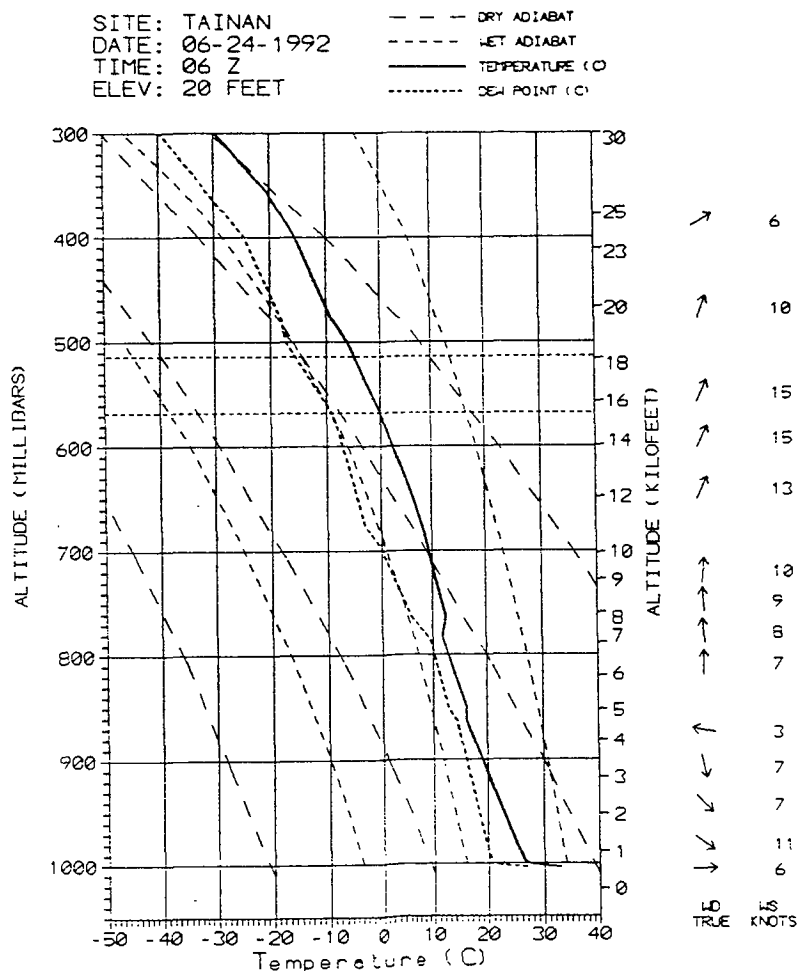


Figure 2 June 24, 1992 - 06Z Project Sounding

There are obviously several assumptions in these calculations. It would be highly desirable to continue the tracer research in an attempt to document SF₆ transport in adequate concentrations to the -10°C level in towering cumulus clouds. This SF₆ tracer research could be refined by concurrently measuring ambient ice particle concentrations in and outside the SF₆ plume to investigate the potential silver iodide seeding signatures.

5.0 CONCLUSIONS

Several conclusions were reached regarding this program. Those conclusions are as follows:

- The Mei-Yu season appears to produce sufficiently frequent opportunity for precipitation increase via cloud seeding to warrant inclusion of that season in an overall cloud seeding program design for southern Taiwan.
- Mei-Yu season cloud seeding opportunities in southern Taiwan occur in two basic categories, organized frontal systems and airmass thunderstorms.
- Ground-based seeding releases appear to have some promise during the Mei-Yu season in certain circumstances in southern Taiwan, primarily with frontal systems having organized low level wind flow. This concept is supported by the frequency of deep convective cloud occurrence, combined with rawinsonde indications of trapping inversions often being overcome when well-organized low level south-southwest flow is established. Limited airborne tracer plume tracking efforts also suggest that vertical displacement of seeding material released from the surface can occur in some cases. The ground-based seeding effectiveness question requires additional investigation.

- Given frequent convective cloud base heights in the vicinity of 1.5 km, and 850 mb temperatures in the seedable situations averaging nearly 10°C, the dynamic seeding approach utilizing aircraft would seem to be well worth serious consideration in deep convective situations with low/warm cloud bases.
- The real-time tracer plume tracking capability provided valuable information regarding the ground-based seeding issue.

REFERENCES

- Benner, R. L. and B. Lamb, 1985: A Fast Response Continuous Analyzer for Halogenated Atmospheric Tracers. *American Meteorological Society Journal of Atmospheric and Oceanic Technology*, Vol. 2, No. 4, pp. 582-589.
- Chen, G. T. and Y. H. Kuo, 1991: The Scientific Results of TAMEX. American Meteorological Society International Conference on Mesoscale Meteorology and TAMEX, Taipei, Taiwan, December 3-6, 1991, pp. 7-15.
- Chin-Fei Hsu, 1981: Weather Modification Activities in Taiwan, 1951-1978. Weather Modification Association, *Journal of Weather Modification*, Vol. 13, No. 1, pp. 161-164.
- DeMott, P. J., 1994: Tests of the ice nucleating ability of aerosols produced by the North American Weather Consultants and Montana State University solution combustion generators. Colorado State University Report to the Utah Division of Water Resources.

THE NOAA ATMOSPHERIC MODIFICATION PROGRAM-- A 1995 UPDATE

Joseph H. Golden, Director
NOAA Atmospheric Modification Program
Silver Spring, Maryland. 20910 USA

1. Introduction

NOAA's Atmospheric Modification Program owes its origins to the Weather Modification Advisory Board Report (1978), that was commissioned by the Secretary of Commerce. One of the key recommendations of that interdisciplinary panel report was the establishment of a new, vigorous research program by NOAA, which was layered on top of some pre-existing operational cloud seeding programs in the States. Concurrently, the water management community within some of the States organized to seek Congressional support for their atmospheric modification efforts. These actions resulted in the formation of the "Federal/State Cooperative Program in Weather Modification Research", now termed the Atmospheric Modification Program (AMP) to reflect the inclusion of research on inadvertent weather modification and climatic change impacts. The AMP is carried forward in the National Oceanic and Atmospheric Administration (NOAA), Oceanic and Atmospheric Research, by renewable two-year cooperative agreements with the six member states: Arizona, Utah, Nevada, North Dakota, Illinois, and Texas. We should emphasize that the AMP Program supports a large fraction of the cutting-edge research in cloud physics and associated laboratory and field measurements in the U.S. The status of the program through 1991 was reported by Reinking (1992). An excellent review of progress in planned weather modification between 1991-1994 will soon be published by Czyns(1995).

2. The Atmospheric Modification Program: Mission and Focus

The AMP research is conducted within the states' universities and research institutes, private industries and collaborating research groups within federal and state agencies (e.g., NOAA, the National Center for Atmospheric Research, and the Bureau of Reclamation). AMP seeks to be technically responsive to regional and national water resource and hydrometeorological issues, and to the needs of our user community. We start from

the premise that better understanding of both natural and modified precipitation will lead to general scientific acceptance of the modification technology. The AMP results to date support the recent Policy Statements on Weather Modification issued by the AMS and WMO(both 1992). The program emphasizes physical design, application of numerical cloud/storm models and new observing technologies, and physical evaluation. The six states are now partners with the federal government in the NOAA/State AMP; indeed, the program of each state reflects its needs and interests with respect to atmospheric modification in its own climate regime. Thus, research in Arizona, Utah and Nevada is focussed on wintertime precipitation in order to secure larger and more reliable spring and summer runoff from the melt of mountain snows. The focus in Illinois, North Dakota and Texas is on precipitation from deep summertime(growing season) convection. Here, the development, testing and application of technologies to increase rainfall and, in the case of North Dakota, to reduce the damaging effects of hail are important. Illinois, at its State Water Survey, has a growing research effort in assessing the socio-economic as well as the physical impacts of climatically or purposely altered precipitation on midwestern crops of national significance. Illinois is also addressing various other aspects of inadvertent weather modification, including the effects of urban heat islands and the Great Lakes on surrounding precipitation.

2.1 Arizona AMP

This State relies on aquifers for about 40% of its water supply. However, in some areas(especially over the densely-populated region centered on Tucson and Phoenix), ground water tables are falling rapidly. Therefore, the Arizona Department of Water Resources has begun a program to encourage water conservation and possibly augment supplies in an attempt to address the 2.5 million acre-ft per year imbalance between supply and demand for renewable water. There is no operational seeding underway in Arizona at this

time; however, since about 40% of the water for central and northern Arizona falls as snow over the Mogollon Rim, attention has naturally focussed on this region as a potential target area for research. Drainage of snowmelt from the Mogollon Rim goes about 50% into the Little Colorado system to the north, and 50% into the Verde and Salt river systems to the south.

The Arizona AMP Program aims to ascertain whether or not winter cloud seeding could be usefully applied in upslope weather conditions over the Mogollon Rim. A critical tool in this effort has been the development, testing and validation with real data of a computer model for winter precipitation over the western Mogollon Rim (Bruitjes et al, 1992a,1992b). One of the major goals of the Arizona AMP Program is to use this three-dimensional prediction model to increase our understanding of the parameters that control the amount of precipitation that reaches the ground. Field programs conducted during the winters of 1987, 1991 and 1992 verified one of the model's most intriguing predictions: the presence of strong gravity waves over Mingus Mountain. These waves were apparent in data from a wind profiler mounted on the top of Mingus Mountain, as well as from rawinsonde releases in the Verde Valley. Some of the waves were manifested by cloud bands containing significant amounts of supercooled cloud water(as verified by research aircraft, Bruitjes et al, 1992a). These waves may provide a key focus for precipitation development not previously noted in other orographic weather modification programs. Future research is aimed at improving the model's microphysics, and a major field program was conducted during January 15-March 15, 1995 in

which the first test releases of seeding material took place. For the first time, limited seeding trials using aircraft AgI and hygroscopic flares were carried out under tightly-controlled conditions. Figure 1 gives an overview of the complex topography in the Arizona AMP field program area and facility locations.

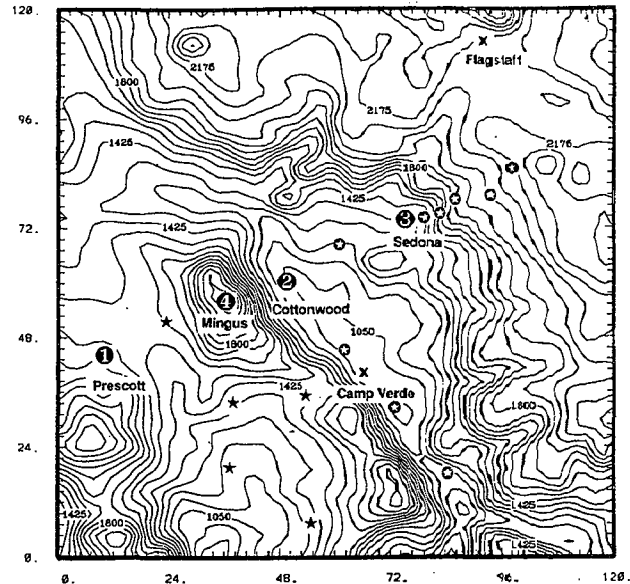


Figure 1. Overview of the Arizona Program Field area and facility locations. The Operations Center, aircraft, modelling activities, and snow sampling will be based out of Embury-Riddle Aeronautical University in Prescott ("●"). The NOAA K- and X-band radars and radiometers, the Univ of Wisconsin Lidar, NASA Ames IR radiometers, and an ALERT surface weather station will all be located at the Cottonwood Airport site ("●"). The Bureau of Reclamation microwave radiometer and an ALERT surface weather station will be located at the Sedona Airport ("●"). Mingus Mountain ("●") will be the location for several chaff and seeding releases, an ALERT surface weather station, and snow, ice crystal, and water vapor measurements and analysis. The other ALERT surface weather stations installed for the Program are located on both private and NFS land, and are shown in Figure 3 with "●" symbols. Other ALERT tipping bucket rain gages not erected specifically for this project are shown by "*" symbols. Axes are in km; all locations are approximate.

Some very intense winter storms were studied with research aircraft(Figure 2); mobile sounding systems and microwave and IR radiometers;



Fig. 2. WMI, Inc. "CHEYENNE" research aircraft used during AMP-AZ winter, 1995 field program, with new hygroscopic wing-flares for test-seedings.

NASA's IR spectroradiometer; electric field mills; radar chaff cutters on Mingus Mtn. and on aircraft; an acoustic sounder; and a pair of NOAA/ETL X-band and single K-band Doppler radars, which documented a low-level jet in one case of 40 m/sec just 700 m AGL.

Additional details on the Arizona AMP results and plans are given in the papers by Sundie, 1994; Bruintjes and Betterton, 1994; Bruintjes, Clark and Hall, 1994a,b).

The Navajo Nation was added to AMP by the US Congress in 1994, with a mandate to assist them in developing a weather modification research capability. The Arizona AMP program has taken the lead in this effort, by extending the computational domain of the three-dimensional cloud model to include the north-south Chuska Mountains, along the Arizona/New Mexico border on Navajo lands. These mountains rise to over 3 km and experience significant snowfall every winter. The orography and synoptic storm patterns appear to favor snowpack enhancement and beneficial runoff for parched Navajo farmlands through carefully-planned seeding efforts. The model will be used along with augmented observations of precipitation and other parameters to test and verify this hypothesis. We have also learned recently that the Navajo Nation has a serious flash-flood warning problem on both sides of the Chuskas, and we are working closely with the NWS Western Region to assist the Navajos to develop a coordinated warning and dissemination capability.

2.2 Utah AMP

The Utah AMP Program has a long and rich history. Its overall goals are to evaluate the effectiveness of the State operational winter cloud seeding program, and to promulgate techniques for improving that program. Previous field programs during the 1980's concentrated on the operational seeding in the Tushar Mountains of southern Utah (Huggins and Sassen, 1990). Field efforts were moved to the Wasatch Plateau (over 3 km elevation) during winter, 1989-90, because the Plateau offers logistical advantages over the Tushar Mountains for transport and dispersion investigations and microphysical studies. In particular, low-level flight through cloud systems is practical over the Plateau, and all-weather highways permit sampling on top of the Plateau (e.g., the "STARSHIP" mobile

platform in Fig.3).

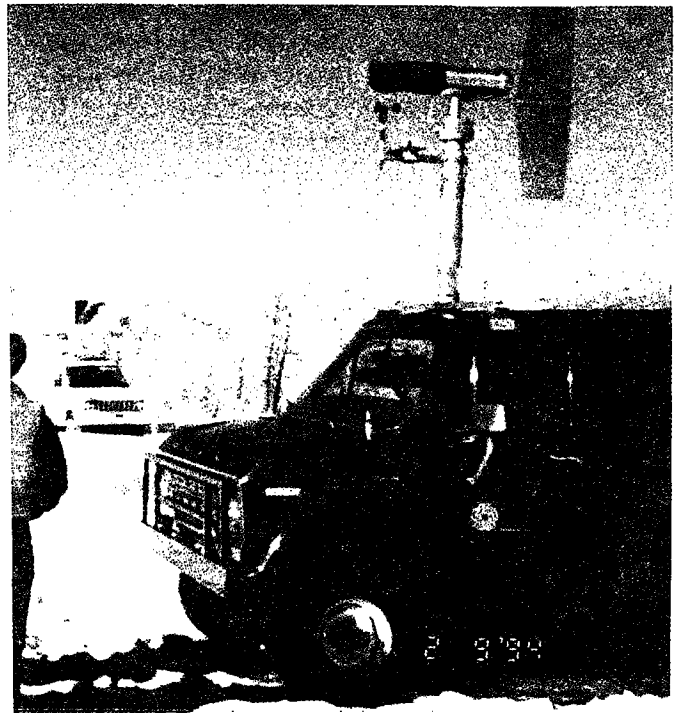


Fig. 3. AMP-Utah's mobile cloud physics vehicle with PMS cloud-particle probe.

The scientific focus of the NOAA/Utah program has emphasized research on the physical processes involved in winter orographic precipitation and its modification. Field efforts over the Wasatch Plateau continue to investigate seeding agent transport and dispersion.

The Utah field programs in the 1980's utilized new technologies such as a microwave radiometer and polarization lidar to significantly improve knowledge concerning SLW over the Tushar Mountains. During a major winter field program over the Wasatch Plateau in 1991, both mobile and fixed microwave radiometers were used to examine the spatial variability of SLW over the barrier. In general, SLW is available during portions of many storms (Super, 1993). Traverses with a new mobile radiometer revealed a consistency in the position of a SLW maxima over the windward slope (Huggins, 1995). Sassen and Zhao (1993) show some intriguing datasets obtained on clouds with supercooled liquid in Utah using a mobile ground-based lidar system.

An adaptation of the same Clark/Hall

three-dimensional cloud model used in Arizona has been made to simulate orographic cloud formation, and transport and dispersion of seeding agents over the Wasatch Plateau (Heimbach and Hall, 1994; Holroyd et. al., 1995). Model simulations of seeding plume dispersion from sources in the valley floor and well up the windward slopes, as well as releases of a tracer gas, were compared with aircraft observations within 300 m of the top of the Wasatch Plateau. Seeding material is mainly confined to a depth of several hundred meters over the terrain, and the position of release points was critical. A unique mobile cloud physics platform, the "STARSHIP", has been used to sample natural and seeded orographic snow clouds, as it was driven along the north-south paved highway on the top of the Wasatch Plateau(Figure 3).

The Utah AMP program carried out an extensive field program during the 1994 winter over the Plateau to expand upon the 1991 observations(Super, 1994) and modelling of transport and dispersion, to document ice crystal characteristics caused by seeding, and to document the ice particle concentrations after seeding(Holroyd et. al., 1995). Figure 4 shows a remote-controlled propane generator that was used during the 1994 Utah field program at a high-altitude site(see Super et al., 1995 for a discussion of propane dispenser testing).

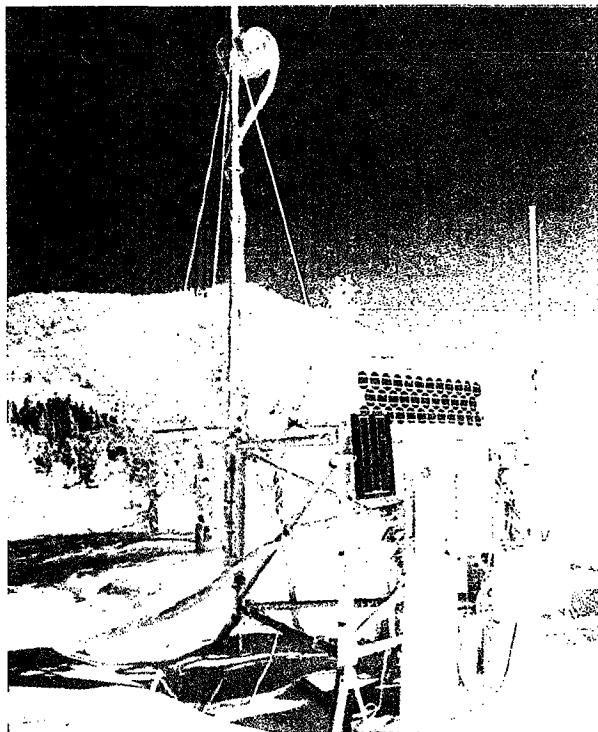


Fig. 4. Remote-controlled liquid propane generator

deployed at high altitude site(2537 m MSL) on upwind slope of Wasatch Plateau.

3.3 Nevada AMP

The long-term goal of the Nevada AMP research program is to develop a method for determining whether or not snowfall enhancement occurs when orographic winter storms are seeded, using ground-based release of ice nucleating aerosols. The Nevada program has recently pioneered in the development and application of chemical tracer techniques to assess cloud seeding and targeting. These techniques, which use an Indium compound, allow the first quantitative estimates of seeding effects due to silver iodide nucleation(see Fig. 5).

NV/NOAA Atmospheric Modification Program Tahoe Meadows, NV, Feb. 17, 1994

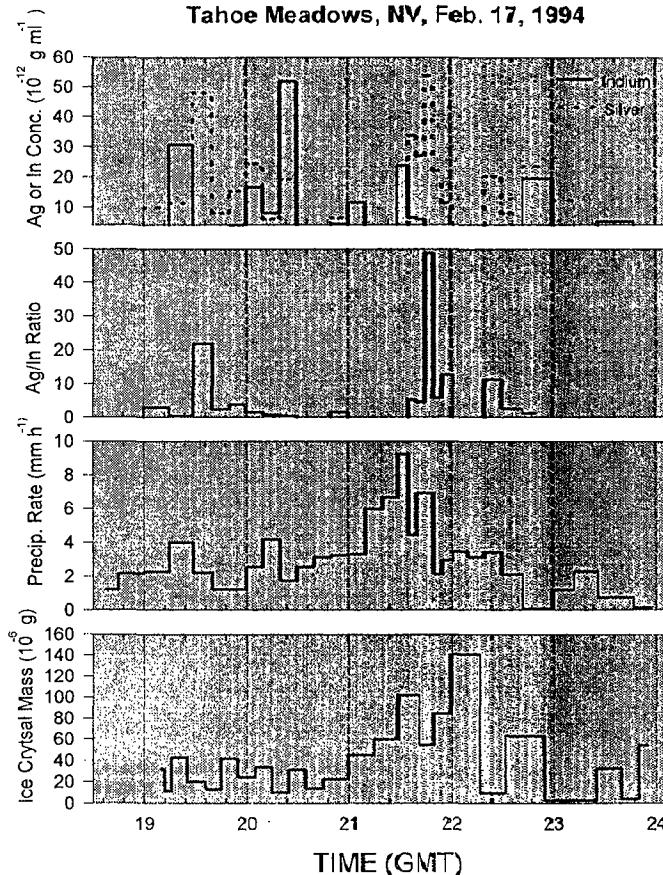


Fig. 5. Data from AMP-NV ice crystal enhancement experiment conducted at the Tahoe Meadows target site just to the east of Mt. Rose. Cloud seeding was conducted from two generator sites slightly upwind of the main Sierra Nevada Crest; both sites releasing AgI and Indium Oxide. Data suggest successful targeting during several subperiods of the experiment. Top Panel: Concentrations of silver

and indium from individual time-sequential snow samples collected at Tahoe Meadows; Second Panel: The ratio of silver mass to indium mass in the samples. Third Panel: Precipitation rate determined from the mass of the time-sequential snow samples. Bottom Panel: Average ice crystal mass determined from paired microphotographs of ice crystals and melted droplets.

Details on the Indium techniques are provided in the paper by Warburton et al(1994). The Nevada AMP Principal Investigator, Mr. Arlen Huggins, participated with one of the DRI mobile radiometers in the 1994 winter AMP-Utah field program on the Wasatch Plateau(results from the 1991 Utah field program are given by Huggins,1995). That radiometer, along with a Ka-band cloud radar from Utah-AMP will be used in a Nevada field effort being planned in the Sierra-Tahoe area during winter 1994-95. Figure 6 gives a three-dimensional portrayal of the mobile radiometer's integrated liquid water transect across the Sierra Nevada on 4 January 1994.

Donner Pass - Truckee - Incline - Mt. Rose - Reno

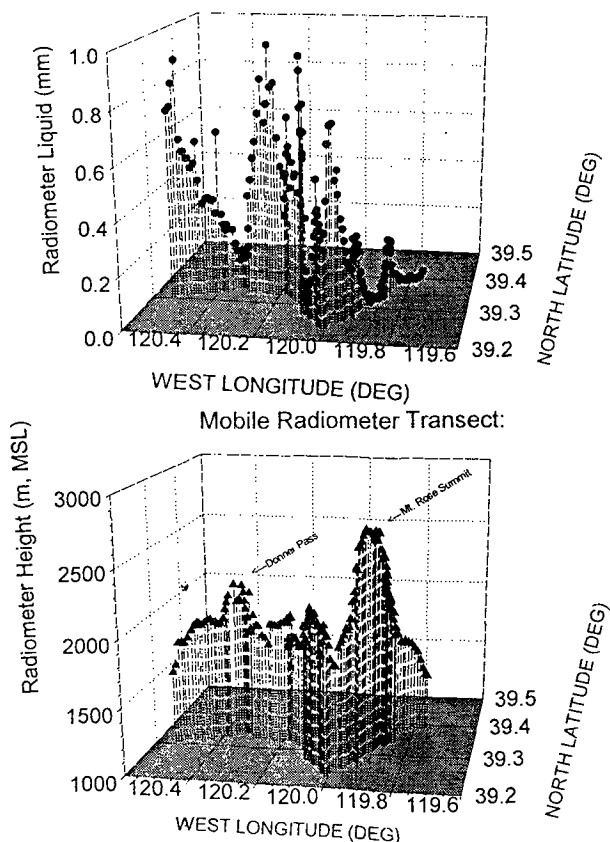


Fig. 6. Distribution of integrated liquid water depth over the Sierra Nevada, as measured on 4 January 1994 by AMP-NV. Transect began to the west of

Donner Pass on I-80 and then passed through Truckee, CA and Incline Village, NV, before proceeding over Mt. Rose summit and back into Reno, NV. Top Panel: Integrated liquid water depth by radiometer position; Bottom Panel: Radiometer height by position as determined by GPS. Donner Pass on the main Sierra Nevada barrier and the Mt. Rose Summit at the crest of the Carson Range are noted.

. Future plans include a greater emphasis on measurements of the air flow over and around the Tahoe Basin(using both special surface remote stations and the new WSR88D data from Reno), and application of an appropriate three-dimensional cloud model to this same region. Additional research is also contemplated on microphysical and chemical studies of snowfall enhancement over the Sierra-Tahoe mountains.

3.4 North Dakota AMP

The long range goals of the North Dakota research in weather modification are: (1) to determine the conditions under which convective rainfall can be enhanced by cloud seeding, (2) assess the feasibility of reducing hail damage through cloud seeding, and (3) improve the understanding of the atmospheric water processes and hazards in northern Great Plains thunderstorms. A study of North Dakota crop-loss insurance data to assess hail damage within and outside the seeding target area has been made by Smith et al(1994). The North Dakota AMP program has recently focussed its research on investigations of transport and diffusion processes in convective clouds, using the release and detection of sulfur hexafluoride gas to trace air motions in the clouds. Ice-phase cloud seeding agents (silver iodide) are sometimes released simultaneously with the tracer, so that any seeding effect can be attributed unambiguously to the actions of the seeding agent. The first North Dakota Thunderstorm Project (NDTP) was carried out in the Bismarck, N.D. area during the summer of 1989. A major new technique, termed TRACIR(Tracking of Air with Circular-polarized Radar), uses the NOAA dual-circular-polarization Doppler radar to follow chaff released from aircraft in a developing convective cloud system. Consecutive scans of the storm at frequent intervals allow determination of the movement and dispersion of the chaff through even precipitating clouds(Martner et al, 1992). Thus, for the first time, we can obtain detailed estimates of

the transport and dispersion of seeding agents in a cloud. Over 50 publications have resulted from NDTP.

During the summer of 1993, the North Dakota AMP Program carried out its most ambitious field program to date, the North Dakota Tracer Experiment (NDTE). Two Doppler radars (one a NOAA X-band and the other, the University of No. Dakota C-band), three research aircraft, a mobile sounding system and other data were obtained to address links in a conceptual model for hydrometeor development. Figure 7 gives some preliminary NOAA/ETL X-band Doppler with chaff results from one of the best-documented hailstorms, which devastated a Airstream trailer congregation at the Bismarck airport. Three different cloud models were used operationally during the project, and will also be tested using these rich data sets.

DOPPLER RADAR DETECTION OF MESOCYCLONE CIRCULATION IN A SEVERE HAILSTORM

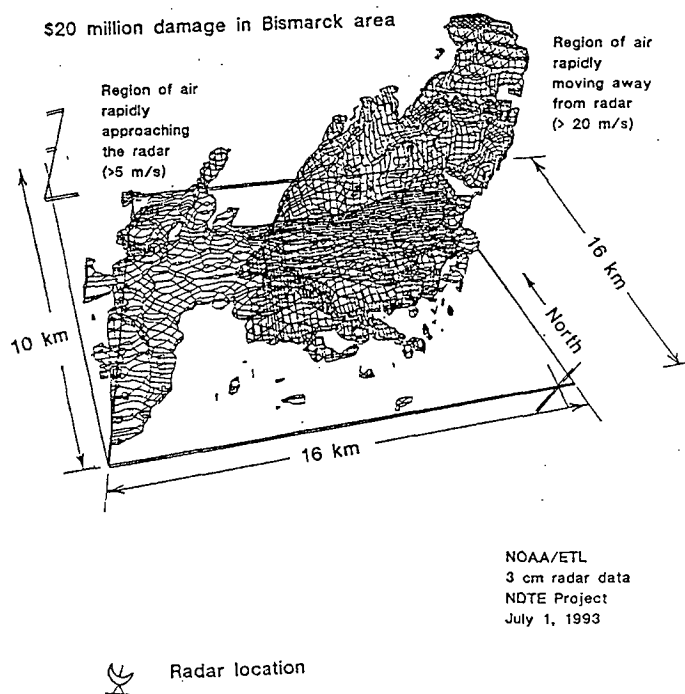


Fig. 7. Three-dimensional depiction of the tilted mesocyclonic circulation in a severe thunderstorm, as observed by the NOAA/ETL Doppler radar.

Surfaces enclosing regions of strong radial velocity toward and away from the radar are indicated by the wire-cage contouring lines. The data for this volume scan were obtained during the NDTE on July 1, 1993, at 1737-38 CDT, approx. one hour before the storm inflicted millions of dollars of hail damage in Bismarck.

3.5 Illinois AMP

The State of Illinois is third nationally in agricultural cash receipts (\$4 billion/yr) and second in agricultural exports. The most critical need is for precipitation optimization, stabilization, and long-range prediction to ensure moisture at critical periods of the growing season. Thus, the AMP focus in Illinois is on agricultural response to both purposeful and inadvertent alterations in precipitation, and on convective cloud physics. Research in the Illinois program is perhaps of the broadest of the six AMP States, and has a 14 year history. Future plans include continuing studies of cloud and precipitation processes; joint Illinois participation in the summer, 1995 AMP-Texas field program on convective cloud rain enhancement with new hygroscopic seeding flares; inadvertent modification of weather and climate conditions in Illinois and the Midwest; and the effects of altered weather and climate conditions. Figures 8 and 9 illustrate some new results on inadvertent weather modification, i.e. the urban 'heat island' effect. Figure 8 reveals a greater incidence of cloud-to-ground lightning flashes downwind from St. Louis, especially in the afternoon and early evening.

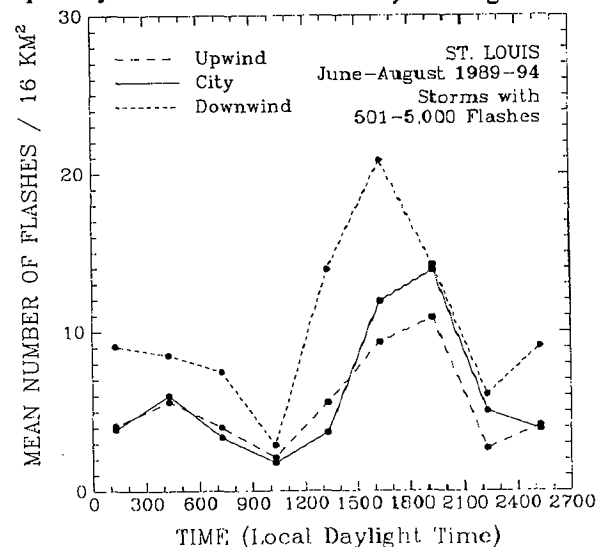


Fig. 8. Frequency of cloud-to-ground lightning flashes(per 16 sq. km) at St. Louis, MO for areas upwind of the city, over the city(urban area) and

downwind(east) of the city. Results reveal greater downwind incidences, particularly in the afternoon and early evening.

Over a larger urban area sample, Figure 9 suggests that cities adjacent to the large Great Lakes(Chicago, Detroit, Milwaukee and Toledo) showed no increase and a slight decrease in lightning. All other cities exhibited downwind increases in lightning.

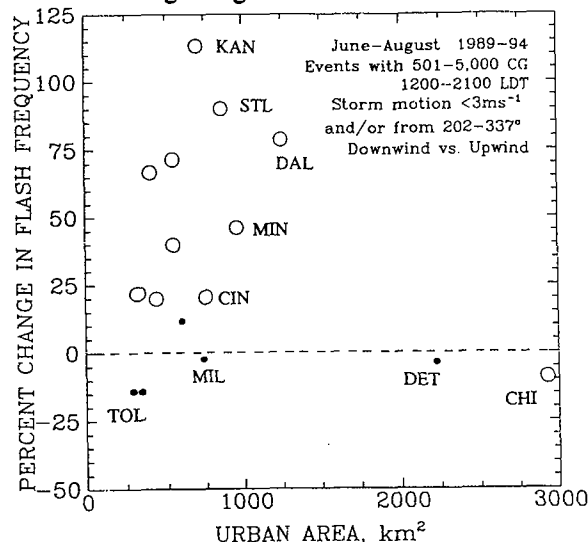


Fig. 9. Percent change of cloud-to-ground lightning flash frequency, from the west upwind to the east-downwind areas for 16 midwestern cities for June-August 1989-1994. Lightning events of a moderate size(501-5,000 flashes), occurring during afternoon hours, and moving slowly or with a westerly component were included. Open circles refer to statistically significant differences and closed circles to non-significant differences. Note that cities adjacent to the large Great Lakes (Chicago, Detroit, Milwaukee and Toledo) showed no increase and a slight decrease, while all other cities exhibited downwind increases in lightning.

Two exploratory seeding experiments were carried out in Illinois during 1986 and 1989(termed PACE), using the dynamic seeding approach(Westcott et al, 1993). The findings so far, using radar and cloud physics aircraft data, have shown some distinct limitations of this approach to Illinois agricultural productivity(Czys et al, 1993). Weather modification efforts on convective clouds in Illinois is greatly complicated by the fact that much of the rainfall occurs in association with severe weather and/or after dark. A comprehensive evaluation of the convective cloud modification efforts to date in Illinois, and possible future

directions is given by Changnon et al(1994). Figure 10 shows that before cloud treatment, there was no sense of organization in the relationship between dynamically-seeded cumuli and rainfall.

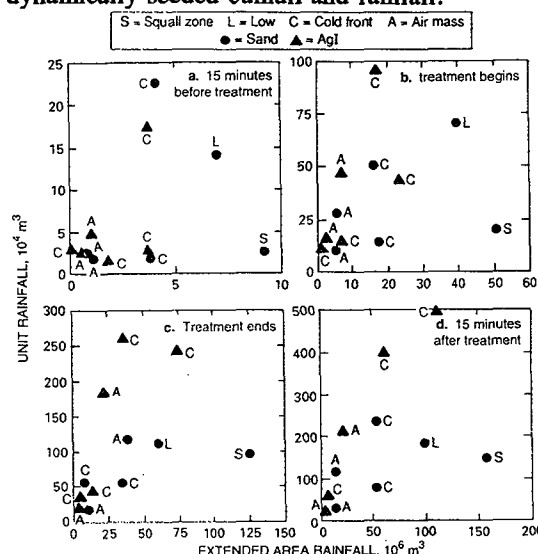


Fig. 10. The 1989 PACE cloud seeding experiment in Illinois involved dynamic seeding of growing cumuliform clouds in groups, or units, and the rainfall from the 6 units treated with AgI was compared with that from 6 units treated with a sand placebo. In this graph, the relationship of the unit-area rainfall(for seeded[treated] and non-seeded units) and that of the extended area (all the other rainfall surrounding the units) is shown for four times, from 15 min before treatment (upper left) until 15 min after treatment.

However, by 15 minutes after AgI seeding, two of six treated units had large values of unit rainfall (relative to extended area amounts). Both cases were with cold fronts, as designated.

With regard to agricultural impacts of purposeful precipitation modification, AMP-Illinois field experiments on agricultural plots have examined how additional water applied during different crop growth stages might affect yields. Figure 11 shows shifts in applications during stage 6 of corn growth for four years. Surprisingly, increased amounts of water had only minor influences on corn yields.

3.6 Texas AMP

Texas was added to the existing five States participating in AMP by the U.S. Congress in 1992. Its research is focussed on summertime convective cloud systems over the semi-arid, agricultural

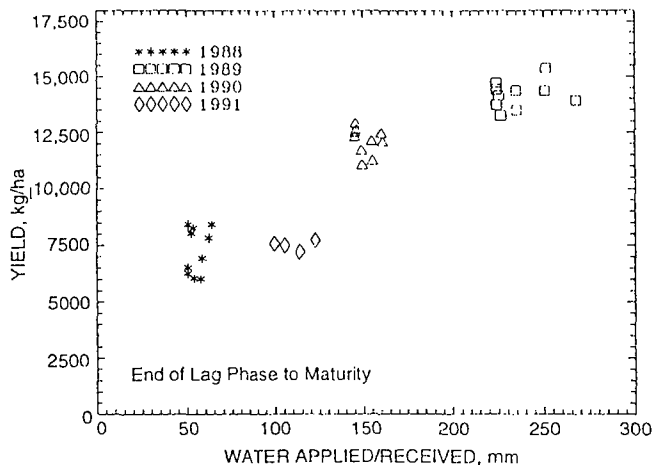


Fig. 11. Illinois field experiments on agricultural plots have examined how additional water applied during different crop growth stages affect yields. Here, shifts in applications during stage 6 of corn are shown for four years. Increased amounts had only minor influence on yields.

cloud systems over the semi-arid, agricultural regions of west Texas. The program has two objectives: to quantify the amount of additional rainwater and runoff that is generated when summertime convective clouds are seeded using the dynamic seeding approach; and to understand the behavior of convective clouds in order to predict the impact of the various cloud seeding methodologies will have on these clouds. A conceptual model for the dynamic seeding hypothesis, as applied to both seeded and nonseeded clouds in Texas has been developed by Rosenfeld and Woodley (1993). Results of a program supported by the Bureau of Reclamation in the 1980's have been reported by Rosenfeld and Woodley (1989). Randomized cloud seeding experiments conducted in 1987 and 1989-90 in conjunction with a State operational program resulted in 183 convective cells (about half seeded and half nonseeded). Dynamic seeding from aircraft increased the areas of the cells by 43%, the durations by 36%, and the rain volume ratios by 130%. The principal dynamic effect of the cloud seeding was the increased mergers of cloud cells.

Another modest field program was carried out in the Big Springs, TX area in late summer, 1994 to obtain additional seeded/nonseeded cases, with emphasis on documenting the microphysics, using the South Dakota School of Mines T-28 aircraft (Fig. 12) and remote sensors.

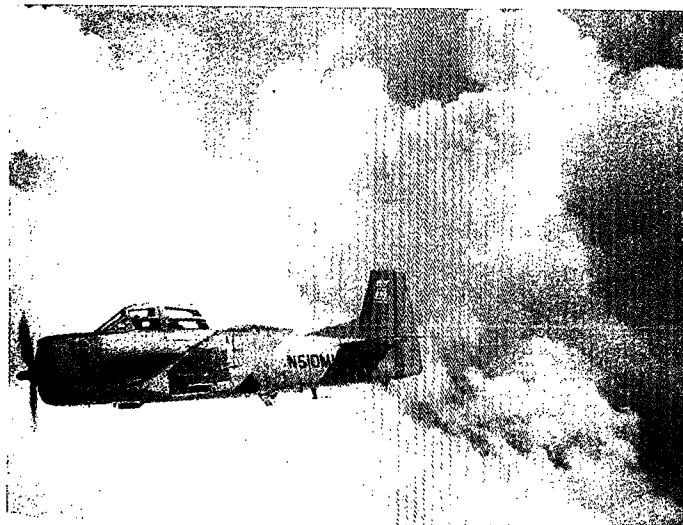


Fig. 12. The South Dakota School of Mines T-28 armoured cloud physics research aircraft, flying cloud-penetration mission on August 15, 1994 during AMP-TX field program southeast of Big Springs.

The T-28 aircraft penetrations of experimental cloud units showed several cases of abundant liquid water with large convective updrafts (some greater than 2 g m⁻³ and 10 m/s, resp.).

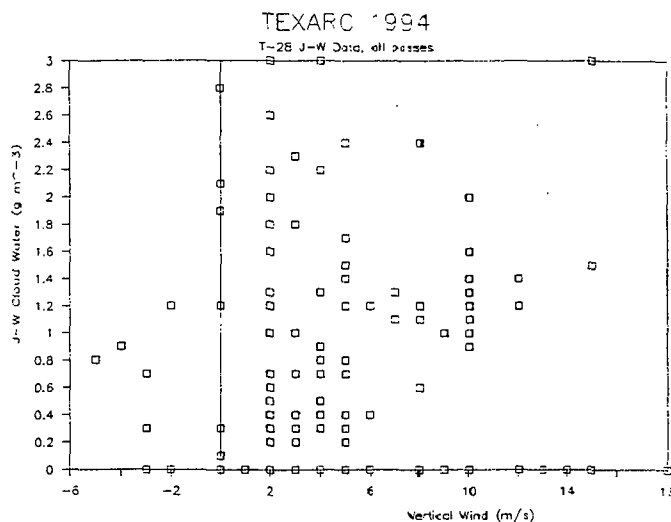


Fig. 13. Plot of J-W cloud water vs. convective updrafts in 1994 AMP-TX field program by T-28 aircraft penetrations of experimental convective cloud units.

Digital data were also archived for the first time on

the NWS NEXRAD at Lubbock.

4. Weather Modification Impacts from the Modernization of the U.S. National Weather Service

The National Weather Service(NWS), NOAA is in the midst of a \$2 billion Modernization program. While the total number of offices will be reduced overall at the completion and certification of the Modernization, there will be 116 modern Weather Forecast Offices(WFOs) equipped with new observing and data processing and display technologies. In addition,

NOAA has installed and operated a 29-station Wind Profiler Demonstration Network over the Central U.S. for 4 years now. These instruments are vertically-pointing, fixed array Doppler radars(405 MHz frequency) that produce virtually continuous tropospheric wind profiles, from about 0.5-16 km. NOAA laboratories have also pioneered in the development of smaller, transportable boundary layer wind profilers(915 MHz frequency), that are used in field experiments. One of these systems was used very successfully during the 1991 Arizona AMP field program. A key new technology component of the NWS Modernization is the WSR-88D(NEXRAD) Doppler radar, which has been deployed at over 100 of the eventual 116 WFO sites. This narrow-beam, 10 cm wavelength Doppler radar has characteristics and advanced data processing summarized by Golden(1989) and Golden et al(1990). It provides high-resolution, three-dimensional volume scans refreshed every 6 min. The WSR-88Ds also provide a synthesized vertical wind profile, using the VAD technique, averaged over the volume scanned above each radar every 6 min. NEXRAD data has already been used in AMP-TX and AMP-AZ field programs over the past year. Together, the wind profilers and WSR-88Ds have many applications to both research and operational weather modification programs in the U.S. In addition, we can now produce high-resolution (1 km or better) hourly, six-hourly and storm-total maps of precipitation accumulation. The WSR-88D software also permits the acquisition and blending of remote raingage data under each radar umbrella in real-time, once the new AWIPS-90 processing system is deployed. We will also be to track seeding materials released from aircraft or the ground much more accurately, using WSR-88D and wind profiler data. Finally, in concert with the FAA and Defense Department, NWS is deploying

over 1200 Automated Surface Observing Systems at large and small airports in the U.S. These new in-situ and remote sensor data, when blended appropriately and assimilated into mesoscale cloud models, will permit highly detailed real-time predictions of cloud and precipitation development, as well as more accurate estimates of transport and dispersion of seeding plumes.

Acknowledgements. The author expresses his gratitude to the Principal Investigators and Principal Scientists in each of the six AMP States for their ongoing leadership and scientific support of the program: Dennis Sundie and Eric Betterton, Arizona; Barry Saunders and Arlin Super, Utah; Arlen Huggins and Joe Warburton, Utah; Bruce Boe, Harold Orville, Paul Smith, and Jeff Stith, North Dakota; Stan Changnon, Bob Czyns, and Steve Hollinger, Illinois; and George Bomar, Bill Woodley and Danny Rosenfeld, Texas. The author also appreciates the early review of this paper by his colleagues at the South Dakota School of Mines, Drs. Harold Orville and Paul Smith. The advice and assistance of my predecessor as AMP Director, Dr. Roger Reinking, NOAA/ETL is also acknowledged.

5. References

- Bruintjes, R.T., T. L. Clark, and W.D. Hall, 1992a: Comparisons between observations and numerical simulations of a winter storm episode over complex terrain. Proceedings, 11th Int'l Conf. on Clouds and Precipitation, Montreal, Canada, August 17-21. ICCP/IAMAP, Innsbruck, Austria, pp. 467-470.
- _____, _____, _____, and R. Gall, 1992b: The use of sophisticated three-dimensional numerical models in winter orographic weather modification efforts. Preprints, Symp. on Planned and Inadvertent Weather Mod., Atlanta, GA, Jan. 5-10, Amer. Meteor. Soc., Boston, MA. pp. 121-125.
- _____, _____, _____, 1994a: The effects of gravity waves on the production of supercooled liquid water(SLW) in complex terrain. Preprints, Sixth WMO Conf. on Wx Mod., Paestum, Italy, 287-290.
- _____, _____, _____, 1994b: The dispersion and transport of tracer plumes in complex terrain and the implications for cloud seeding experiments. Op.Cit., 291-294.

_____, and E.A. Betterton, 1994: The Arizona Atmospheric Modification Program. Op.Cit., 267-270.

Changnon, S.A., R.C. Czyns, and S. Hollinger, 1994: The integration of meteorological, technological, economic and legal factors affecting use of precipitation modification in the central U.S. Preprints, Sixth WMO Conf. on Wx Mod, Paestum, Italy, 271-274.

Czyns, R.R., S.A. Changnon, N.E. Westcott, M.S. Petersen and R.W. Scott, 1993: Evaluation of echo core responses in the 1989 Illinois exploratory cloud seeding experiment using a seedability index. J. Wea. Modification, 25, 12-25.

Golden, J. H., 1989: The prospects and promise of NEXRAD: 1990s and beyond. Proceedings, Weather Radar Networking--Seminar on COST 73 Project, Kluwer Academic Publishers, London, pp. 26-45.

_____, and others, 1990: Severe Storm Detection--Panel Report. Chapter 30b in "Radar in Meteorology", D. Atlas, Ed., Amer. Meteor. Soc., Boston, MA, pp. 648-656.

Heimbach, J.A. and W. D. Hall, 1994: Applications of the Clark model to winter storms over the Wasatch Plateau. J. Weather Mod., 26, 1-11.

Holroyd, E.W., J.A. Heimbach and A.B. Super, 1995: Observations and model simulation of AgI seeding within a winter storm over Utah's Wasatch Plateau. J. Weather Mod., this issue.

Huggins, A.W. and K. Sassen, 1990: A high altitude ground-based cloud seeding experiment conducted in southern Utah. J. Wea. Mod., 22, 18-29.

_____, 1995: Mobile microwave radiometer observations: Spatial characteristics of supercooled cloud water and cloud seeding implications. J. Appl. Meteor., 34, 432-446.

Martner, B.E., J.D. Marwitz, and R.A. Kropfli, 1992: TRACIR observations of transport and diffusion in clouds and precipitation. J. Atmos. and Ocean. Tech., 9, 226-241.

Reinking, R.F., 1992: The NOAA Federal/State

cooperative program in atmospheric modification research: A new era in science responsive to regional and national water resource issues. Preprints, Symp. on Planned and Inadvertent Weather Modification, Amer. Meteor. Soc., Boston, MA, pp. 136-144.

_____, (editor), 1993: The NOAA Federal/State Cooperative Program in Atmospheric Modification Research--Collected Publication Titles and Abstracts. NOAA Tech. Memo. ERL WPL-231, Wave Propagation Laboratory, NOAA, Boulder, CO. 86 pp.

Rosenfeld, D., and W. L. Woodley, 1989: Effects of cloud seeding in west Texas. J. Appl. Meteor., 28, 1050-1080.

_____, and _____, 1993: Effects of cloud seeding in West Texas: Additional results and new insights. J. Appl. Meteor., 32, 1848-1866.

Sassen, K. and H. Zhao, 1993: Supercooled liquid water clouds in Utah winter mountain storms: Cloud-seeding implications of a remote-sensing dataset. J. Appl. Meteor., 32, 1548-1558.

Smith, P.L., L.R. Johnson, D.C. Priegnitz, and P.W. Mielke, 1994: Statistical evaluation of the North Dakota CLOUD Modification Project. Preprints, Sixth WMO Conf. on Wx Mod., Paestum, Italy, 281-284.

Super, A.B., 1994: Implications of early 1991 observations of supercooled liquid water, precipitation and silver iodide on Utah's Wasatch Plateau. J. Weather Mod., 26, 19-32.

Super, A.B., and A.W. Huggins, 1993: Relationships between storm total supercooled liquid water flux and precipitation on four mountain barriers. J. Weather Mod., 25, 82-92.

_____, E. Faatz, A. J. Hilton, V.C. Ogden, and R.D. Hansen, 1995: A status report on liquid propane dispenser testing in Utah with emphasis on a fully-automated seeding system. J. Wea. Mod., this issue.

Weather Modification Advisory Board, 1978: The management of weather resources, Vol. I. Report to the Secretary of Commerce, U.S. Govt. Printing Office, Washington, D.C., 229 pp.

Warburton, J.A., S.K. Chai, and L.G. Young,
1994: A new concept for assessing snowfall
enhancement in winter orographic cloud-seeding
experiments. Preprints, Sixth WMO Conf. on Wx
Mod., Paestum, Italy, 699-702.

Westcott, N.E., S.A. Changnon, R.R. Czys, R.W.
Scott, and M.S. Petersen, 1993: Results of the 1989
exploratory cloud seeding experiment in Illinois
based on synoptic weather conditions.
J. Wea. Modification, 25, 26-49.